

**Exercising demons: How to drive a  
chemical system away from equilibrium**

**By  
Viviana Serreli**

Degree of Doctor of Philosophy  
Department of Chemistry  
University of Edinburgh  
June 2008

# Table of Contents

<b>Abstract.....</b>	<b>v</b>
<b>Declaration.....</b>	<b>vi</b>
<b>Attended Lectures and Meetings .....</b>	<b>vii</b>
<b>Acknowledgements .....</b>	<b>viii</b>
<b>List of Abbreviations .....</b>	<b>ix</b>
<b>General Remarks on Experimental Data .....</b>	<b>x</b>
<b>Layout of the Thesis.....</b>	<b>xi</b>
<b>Chapter 1: Making Molecular-Level Machines.....</b>	<b>13</b>
Introduction.....	14
1.1 From Natural to Artificial Molecular-Level Machines.....	14
1.1.1 Nanotechnology: a challenge from nature.....	14
1.1.2 Breaking into motion.....	16
1.2 Covalently Bonded Molecular Systems with Rotating Parts.....	18
1.2.1 Molecular propellers and gears.....	18
1.2.2 Controlling rotational motion:a molecular breake.....	19
1.2.3 A chemically powered unidirectional rotor .....	20
1.2.4 The first 360 <sup>o</sup> unidirectional rotation about a double bond .....	21
1.2.5 Reversible, 360 <sup>o</sup> unidirectional rotation about a single bond .....	23
1.3 Molecular Level Devices with Mechanically-Bonded Shuttling Parts.....	25
1.3.1 Catenanes and rotaxanes.....	25
1.3.2 Rotaxane-based molecular shuttles.....	26
1.3.2.1 Degenerate molecular shuttles.....	26
1.3.2.2 Stimuli-responsive molecular shuttles: a physical description.....	29
1.3.2.3 Reversible molecular switches.....	31
1.4 Compartmentalizing molecular machines.....	33
1.4.1 The two-compartment Brownian motion "though machines".....	34
1.4.1.1 Maxwell's Demon.....	34
1.4.1.2 Szilard's Engine.....	37

1.4.1.3	Smoluchowski's Trapdoor.....	38
1.4.2	Brownian ratchet molecular motors.....	39
1.4.2.1	Compartmentalizing synthetic molecular-level machines.....	40
1.4.2.2	A reversible synthetic rotary molecular motor.....	42
1.4.2.3	A compartmentalized stimuli-responsive molecular shuttle..	45
1.5	Summary.....	49
1.6	References and notes.....	51

## **Chapter 2: Exercising demons: How to drive a chemical system away from equilibrium.....60**

### **Synopsis.....61**

2.1	Introduction.....	63
2.1.1	Driving chemical system away from equilibrium .....	63
2.1.2	Driving chemical system away from equilibrium using molecular-level motion.....	66
2.1.3	Design of a non-adiabatic molecular Maxwellian pressure demon.....	67
2.2	Experimental results.....	70
2.2.1	Photochemical studies on the model compounds .....	70
2.2.2	Photochemistry behavior of rotaxane 1 .....	73
2.2.3	Binding studies .....	74
2.2.4	Operation of the molecular machine.....	75
2.2.5	Kinetic model for the operation of rotaxane 1 .....	79
2.2.6	Control experiments.....	81
2.3	Discussion .....	83
2.3.1	Free-energy increase on moving away from equilibrium.....	84
2.3.2	Information, entropy and useful work .....	84
2.3.3	An information ratchet molecular machine mechanism.....	86
2.3.4	Chemical games.....	89
2.3.5	Information ratchets in biology .....	91
2.4	Conclusions.....	92
2.5	References and notes.....	93

<b>Chapter 3: Experimental part .....</b>	<b>101</b>
3.1 Synthesis .....	102
3.2 Experimental procedures.....	109
3.3 References and notes.....	134
 <b>Appendix : Published Paper .....</b>	 <b>135</b>

## Abstract

The concept of tiny machines capable of selectively transporting particles between two compartments by Brownian motion dates back to the 19th century when James Clerk Maxwell pondered the significance of a hypothetical ‘sorting demon’ being able to perform such a task adiabatically. This thesis report the design, synthesis and operation of a compartmentalized molecular machine in which the distribution of a Brownian particle, the macrocycle in a rotaxane, is controlled by using the light-induced transmission of information to lower a kinetic barrier according to the location of the particle. For an ensemble of such machines the particle distribution is driven further and further away from equilibrium, providing a non-adiabatic realization of Maxwell’s pressure demon in molecular form. The nanomachine does not break the Second Law of Thermodynamics because the energy cost of the information transfer is met by externally supplied photons. As the molecular structure can be understood in chemical terms, it is possible in this experimental system to pin-point precisely how information is traded for energy. Intriguingly, the chemical mechanism can also be understood in terms of game theory. This is the first example of a synthetic molecular machine designed to operate via an information ratchet mechanism, where knowledge of the object’s position is used to control its transport away from equilibrium.

## Declaration

The scientific work described in this Thesis was carried out in the Department of Chemistry at University of Edinburgh between November 2003 and November 2006. Unless otherwise stated, it is the work of the author and has not been submitted in whole or in support of an application for another degree or qualification of this or any other University or institute of learning.

Signed.....

Date.....

## Lectures and Meetings Attended

1. **Organic Research Seminars**, School of Chemistry, University of Edinburgh, Scotland, 2003-2006.
2. **Firbush Organic Talks**, School of Chemistry, University of Edinburgh, Scotland, 2004-2006.
3. **Perkin Organic Chemistry Conference**, School of Chemistry, University of Edinburgh, Scotland, 12/03.
4. **EMMA European Network**, Netherlands, 6/04, oral presentation: *“Exercising Maxwell’s Demon, Using information to do work at the molecular level”*.
5. **European Science Foundation: “Chemistry and Physics of Multifunctional Materials”**, Portugal, 9/04, Presented poster: *“Exercising Maxwell’s Demon”*.
6. **EMMA European Network**, University of Edinburgh, Scotland, 5/05, oral presentation: *“Exercising Maxwell’s Demon: How to drive a chemical system away from equilibrium”*.
7. **InterConsortia European Meeting**, Italy, 6/06, oral presentation: *“Exercising demons: A Molecular Information Ratchet”*.

## Acknowledgements

I would like to express profound gratitude to my Supervisor Prof. Dave Leigh, for his invaluable support, encouragement, supervision during these years. His moral support, criticism and continuous guidance enabled me to overcome all the difficult times and failures I faced working on this project and to turn them into useful learnings without ever giving up.

I am also highly thankful to Dr. Euan Kay who shared his knowledge and expertise with me, always willing to help me answer all my questions without hesitation, gave me so much important advice throughout this research work and guided me about the direction of my thesis. Thanks to Dr. Chin-Fa Lee for his support in completing this research project.

I spent in the Leigh group three wonderful years from the scientific point of view during which I had the chance to meet fantastic people from all the world that I would like here to thank. A huge thanks to Ale, Andrea and Smjlia, ones of the most genuine persons I met in my life and with which I shared happy and sad moments in these years. Thanks for all the good time, the laugh we had together and for being such good friends...Thanks to all the Leigh group, especially to Dana, Jose', Julia, Manashj, Vince, Pepe, Nick, Annemarie, Diego, Aurelian.

Moreover I am so grateful to the University of Edinburgh, the teaching and technical staff of the Chemistry department for providing me with a stimulating and exciting learning environment.

I am as ever, especially indebted to my husband, my parents and relatives for their love, for giving me the extra strength, motivation and love necessary to get things done, and for all the emotional support, entertainment, and caring they provided. In particular, my last but not least thought goes to my dear granddaddy Nonno Tutuccio, Zietta, zia Elena and Prof. Stefana Melis that unfortunately could not see the end of this PhD. To them I dedicate this thesis.



## List of Abbreviations

DMSO dimethylsulphoxide

DMF *N,N'*-dimethylformamide

THF tetrahydrofuran

TFA trifluoroacetic acid

EDTA ethylenediamine tetraacetic acid

Boc<sub>2</sub>O di-*tert*-butyl dicarbonate

Alloc allyl chloroformate

Et ethyl

Me methyl

CBS Corey, Bakshi, Shibita reagent (chiral borohydride reducing agent)

PMB *p*-methoxybenzoate group

TBDMS *t*-butyldimethylsilyl group

THP tetrahydropyranyl group

DIBAL-H di-isobutylaluminium hydride

EDCI 1-(3-dimethylaminopropyl)-3-ethyl carbodiimide

DB24C8 dibenzo-24-crown-8

*E trans* isomer

*Z cis* isomer

*dba* dibenzyl ammonium station

*mba* monobenzyl ammonium station

PPS photostationary state

ET electron transfer

NMR Nuclear Magnetic Resonance

ppm part per million

mins minutes

$\delta$  chemical shift

m.p. melting point

TLC Thin Layer Chromatography

FAB Fast Atom Bombardment

rt room temperature

mL millilitres

g grams

HRMS High Resolution Mass Spectrometry

Calcd. calculated

$\Delta G^\circ$  Gibbs energy

## General Remarks of Experimental Data

Unless stated otherwise, all reagents were purchased from commercial sources and used without further purification. Dry acetonitrile, chloroform, dichloromethane, *N,N*-dimethylformamide (DMF), methanol and tetrahydrofuran (THF) were obtained by passing these solvents through activated alumina columns on a PureSolv<sup>TM</sup> solvent purification system (Innovative Technologies, Inc., MA). Column chromatography was carried out using Kiesegel C60 (Fisher) as the stationary phase, and TLC was performed on precoated silica gel plates (0.25 mm thick, 60F<sub>254</sub>, Merck, Germany) and observed under UV light. Routine <sup>1</sup>H and <sup>13</sup>C NMR spectra were recorded on a Bruker AV 400 instrument, at a constant temperature of 25 °C, while <sup>1</sup>H spectra for analysis of rotaxane operation were recorded on a Varian INOVA 600 instrument, also at 25 °C. Chemical shifts are reported in parts per million from high to low field and referenced to residual solvent. Standard abbreviations indicating multiplicity were used as follows: m = multiplet, br = broad, d = doublet, q = quadruplet, t = triplet, s = singlet. All melting points were determined using a Sanyo Gallenkamp apparatus and are uncorrected. FAB mass spectrometry was carried out by the services at the University of Edinburgh.

Photoisomerizations were carried out at 298 K using a multilamp photoreactor (model MLU18) manufactured by Photochemical Reactors Ltd, Reading, UK.

## Layout of this Thesis

This thesis describes the design, synthesis and operation of a photo-operated molecular information ratchet based on a compartmentalized stimuli-responsive molecular shuttle. A brief review of the literature is given in Chapter One describing the background to controlled motion at the molecular level and the advancements achieved in the field with the latest compartmentalized molecular machines.

The remainder of the Thesis discusses my own experiments in this area – contributions of others are gratefully acknowledged before Chapter Two - and is presented in the form of three chapters as integration of the article that has already been published with addition of experimental parts and concepts that were reported as Supporting Information.

Chapter Two is focused on the design and operation of the rotaxane machine with the photochemical experiments (the photochemistry of model compounds is also discussed) exploited by photo-sensitized isomerization and the investigation of the machine-performance by  $^1\text{H}$  NMR spectroscopy. The results have also been discussed in terms of physics and thermodynamics. A brief synopsis is included at the start of chapter to help put the reader in perspective.

Chapter Three contains the synthesis and characterization of the rotaxane machine and the model compounds.

Viviana Serreli

June 2008

*I dedicate this Thesis to my husband and my daughter,  
to my family,  
to all my relatives and friends  
for their love and support throughout these years.*

*Grazie!*

## *Chapter One*

## Making Molecular-Level Machines.

## Introduction

### 1.1 From Natural to Artificial Molecular-Level Machines

#### 1.1.1 Nanotechnology: a challenge from nature

The development of civilization has always been strictly related to the design and construction of devices capable of facilitating man's everyday needs.

Technological progress also unravels a lot of hidden areas, shows how nature performs its miracles and helps us understand its power and greatness. Imagine a primitive man who sees an automobile, he might guess that it was powered by the wind or by an antelope hidden under the car, but when he opens up the hood and sees the engine he immediately realizes that it was designed! In the same way modern biochemistry opens up the cell to examine what makes it run and we see that it, too, was organized.

Nature provides us with living examples of fantastically complex biological molecular systems such as assemblies of proteins which work inside a cell like machines with the task to provide the energy necessary for everyday life.

In the past two decades the outstanding development of scientific breakthroughs and new technologies for the manipulation and observation at the molecular scale has thrown light on the working mechanism of many key biological machines from  $F_0F_1$ -ATPase to kinesin and myosin.

A new science inspired by nature is taking place with the challenge to reproduce at the nanoscale synthetic analogues of natural molecular motors and their macroscopic counterparts. However because of their deep complexity the structures and detailed working mechanism of natural motors have been elucidated only in a few instances, and the problems posed by interfacing artificial molecular machines with the macroscopic world still need to be overcome.

Despite tremendous advancements in recent years synthetic molecular machines remain very much in their infancy in terms of experimental systems and any attempt to reproduce natural molecular motors artificially, at least in the short term, would be hopeless. What chemists can do, at present, is to construct simple prototypes consisting of a few molecular components capable of moving in a controllable way. Improving the ability to control the movement of matter has long been a major aim of technology and the consequences of such ability at the nanoscale will be enormous, in areas as diverse as medicine, computation, manufacturing, and environment.

The first time the possibility of constructing artificial molecular-level machines was contemplated was in 1959 by the Nobel Laureate Richard Feynman during the annual meeting of the American Physical Society in his historical address: “There’s Plenty of Room at the Bottom”<sup>1</sup>. Here are some prophetic sentences from this lecture:

*What would be the utility of such machines? Who knows? I cannot see exactly what should happen, but I can hardly doubt that when we have some control of the arrangement of things on a molecular scale we will get an enormously greater range of possible properties that substances can have, and of the different things we can do.*

In this introduction I will present a short outlook on the progresses made so far in the manipulation and control over submolecular motion in synthetic molecular machines and the resulting remarkable achievements in terms of task performance.

With the intention of introducing the reader to the systems discussed this thesis, I shall focus the following review on rotaxane-based molecular devices, the design and the physics of their working mechanism.



### 1.1.2 Breaking into motion

The design and synthesis of molecular-level devices is not always intuitive and it is not enough just to make a miniature version of a macroscopic motor since the physics of the nano-world is essentially different from that in the macroscopic world. We can define a macroscopic *machine* as “an apparatus for applying mechanical power, having several parts, devices, each with a definite function”<sup>2</sup>.

This leads us to the definition that a *molecular-level machine* is an assembly of a discrete number of molecular components designed to perform mechanical-like movements (output) as a consequence of appropriate external stimulus (input). The main features of such a machine are i) the kind of energy by which it is powered, ii) the type of movement performed, iii) the manner in which the motion can be monitored and controlled and iv) the function performed by the machine.

In the “real word” machine parts (e.g. cogs, flywheels, pistons) are generally unaffected by ambient thermal energy and they do not move until and unless a force is applied to make them do so. At the molecular scale however inertia is negligible and at any temperature above 0 K molecules and their parts are constantly subject to random and incessant thermal and quantum fluctuations so that for molecules, moving deterministically is like trying to walk in a storm!

The effects of random motion at the molecular scale were first observed in 1827 by the Scottish botanist Robert Brown (from here comes the name Brownian motion) when he noted through his microscope an incessant, haphazard motion of particles within pollen grains suspended in water.<sup>3</sup> Later Einstein<sup>4</sup> provided a molecular explanation of this phenomenon and Perrin gave the experimental proof over the next decade<sup>5</sup>. Since then and for nearly two centuries scientists have been working on the fascinating implications of the stochastic nature of molecular-level motion.

Although biological systems face this chaos in their everyday operations, cells thrive: they ferry materials, pump ions, build proteins. How can they make order out of anarchy? In his *Making molecules into motors*<sup>6</sup> R. D. Astumian quotes

“Molecular turmoil and quantum craziness: microscopic machines must operate in a word gone mad. But if you can’t beat the chaos, why not exploit it?”

In other words, like “Mohammed and the mountain”, for biological motors to work the preferable choice seems to be working with Brownian motion rather than fighting against it. Starting from this consideration over the past years, biologists, physicists and chemists have been working together to understand how they take advantage of these random pushes and use them to harness directionality in motion.

The solution to this represents the basic principle for a working molecular level machine: an external trigger is used to control a change in property of some component, which provokes net directional motion of one component relative to another through Brownian motion. The result will be a net task being performed and the displacement will then be monitored by following changes in some of the physical properties of the molecular species.

The behaviour of molecular-level machines is strictly dependent upon their architecture, the way with which the molecular components are linked to others and the kind of movement that they perform to achieve a mechanical task. In the next session I have discussed some literature examples of two distinct categories of molecular-level machines i) covalently bonded systems with rotating moving parts and ii) mechanically bonded systems with translating moving parts. An extra care has been recently dedicated in updating the language used to describe molecular-level machines<sup>7</sup> dated respect the advances in this field. This leads us to further distinguish two main classes of molecular machines, depending on the mechanism of their operation: “molecular motors” where the task is performed as a function of the “trajectory” of the system, and “molecular switches” where the task is performed as a function of the “state” of the system.

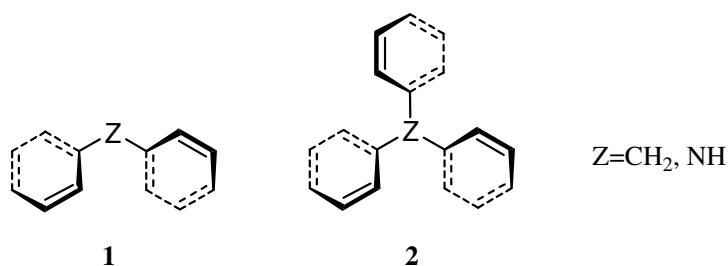
In other words switches can use chemical energy to do mechanical work but this is undone by resetting the machine to its original state whereas a motor does not.

Returning a motor to its original position by different pathway to that used initially allows the use of chemical energy to repetitively and progressively drive the system away from equilibrium whereas the switches cannot. The terms motor and switch have been sometimes used interchangeably in the chemistry literature but it is important to remark that the most of the molecular-level machines developed so far in this field are switches and not motors.

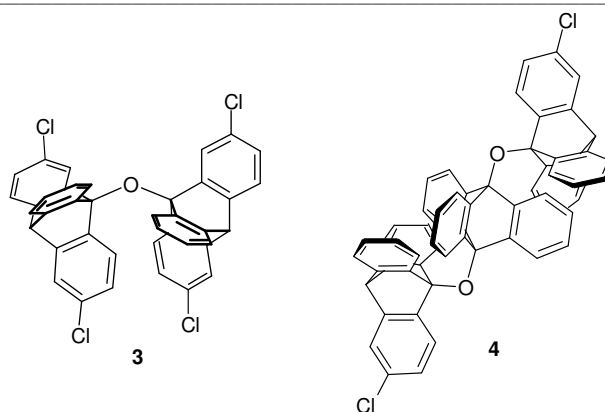
## 1.2 Covalently Bonded Molecular Systems with Rotating Parts.

### 1.2.1 Molecular propellers and gears.

The consideration of the restriction of thermal motion in chemistry first arose in regard to a fundamental question of molecular stereochemistry.<sup>8a</sup> The rotational triple energy minima about C-C single bonds follows directly from the tetrahedral geometry of saturated carbon centres, yet it was not proven experimentally until 1936.<sup>8b</sup> These studies inspired the first molecular analogues of macroscopic machine parts: propellers (**1** and **2**)<sup>9</sup> and gears. A combination of NMR spectroscopy and X-ray crystallography provided evidence that the aromatic rings are tilted in the same direction relative to the reference plane in an arrangement similar to the blades of a propeller.



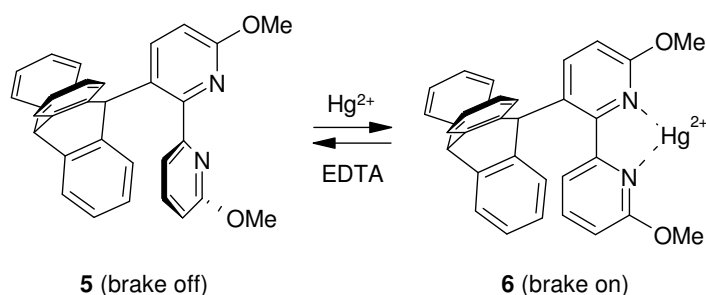
The concept of the interdependent motion of aryl units in molecular propellers has been exploited in the design of a new class of molecules presenting restricted internal motion, the molecular “bevel gears”. These molecules present two or more tightly intermeshed rotating units arranged in such way that the rotation of these groups are mutually dependent. An example of this phenomenon is **3**, which consists of two bridged triptycene groups in which the rotational movement of one of the units induces the concerted motion of the second one as the two units are interdigitated.<sup>10a</sup> A combination of  $^1H$  and  $^{13}C$  NMR spectroscopy quantified the energy barrier of the “gear rotation” of the triptycyl unit as  $8 \text{ kcal mol}^{-1}$ , whereas molecular modelling showed a much higher value,  $30\text{--}40 \text{ kcal mol}^{-1}$  for the uncorrelated rotation of the tridentate unit, referred to a “gear slippage”.



The concept of a double connected bevel gear has been implemented by the synthesis of **4**, which consists of three triptycyl units.<sup>10b</sup> In this system the rotation of the two external non-directly connected triptycyl groups is mutually influenced and the concerted rotational motion made possible by the presence of the central bridging triptycyl group.<sup>11</sup>

### 1.2.2 Controlling rotational motion: a molecular brake.

In the molecular rotors mentioned so far the interdependent rotational motion of the triptycyl units is powered by the thermal energy of the system and thus uncontrolled. Kelly and co-workers attempted to overcome this limitation by synthesising a “molecular brake”.<sup>12</sup> The molecule **5** is a triptycyl derivative covalently connected to a chelating 2,2'-bipyridine unit (Scheme 1.1). The rapid rotation around the carbon-carbon bond connecting the two units is demonstrated by the presence in the <sup>1</sup>H NMR at 30 °C of four distinct signals for the aromatic protons of the triptycyl unit (*brake off*).

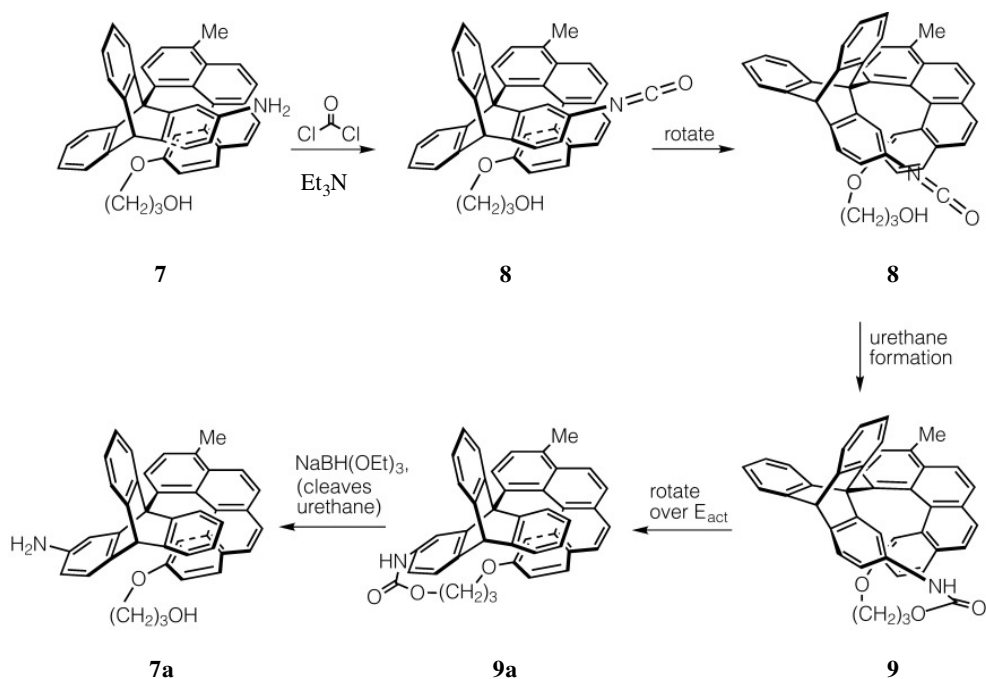


**Scheme 1.1** The “molecular brake” is controlled through the complexation-decomplexation of the bipyridine unit.

Treatment of **5** with  $\text{Hg}^{2+}$  affords a new molecular species **6** where the metal cation is coordinated to the two pyridine nitrogens. This chelation aligns the two pyridine units and results in “blocking” of the rotation of the triptycyl unit as confirmed by the non equivalence of some of its aromatic protons at  $-30\text{ }^{\circ}\text{C}$  (*brake on*). At  $30\text{ }^{\circ}\text{C}$  however the protons of the triptycene coalesce in a broad signal indicating that the steric hindrance of the pyridyl group is not sufficient to stop the spontaneous rotation of the triptycene and slipping of the brake is occurring. The original demetallated species **5** can be restored by adding EDTA to **6** proving the reversibility of the system.

### 1.2.3 A chemically powered unidirectional rotor.

In order to generate a chemical rotor that exhibits unidirectional motion, the design of the molecular brake **5** was modified. The 2,2'-bipyridine group was replaced by a [4]helicene unit functionalised with a hydroxypropyl group whereas the triptycyl unit was functionalised with an amine, to obtain the molecular rotor **7** (Scheme 1.2).<sup>13</sup>



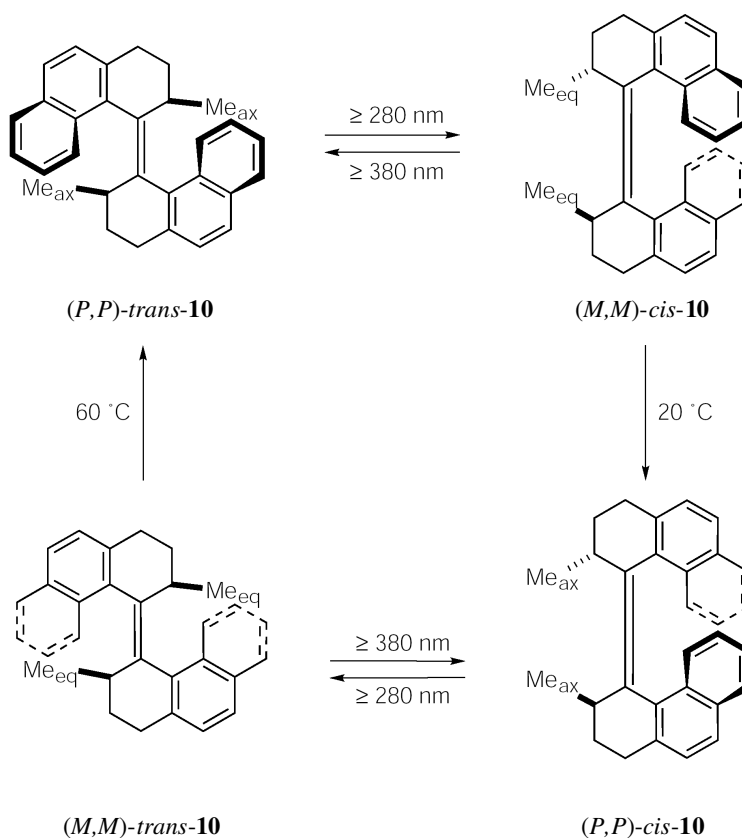
**Scheme 1.2** Sequence of the  $120^{\circ}$  unidirectional rotation of a chemically powered rotor **7**.

Treatment of **7** with  $\text{COCl}_2$  and  $\text{Et}_3\text{N}$  gives the isocyanate **8** which once formed can react intramolecularly with the hydroxyalkyl group of the helicene affording the

urethane **9** in a highly strained conformation. Compound **9** then rotates around the single bond connecting the helicene to the triptycyl unit forming the isomer **9a** and thus releasing the strain. Finally cleavage of the urethane with H<sub>2</sub>O affords the compound **7a** in a conformation which is different from its isomer **7**. This new conformation is obtained as result of a unidirectional 120° rotation promoted by the formation and breaking of a covalent bond.

#### 1.2.4 The first 360° unidirectional rotation about a double bond.

Feringa and co-workers reported the first example of molecular motor displaying repetitive and controlled 360° unidirectional motion around an alkene bond in response to photonic and thermal stimuli (Scheme 1.3).<sup>14</sup>



**Scheme 1.3** The 360° unidirectional rotation is achieved in a four-step process involving alternate isomerisation of double bond and thermal interconversion of helicity.

The system is constituted of two tetrahydrophenanthrene units covalently connected by a carbon-carbon double bond.<sup>15</sup> Each of the two phenanthrene groups, due to steric reasons, can adopt a right-handed (*P*) or a left-handed (*M*) helicity, distorting the expected planarity imposed by the double bond. The four step rotation is achieved by an initial irradiation at  $\lambda \geq 280$  nm at  $-55$  °C of (*P,P*)-*trans*-**10** to obtain the (*M,M*)-*cis*-**10** isomer. Interconversion of helicity, while maintaining the *Z* configuration, is achieved by heating the solution of (*M,M*)-*cis*-**10** at  $20$  °C generating the thermodynamically more stable (*P,P*)-*cis*-**10** isomer bearing the two methylene groups in a less sterically demanding axial position. A further  $180^\circ$  rotation is obtained by *Z*→*E* isomerisation at  $\lambda \geq 280$  nm to afford (*M,M*)-*trans*-**10** whose helicity can be inverted by heating the solution at  $60$  °C to obtain the original (*P,P*)-*trans*-**10** isomer, the most thermodynamically stable of all four isomers of the cycle, where the methylene substituents are, once again, adopting a more stable equatorial orientation. The overall process can be monitored by following the changes in the absorption intensity of circularly polarised light at 217 nm.

Control over the speed of the unidirectional rotation in molecular rotors has been achieved by synthesising a series of overcrowded alkenes, **11a-11i**.<sup>16</sup> Changing the nature of the heteroatoms X and Y modifies the energy barrier of the helical inversion, the rate-determining step of the unidirectional rotation (Figure 1.1). The speed of the thermal inversion of helicity changes up by a factor of 400 from **11f** to **11g**.

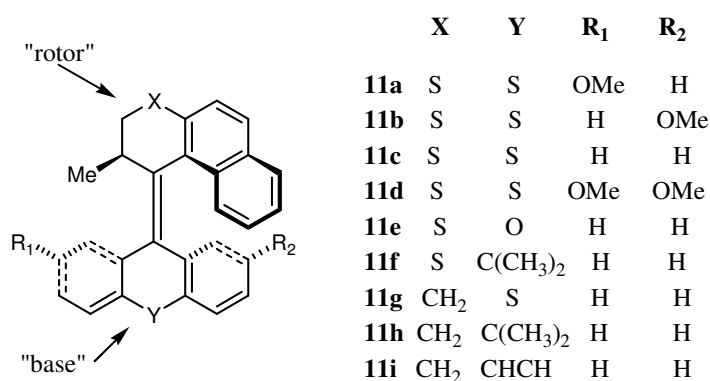


**Figure 1.1** Second generation of light-driven unidirectional rotor **11a-11i**.

The construction of stimuli-responsive molecular species that could lead to changes in some of the macroscopic properties of a system is one of the major endeavours in contemporary science. Recently, Feringa and co-workers demonstrated that if the molecular rotor *(P,P)*-**trans-10** is doped into a nematic liquid crystal film and irradiated at  $\lambda \geq 280$  nm, the demonstrated unidirectional rotation of the molecular rotor induces a rearrangement of the mesogenic molecules which leads to a gradual change in the colour of the doped film from purple to red after only 80 seconds of irradiation (Figure 1.2).<sup>17</sup> The colour of the mesogenic film can be finely tuned by changing parameters such as irradiation time, wavelength used or light intensity.

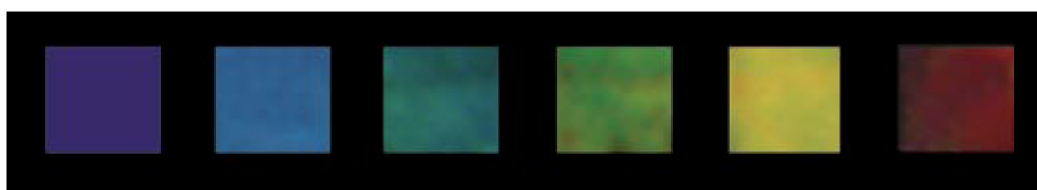


**Figure 1.2** Colours of a molecular rotor doped liquid crystal phase, starting from pure *(P,P)*-**trans-10** (far left) upon irradiation at  $\lambda > 280$  nm at room temperature, until an irradiation time of 80 s (far right).

### 1.2.5 Reversible, 360° unidirectional rotation about a single bond.

In 2005 Feringa and co-workers have realized a reversible unidirectional rotary motor fuelled by chemical energy<sup>18</sup>. The system works by stereoselective ring-opening and ring-closing of a biaryl-lactone to direct rotation about a single bond (Figure 1.3a). The molecule consists of upper phenyl rotor half (green and blue) connected to a lower naphthyl stator (red) by a single carbon-carbon bond (black) which acts as the axis of rotation. The rotary cycle involves four chemical transformations each one generates directional rotation of 90° around the biaryl bond and four intermediates (A-D, Figure 1.3b). Lactones **12** and **14** exist as racemic mixtures as a result of a low barrier for small amplitude rotations around the aryl-aryl bond. In states A and C the rotor and stator are locked by the presence of a lactone unit (covalent linkage); in states B and D rotation is restricted because of steric interactions of the *ortho* substituents on the aryl rings between the two halves



of the system (red and green/blue). These forms are configurationally stable. The rotation relies on stereospecific cleavage of the covalent linkages in steps (i) and (iii), then regiospecific formation of covalent linkages in steps (ii) and (iv). The four chemical transformations involved are: i) Stereoselective reduction with (*S*)-CBS with high enantioselectivity (96.8:3.2 and 90.3:9.7 starting from **12** and **14**, respectively) and high preference to move in a clockwise direction ((*R*)-CBS could be used to invert the sense of rotation in a counterclockwise direction). The resulting phenolic alcohol is protected with an allyl group and the alcohols **13a** and **15a** are oxidized to the acids **13b** and **15b**. ii) Chemoselective PMB removal resulting in spontaneous lactonization. iii) Stereoselective reduction with (*S*)-CBS then PMB protection. iv) Chemoselective allyl removal resulting in spontaneous lactonization.

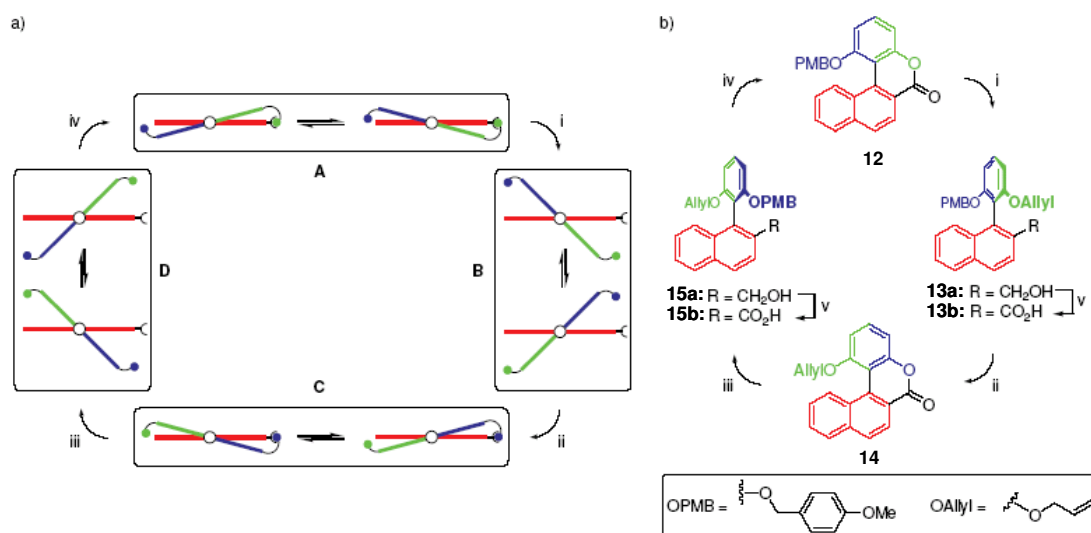


**Figure 1.3** a) Cartoon representation of unidirectional rotation around a single bond. b) Structure and chemical transformations of a unidirectional rotor.

The whole reaction sequence generates a net  $360^\circ$  rotation of the rotor about the stator in clockwise or anticlockwise direction depending exclusively of the choice of chemical reagents, respectively (*S*)-CBS or (*R*)-CBS asymmetric catalysts.

## 1.3 Molecular Level Devices with Mechanically-Bonded Shuttling Parts.

### 1.3.1 Catenanes and rotaxanes.

Catenanes and Rotaxanes are both examples of interlocked molecules.<sup>19</sup>

They consist of two or more separate components mechanically linked to each other, but not connected by chemical bonds – resulting in a *mechanical bond* which prevents dissociation without cleavage of one or more covalent bonds.<sup>20</sup> Thanks to their interlocked architecture catenanes and rotaxanes are ideal candidates for the manipulation and control of submolecular motion and the development of molecular machinery. In these structures<sup>20</sup> the mechanical bond restricts the relative degrees of freedom of the components in space while permitting a relatively large amplitude of motion along certain directions (Figure 1.4).

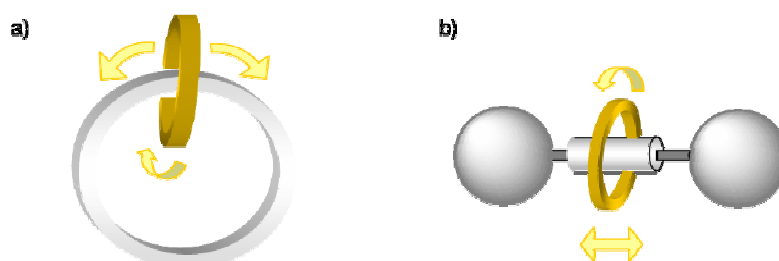


**Figure 1.4** Cartoon representing the topology of a) a [2]catenane and b) a [2]rotaxane. The components can move one relative to the other by large-amplitude movements: “pirouetting” and “shuttling”.

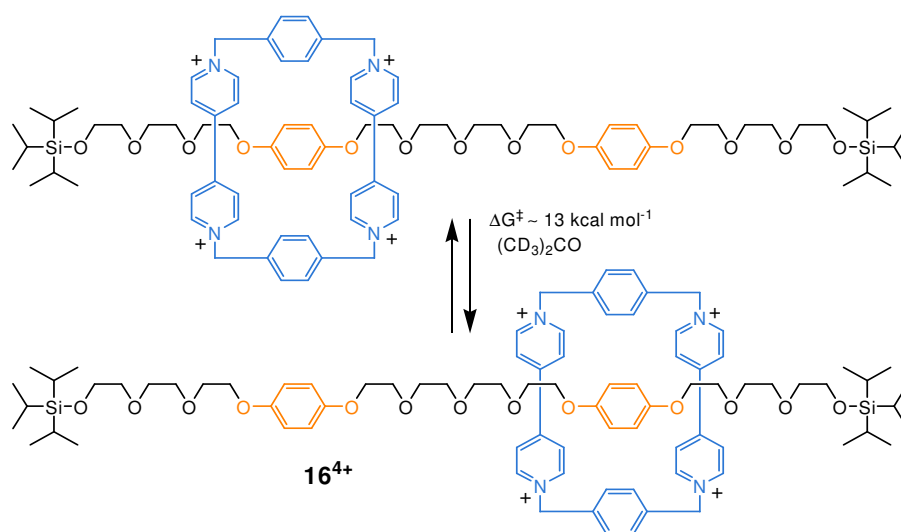
A catenane, from the Latin *catena*, meaning chain, is a molecular species formed by two, or more, interlocked macrocycles which can be separated only by breaking one or more covalent bonds. Instead a rotaxane, from the Latin *rota* and *axis* meaning respectively wheel and axle, consists of one or more a macrocycles mechanically prevented from dethreading from a linear unit by bulky “stoppers”<sup>19</sup>.

### 1.3.2 Rotaxane-based molecular shuttles.

In rotaxanes the thread usually consists of one or more binding sites for the ring called “stations”. If two or more stations are present on a thread with a traversable path between them the rotaxane can be considered a ‘molecular shuttle’ in which the ring is incessantly and randomly moving on, off or between them through Brownian motion. The shuttling movement of the ring is constricted to one dimension by the linear thread, a situation in many ways analogous to the restriction of movement imposed on biological motors (e.g. kinesin, myosin, ion pumps) by a track.<sup>21</sup>

#### 1.3.2.1 Degenerate molecular shuttles.

The first example of molecular shuttling behaviour in a rotaxane was reported by Stoddart and co-workers in 1991 (Scheme 1.4).<sup>22</sup>



**Scheme 1.4** The first “molecular shuttle”  $16^{4+}$ .

The rotaxane  $16^{4+}$  consists of a  $\pi$ -electron poor tetracationic cyclophane mechanically interlocked onto a linear thread containing two isoenergetic  $\pi$ -electron rich hydroquinone stations separated by a polyether spacer. Since the two stations are identical, the macrocycle shuttles back and forth between the two isoenergetic, and thus equally occupied, stations in a temperature-dependent fashion.

A [2]rotaxane containing two degenerate and well-separated stations on its thread can be considered as the simplest example to study the shuttling phenomenon.

For the shuttling to take place the macrocycle needs first to escape the forces exerted through non-covalent binding interactions at one station and then to move to the other where new interactions will form. The resulting free energy profile for the shuttling (simplified in Figure 1.5) will be a combination of two main components: i) the energy required to break the non-covalent interactions holding it to the station and ii) the distance required to achieve the other station.

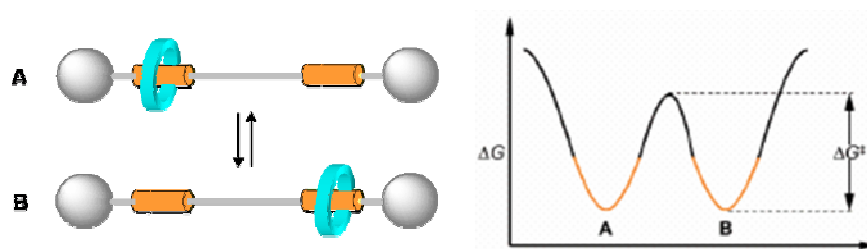


**Figure 1.5** Idealized free energy profile for the shuttling in a degenerate molecular shuttle.

From here we can deduce that temperature and environmental factors with disrupting effects on the interactions in the recognition sites will enhance the shuttling rate. The effects of hydrogen-bond-disrupting solvents as  $[D_6]$ DMSO or  $[D_4]$ methanol on hydrogen bonds has been proved in studies on peptide-based molecular shuttles in which the two glycylglycine stations are separated by aliphatic linkers.<sup>22b</sup>

The effect of the temperature on the shuttling rate can be better understood in terms of kinetic energy of the macrocycle. Lets consider the thread portion of the molecule as a machine which moves a particle, the macrocycle, along a one-dimensional potential energy (rather than free energy  $\Delta G$ ) surface. At temperature,  $T$ , the macrocycle – like all molecular-level particles – possesses translational kinetic energy  $\frac{1}{2}mv^2$  equal to  $\frac{1}{2}k_B T$  per degree of freedom (where  $k_B$  is the Boltzmann constant) which allows it to escape from the energy wells located at each station and explore the full length of the thread. The graphic below (Figure 1.6) gives a physical representation of the energy  $\Delta E^{act}$  required from the macrocycle to escape the forces exerted by non-covalent interactions as a function of its position on the thread (while the free energy  $\Delta G$  includes also the distance-dependent contribution). The gradient

of the line is maximum when the macrocycle is near to the stations and zero when it is on the thread between them, where all attractive non-covalent interactions are broken.

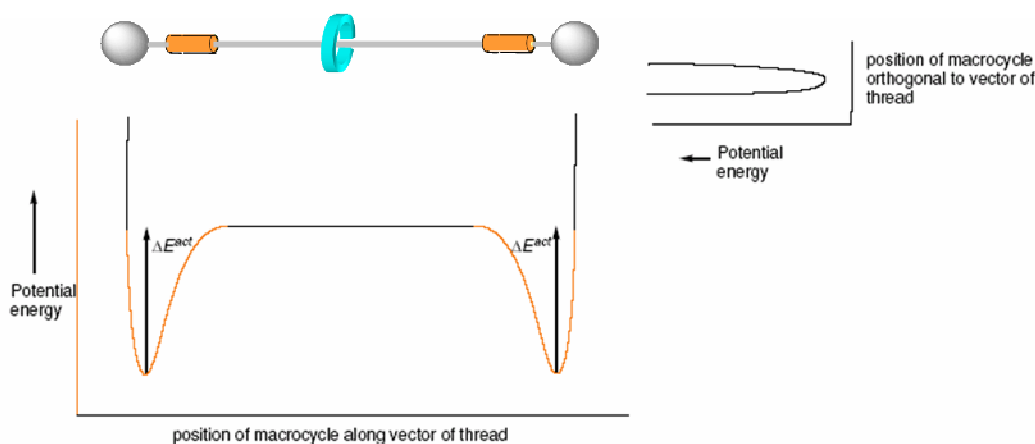


**Figure 1.6** Idealized potential energy of the macrocycle in a degenerate molecular shuttle.

Although the rate of shuttling can be regulated by temperature, solvent composition or binding events, even for a molecular shuttle with two different stations, at equilibrium no net task can be performed by these movements.

This is a consequence of the “Principle of Detailed Balance”<sup>23</sup> which states that at equilibrium transitions between any two states take place in either direction at the same rate so that no net flux is generated. However if the system is pushed out of equilibrium so that detailed balance is broken, net work can be done by the fluxional exchange process when the system returns spontaneously toward equilibrium. The requirement for the detailed balance to be broken is the first key to doing mechanical work and it represents the starting point in the design of molecular-level machines that operate with Brownian motion.

From here generations of “stimuli-responsive molecular shuttles” have been developed, where an external stimulus is applied to break the detailed balance and change the net location of the macrocycle on the thread (i.e., the statistical distribution of the ring between the stations). The use of an external trigger provides a greater level of positional control over the machine and allows a variety of tasks to be performed. With the topics discussed in the next chapters in mind, I found it more

appropriate to describe these systems from the point of view of their general systematic behaviour rather than provide a list of examples from the literature, divided according to the kind of stimulus used (light<sup>24</sup>, heat<sup>25</sup>, electrons<sup>26</sup>, chemical<sup>27</sup>, pH<sup>28</sup>, binding events<sup>29</sup>, etc.).

### 1.3.2.2 Stimuli-responsive molecular shuttles: a physical description.

In a stimuli-responsive molecular shuttle (Figure 1.7) the stations (orange **B** and blue **A'**) have different binding affinities for the macrocycle so that it resides preferentially over the station that provides the best stabilisation energy, i.e. highest  $\Delta E^{\text{act}}$  in the potential energy profile (Figure 1.8).

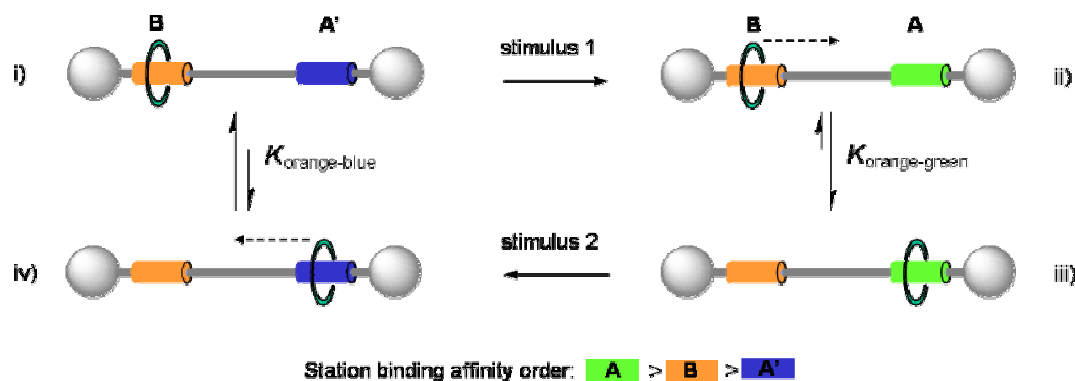


**Figure 1.7** Translational motion in a stimuli-responsive molecular shuttle.

At equilibrium the macrocycles populate the different stations and the thread according to a Boltzmann distribution (Eq. 1), which depends on the energies of the various co-conformations and the temperature. For a single molecule, the populations correspond to the amount of time the macrocycle spends on each site.

$$\frac{P_B}{P_{A'}} = \exp\left(-\frac{(\Delta E_B - \Delta E_{A'})}{k_B T}\right) \quad \text{where } \Delta E_B > \Delta E_{A'} \quad (1)$$

When an external stimulus 1 is applied to chemically modify the system, in order to increase the binding affinity for the initially less favourite station (blue station **A'** →

green station A), the difference in activation energies is reversed and the green station now becomes energetically more favoured ( $\Delta E_{A \text{ to } B}^{\text{act}} > \Delta E_{B \text{ to } A/A'}^{\text{act}}$ ).

This ultimately results in the shuttling of the macrocycle to the new green station A (Figure 1.8). Applying a second stimulus 2 restores the original state and closes one cycle of shuttling motion which may be achieved also by destabilising the binding affinity for the initially preferred site. It is important to remark that in both cases the role of the external input is not to induce directional motion per se. As we discussed before the macrocycle is continuously moving on, off and between the two stations, it just spends more time on the station with higher binding. The stimulus is rather used to alter the structure and binding affinity of one of the stations for the macrocycle and therefore put the system out of co-conformational equilibrium<sup>30</sup>, (i.e. to break the initial detailed balance). The net directional transport of the macrocycle occurs via biased Brownian motion from the relaxation of the system towards the new energy minimum allowing the new co-conformational equilibrium to be restored.

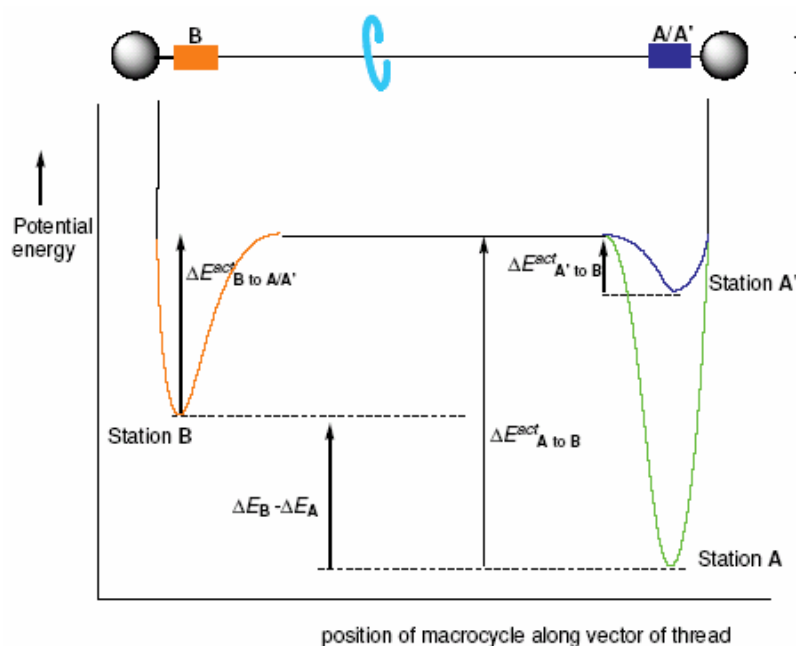


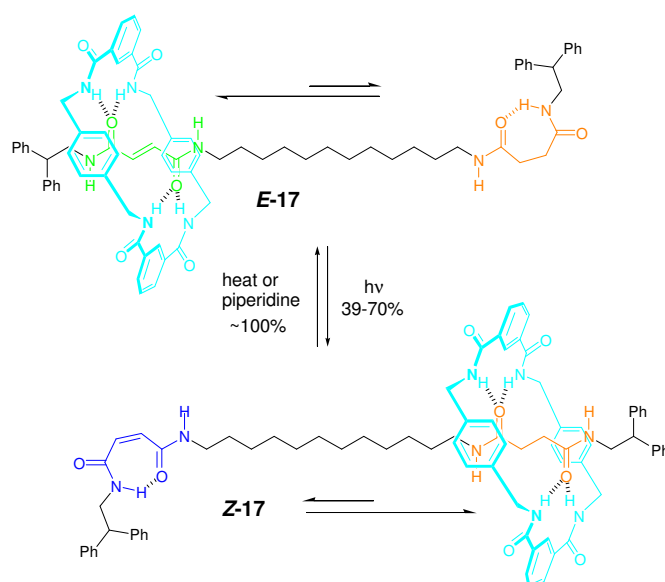
**Figure 1.8** Idealized potential energy profile of the macrocycle in a stimuli-responsive molecular shuttle.

In other words when the detailed balance is broken the system moves spontaneously towards equilibrium with a net flux that *can* be used to do work. However, as we

have mentioned in section 1.1.2, can a simple stimuli-responsive molecular shuttle be considered a “motor”? Does it really perform any mechanical work and if it does, how is such a task performed? In the next pages we will go into the systematic behaviour of a classic stimuli-responsive molecular shuttle giving a mechanical, chemical and physical description of its performance<sup>31</sup>.

### 1.3.2.3 Reversible molecular switches.

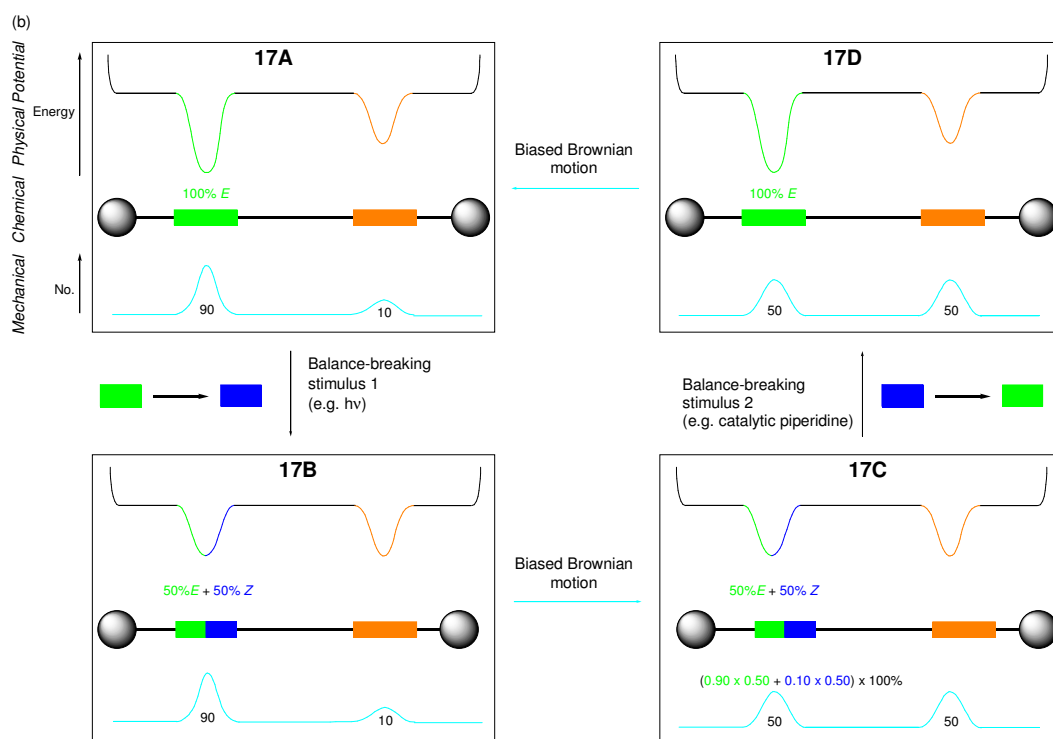
Consider a typical light-switchable amide-based molecular shuttle *E/Z* **17**, developed a few years ago by Leigh and co-workers<sup>24j</sup>. It consists of a succinamide (orange) and isomerizable fumaramide/maleamide (green/dark blue) stations – and a substrate (the ring, light blue, Scheme 1.5). Rather than considering this system as a single molecule that changes when light is shone, we can think of stimuli-responsive molecular shuttle as a machine – the thread - that directionally transports a particle - the macrocycle- between the two stations (compartments) on a one-dimensional potential energy surface. The relevance of this approach is that we can consider both thread and macrocycle existing in more than one state/position and we can represent the performance of the machine at each stage in terms of chemical structure (fraction of olefin geometrical isomers), average potential energy surface of the thread and statistical distribution of the macrocycle along the thread (Scheme 1.6)<sup>31</sup>



**Scheme 1.5** Example of light-switchable stimuli-responsive molecular shuttle **17**.<sup>24j</sup>



In Scheme 1.6 we assume the photostationary state is 50:50 *E*:*Z*, the natural balanced distribution of the ring between fumaramide (green) and succinamide (orange) stations is 95:5 and between maleamide (blue) and succinamide 5:95. The initial state of the system is statistically balanced (**17A**) according to the Boltzmann distribution. When the balance breaking stimulus (i.e. irradiation at 312 nm) is applied 50% of *E* isomerizes to *Z* putting the system temporarily out of equilibrium (**17B**) since the maleamide binds the ring more weakly than the fumaramide. The system acts to restore the balance and by a thermally activated relaxation step the macrocycle moves through biased Brownian motion to the succinamide station, which is now energetically more favoured (**17C**). Net displacement of the substrate has occurred. However, when a second balance-breaking stimulus (e.g. catalytic piperidine) is applied to reset the machine, the macrocycle moves back to the green station again, *undoing* the previous transportation task (**17D**).



**Scheme 1.6** “Machine-performance representation” of the forward (**17A**→**17C**) and backward (**17C**→**17A**) operations of the machine-substrate system **17**.

In other words at each stage the average position of the particle is dependent on the state of the machine (the thread) so that the transport is undone every time the machine is reset. All the stimuli-responsive molecular shuttles where the task performance is influenced by the state of the system have been called “molecular switches” to be distinguished from “molecular motors” (where the system is influenced as function of its trajectory).

Most of the systems developed thus far make use of a variety of stimuli<sup>24-29</sup> and some of them can perform useful tasks like fluorescence switching<sup>32a-f</sup>, conductivity of solid-state electronic junctions<sup>32h-k</sup>, conductivity at electrode interfaces<sup>32l-o</sup>, exertion of a mechanical force on a macroscopic object<sup>32p-q</sup>, macroscopic transport of a droplet of liquid across a surface.<sup>32s</sup> However despite their highest level of sophistication all these systems basically work in the same way as illustrated in Scheme 1.6 and so they still remain molecular switches and not motors.

## 1.4 Compartmentalizing molecular machines.

As discussed above, in rotaxane-based molecular switches the net transport of the macrocycle is reversibly undone every time the machine is reset. Looking at their design we can appreciate the reason for this behaviour: at each stage the particle is free to dynamically exchange between the two stations. In order to make the transport irreversible in one direction, the substrate should be prevented from moving backward in the resetting stage. This would require the presence of a controllable and temporary barrier to enable the disconnection of the two binding sites at various stages during the operation – creating a so-called “compartmentalized” molecular machine<sup>31</sup>. The idea of compartmentalizing systems that work with Brownian particles has been previously discussed by several illustrious physicists through a number of celebrated “thought machines”.<sup>34-38</sup> In the next pages I have reported the most significant examples of such machines (recently discussed in the literature<sup>7, 31</sup>) with the intention of highlighting the concepts and guidelines that they can provide us with in terms of harnessing Brownian motion in synthetic molecular-level machines that are only now becoming accessible through modern synthetic

chemistry. The design of these “thought machines” has inspired the development of “compartmentalized molecular-machines”<sup>31, 33</sup>, much more sophisticated in terms of task performance than simple switches. In order to better introduce the contents discussed in the following chapters, I will go more in to the description of the “Maxwell’s Demon” thought experiment that has, in part, inspired this PhD work.

#### 1.4.1 The two-compartment Brownian motion ‘thought machines’.

The concept of Brownian “thought machines” dates back to the middle 19<sup>th</sup> century, when the Second Law of Thermodynamics was first formulated and then carefully analyzed. In 1856, following Carnot’s earlier observations, Clausius phrased the Second Law as “*Heat can never pass from a colder to a warmer body without some other change, connected therewith, occurring at the same time*”.<sup>34</sup>

Modern textbook formulations specify that the “other change” in question was implicit to be the performance of external work on the system. Many physicists in those years had proposed sophisticated “thought machines” in order to show the limitations of the Second Law. The first provocation came from James Clerk Maxwell<sup>35</sup>, the famous Scottish physicist and father of statistical mechanics. Along with Boltzmann he had been investigating the relationship between particle energy and heat and he played a major role in developing the kinetic theory of gasses.

##### 1.4.1.1 Maxwell’s Demon.

The point to be stressed in Clausius’ definition of the Second Law was the universality of the statement, signalled for example by the word “never” in the quotation. It was here that Maxwell chose to “pick a hole” when, in 1867, he wrote a letter to his friend and colleague Peter Tait<sup>36a</sup> to claim the limitation and the statistical nature of the Second Law. His dissertation was introduced to the public audience in 1871 in his book “*Theory of Heat*” where, in the section called “Limitation of the Second Law of Thermodynamics” he wrote one of the most discussed quotations in physics:

“...One of the of the best established facts in thermodynamics is that it is impossible in a system enclosed in a envelope which permits neither change of volume nor passage of heat, and in which both the temperature and the pressure are everywhere the same, to produce any inequality of temperature or of pressure without the expenditure of work. This is the Second Law of Thermodynamics, and it is undoubtedly true as long as we can deal with bodies only in mass, and have no power of perceiving or handling the separate molecules of which they are made up. But if we conceive a being whose faculties are so sharpened that he can follow every molecule in its course, such a being....

... would be able to do what at present is impossible for us”.

In his “thought experiment” Maxwell imagined a vessel with two compartments (labelled L and R in Figure 1.9) filled with gas at uniform temperature, separated by a controllable door (Figure 1.9 a). A “being” (that Thomson later called “Maxwell’s Demon”<sup>37</sup>) sits on the door, looks at the oncoming gas molecules and, depending of their speed, it opens the door to collect only hot molecules (faster than the average) from R to L and only cold molecules (slower than average) from L to R. In this way the demon establishes a temperature difference between two compartments that, for example, could be used to drive a thermal engine. In other words the demon could convert (without expenditure of work as he carries out all the operations slowly) the thermal energy of molecules at equilibrium into useful work in contradiction with the Second Law. Maxwell later applied the same principle to a simpler system where a “pressure demon”<sup>36c</sup> could sort molecules only depending of their direction of approach (from L to R) and not their speed, which would require less information to operate than the original temperature demon (Figure 1.9 b). Although Thomson’s nomenclature of “demon” was not intended as malicious, but rather as a supernatural creature between god and human (from the Greek *daemon*), Maxwell’s specification of the demon was vague enough to leave considerable room for wrong interpretation by successive investigators. The experiment has been viewed by some as an attempt to construct a perpetual motion machine that can continually extract work from the thermal bath.

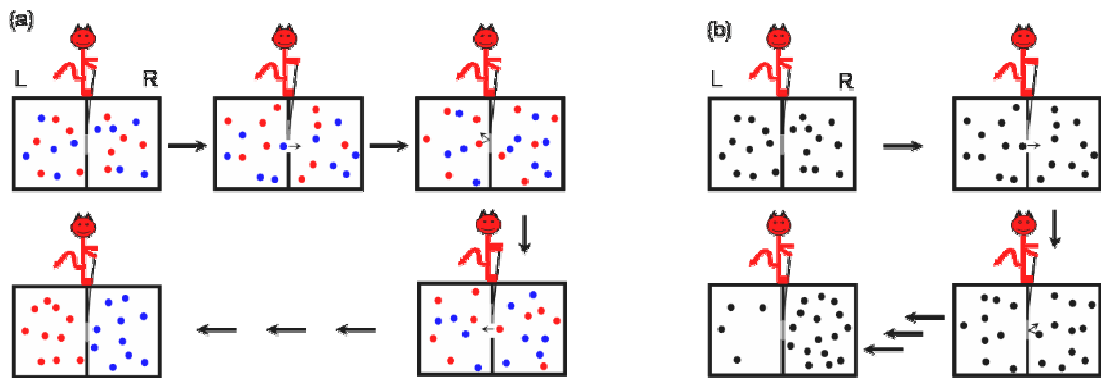


**Figure 1.9** Cartoon representation of (a) Maxwell's "temperature demon"<sup>36a, b</sup> and (b) Maxwellian "pressure demon"<sup>36c</sup>.

On the other hand, motivated by the purpose of exorcising Maxwell's demon (i.e. determining what part of the process must be dissipative in order to satisfy the Second Law), generations of physicists including Szilard, Rothstein, Brillouin, Gabor, Lloyd etc. have deeply investigated the connection between entropy and information, creating the foundations of modern information theory, thermodynamics of computation, quantum measurements and cybernetic theory.<sup>35</sup> A remarkable achievement was reached by Landauer in 1961, when he discovered that memory erasure in computers feeds entropy to the environment. Erasing one bit of information produces  $kT \log 2$  joules of heat, where  $T$  is the absolute temperature and  $k$  is Boltzmann's constant, a concept known as "Landauer's Principle"<sup>38</sup>. This result inspired Bennett's observation (1982)<sup>39</sup> that nullified the demon paradox: the essential irreversible act which prevents the demon from violating the second law, is not the measurement itself (the demon begin by registering the state of the system about the particle's position, which uses one bit of storage) but rather the *erasure of* that bit to reset the system in preparation for next measurement and close a thermodynamic cycle.

It is important to appreciate how those linkages and applications make Maxwell's demon strongly entrenched in the entire scientific literature and culture.

### 1.4.1.2 Szilard's Engine.

In 1929 Leo Szilard wrote a paper<sup>40</sup> where for the first time he tried to establish a quantitative connection between entropy and information, earlier envisaged by Maxwell and Thomson only in terms of the fact that the demon required “intelligence”.

Szilard proposed a “pressure demon”-based machine where he tried to utilize the pressure exerted on a piston by one Brownian particle to do work. He realized that the demon's operation can be reduced to a simple computational process consisting of the detection of the particle, the information gathering about its position, memorizing the information acquired and then acting upon it (Figure 1.10). In doing so Szilard discovered the idea of a “bit” of information (the term “bit” or binary digit, was suggested almost 15 years later by John Tukey), now central in computer science.

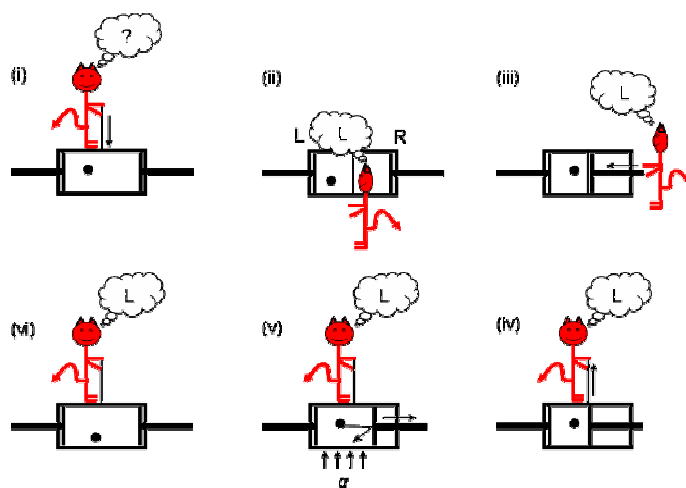


**Figure 1.10** Cartoon representation of the “pressure-demon” based Szilard’s Engine.

The cylinder has a piston at either end. Initially the molecule wanders freely in the apparatus and the demon doesn’t know where the molecule is (i). He randomly inserts a frictionless partition dividing the container into two compartments and trapping the molecule in one compartment. The demon then performs a measurement to learn about the position of the molecule (ii). Now he is able to move the appropriate piston into position (iii) in order to be able to extract work from the system when the partition is removed (iv). The molecule can expand against the

piston, doing work against any attached load (v). Heat must be drawn from the surroundings in order to replenish the energy used by the gas and maintain a constant temperature. Crucially, however, to complete the thermodynamic cycle and reset the machine, the demon's memory of where the particle was must finally be erased (vi).

### 1.4.1.3 Smoluchowski's Trapdoor.

In 1912 Marian von Smoluchowski proposed the first version of an automatic (non-intelligent) mechanical demon<sup>41</sup>. He imagined a vessel with two gas-containing compartments separated by spring loaded trapdoor (in place of the demon). The trapdoor is a wholly mechanical device that is intended to open only when hit from the left but not from the right, allowing passage of molecules with a directionally-discriminating-behaviour (Figure 1.11).

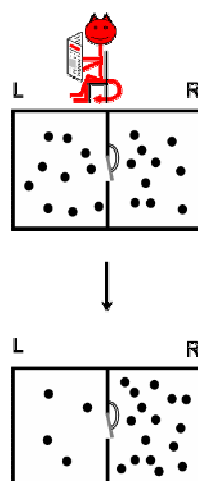


**Figure 1.11** Cartoon representation of Smoluchowski's Trapdoor.

However, if the door has no way of dissipating energy it will be at thermal equilibrium with its surroundings. This means it must spend much of its time open, unable to influence particle transport. Rarely, it will be closed when a particle approaches from the right and will open on collision with a particle coming from the left – doing its job as intended. Such events are balanced, however, by the door snapping shut on a particle from the right, pushing it into the left chamber. Overall,

the probability of a particle moving from left to right is equal to that for moving right to left and so the trapdoor cannot accomplish its intended function adiabatically.

#### 1.4.1.4 Feynman's Ratchet-and-Pawl.

In his *Lectures on Physics* (1963) Richard Feynman proposed his thought experiment, a miniature Brownian ratchet-and-pawl<sup>38</sup>, as an illustration of the Second Law.

The device (Figure 1.12) consists of a gear with asymmetric teeth and a pawl, a little arm that jams the gear and prevents it from turning backward. The gear is connected by an axle to a propeller surrounded by a gas at temperature  $T_1$ , while the ratchet-and-pawl system is held at temperature  $T_2$ . Can the random bombardment of the gas molecules hitting the propeller bring a net unidirectional motion of the gear?

Feynman showed that only if  $T_1 > T_2$  does the system rectify thermal motions and is therefore able to do work, for example lifting a hypothetical load. However, for the gear to keep moving, an external means must maintain this temperature difference and replenish the heat dissipated during the rotation (note that the machine, therefore, does not violate the Second Law). In the absence of an external heat source, when the two compartments come to equilibrium, i.e.  $T_1 = T_2$ , the system cannot extract any more energy from the thermal bath to do work (as in Smoluchowski's Trapdoor).

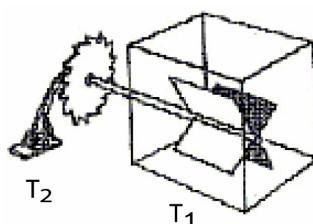


**Figure 1.12** Feynman's Ratchet-and-Pawl.

Feynman's Brownian ratchet represents the first example of a plausible mechanism for a molecular motor, whereby the random Brownian motion is harness and rectified in one net direction<sup>39</sup>.



### 1.4.2. Brownian ratchet molecular motors.

Over the past several years scientists have tried to understand how molecular motors can be so efficient in converting chemical energy, barely more powerful of the surrounding thermal noise, into kinetic energy. In contrast, artificial macroscopic machines operate at energies much higher than the thermal noise. The development of new technologies to manipulate molecules and to identify tiny movements and forces has led the suggestion that many biological motors work by principles similar to Feynman's Brownian ratchet as biological rectifiers. Ion pumps for example can drive ions through a cell membrane in one direction only, against a natural electrochemical potential. The Brownian ratchet model has recently helped in understanding the stochastic nature of important biological transports such as Kinesin, Myosin, ion channels previously explained by long-held deterministically theories. Kinesin is a dimeric motor protein that walks along a microtubule to transport organelles, mRNA and signalling molecules within the cell. Only recently has it been proposed that the kinesin walks with a "hand-over-hand"<sup>44</sup> mechanism (rather than with an "inchworm" movement) whereby the ATP hydrolysis serves as a "switching mechanism" to only push the molecule forward making the backward step virtually irreversible, allowing to rectify transport in one direction. Myosin motion along the actin filament is crucial to the functioning of muscle contraction. Although it is still not clear how exactly the ATP transforms the random Brownian motion into forward movement, recent studies have established that the myosin head moves stochastically with regular steps of 5.3 nanometres, not just forward but also backward and with multiple jumps.<sup>45</sup> This is in contradiction with the previous long-held deterministic theory by which the molecule of myosin changes shape when it cleaves a molecule of ATP and pulls the actin filament along by a single step.

Inspired by the wish to explain the working mechanism of such and more complex biological motors, by Feynman's ratchet-and-pawl principle and by the design of the previous celebrated "thought machines" chemists have started to re-visit the question of how to transport a Brownian particle between two distinguishable sites. The new perspective however is not to test the Second Law in an adiabatic system as in the thought machines, but rather to see how the Brownian ratchet principle could be

applied in a working molecular-level machine and what outcomes can be achieved in the performance of the transportation task. Numerous mathematical models and formal mechanisms based on nonequilibrium statistical mechanics have been developed by theoretical physicists to explain how the directional transport of Brownian particles can occur from periodic changes in a potential energy surface<sup>46</sup>. These mechanisms include different types of theoretical Brownian ratchet like energy ratchets, information ratchets, flashing ratchets and rocking ratchets<sup>47</sup>.

Only now modern synthetic chemistry has reached a point where we can consider investigating such mechanisms at the molecular level in artificial systems and we can make molecules whereby the positional displacement of the substrate occurs by Brownian motion between two defined locations. Rotaxane and catenanes are ideal candidates for doing this because 1) they can be thought of in terms of a machine – the thread - that directionally transports a particle - the macrocycle- between the two stations (compartments) on a one-dimensional potential energy surface, 2) they are also reasonably synthetically accessible.

If we analyze the design and behaviour of the previous “thought machines” we can deduce how underlying a Brownian ratchet mechanism are three main components (the first two of which were implied in the working mechanism of stimuli-responsive molecular shuttles): (i) a randomizing element, given by a Brownian particle that moves under thermal motion, (ii) the use of an external source of energy not to generate unidirectional motion per se but rather to continually or cyclically drive the system away from equilibrium and to avoid falling foul of the Second Law, and (iii) asymmetry in the dimension in which the motion occurs, intended to allow movement in only one direction and not the other (see Maxwell’s demon, Smoluchowski’s trapdoor and Feynman’s ratchet-and-pawl).

#### **1.4.2.1 Compartmentalizing synthetic molecular-level machines.**

It is not a coincidence that all thought machines used a kind of controllable door or a ratchet device to disconnect the two compartments at various stages during their operation and obtain net particle transportation thermodynamically uphill. Indeed the compartmentalization is the key element missing from the past generation of stimuli-

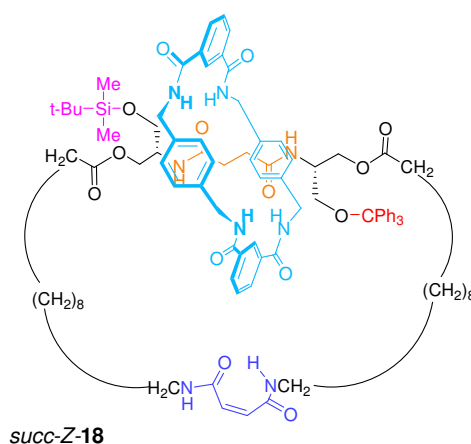
responsive molecular shuttles whereby the transport of the macrocycle was only resulting from moving energetically downhill and the unidirectionality of the motion was reversibly undone at the resetting stage of the machine (see sections 1.3.2.3. and 1.4.).

Starting from this consideration chemists have recently started to revise the design of previous generations of molecular shuttles by introducing controllable barriers between the stations, resulting in compartmentalized molecular machines.

Remarkable results have been achieved from the studies of such systems and although this entire introduction has thus far focused solely on rotaxane-based molecular shuttles, the work of Leigh, Hernández and Kay on a reversible synthetic rotary molecular motor<sup>33</sup>, the first example of a compartmentalized molecular-level machine, deserves to be an exception to that rule.

#### 1.4.2.2 A reversible synthetic rotary molecular motor

In 2004 Leigh and co-workers reported catenane **18** (Scheme 1.7) whereby the small ring can move clockwise or anti-clockwise between the two stations with two routes, each of which can be independently blocked by two bulky stoppers.<sup>33</sup> The physical principles behind the transport mechanism are the same that occur in a typical stimuli-responsive molecular shuttle but with the addition of control over kinetics.



**Scheme 1.7** Chemical structure of a compartmentalized [2]catenane **18** that works as a reversible rotary molecular motor.

We can better follow the operation of the machine by using a cartoon illustration of the structure of the [2]catenane **18** and the potential energy surface diagram of the small ring along the bigger one (Figure 1.13 A and B). The succinamide station is shown in orange, maleamide in blue and fumaramide in green. The coloured spheres represent the two bulky stoppers: TBDMS-group in violet and trityl-group in red. The net change in position of the smaller ring is achieved by the combination of two kind of chemical transformation which alter the potential energy surface in different ways: (i) balance-breaking reactions (isomerization  $E \rightarrow Z$  or  $Z \rightarrow E$  of the olefin) to switch on/off the binding affinity of this station for the macrocycle and (ii) linking/unlinking reactions to modulate the rate of exchange between the stations along two different pathways.

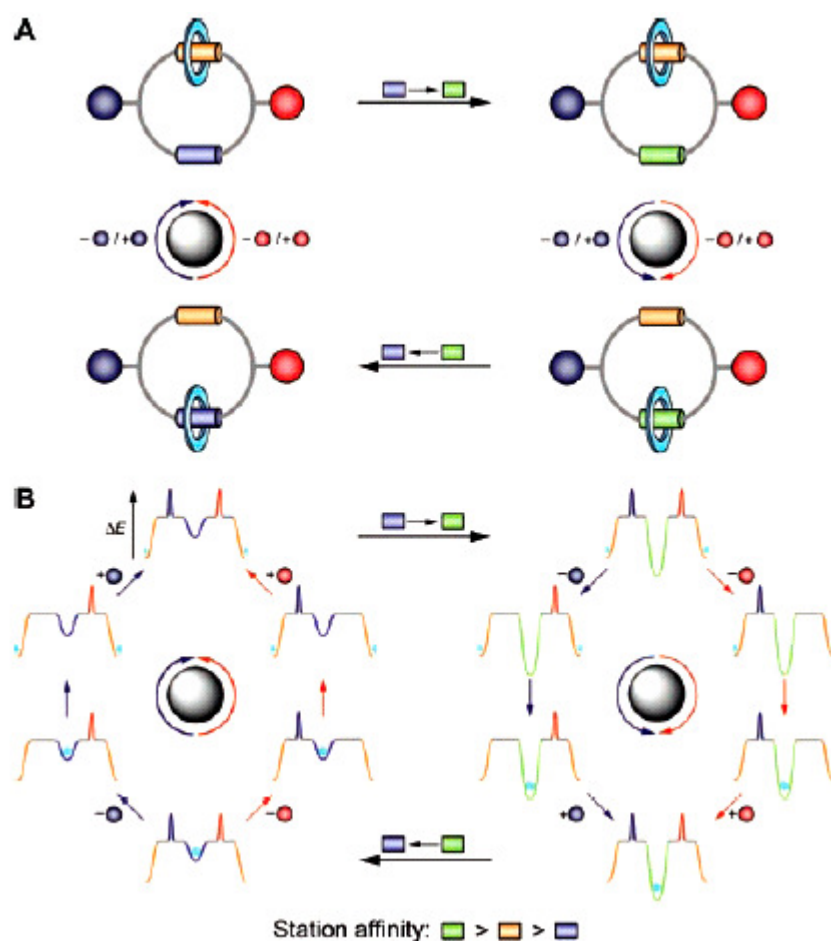


**Figure 1.13** (A) Schematic illustration and (B) potential energy surface of the small ring in a [2]catenane rotary molecular motor.

Initially the small macrocycle is sitting on the succinamide station (orange). Catalytic piperidine (balance-breaking stimulus) provokes isomerization of the maleamide into fumaramide ( $Z \rightarrow E$ ) producing the green station which is energetically more favourable for the macrocycle. Deprotection of TBDMS-group (linking stimulus) lowers the kinetic barrier between the stations, so that the macrocycle is free to exchange and redistributes itself according to the new Boltzmann distribution by moving in an anti-clockwise direction to the green station. Resilylation restores the barrier (unlinking stimulus) and ratchets the transported quantity on the green station. Reisomerization of fumaramide into maleamide ( $E \rightarrow Z$ ) by UV light makes the orange station energetically more favourable (external energy input, balance-breaking stimulus). The Trityl-group is removed and the ring moves in an anti-clockwise direction because the TBDMS-stopper prevents it from going backward. Re-tritylation resets the machine and completes a net unidirectional circumrotation of the small ring about the larger one. A clockwise rotation can be obtained by exchanging the order of the protecting-deprotecting steps. As a consequence of the ratcheting mechanism exploited by the use of the two barriers, the transportation task is not undone on the resetting machine and the system can cyclically use chemical energy to do work, unlike in the previous generations of molecular switches (1.3.2. and 1.4). Although unidirectional rotary motors were previously developed in the past by the groups of Kelly<sup>13</sup>, Feringa<sup>14-17</sup> and Leigh<sup>43c</sup>, those systems could only rotate in one direction but not the other. The [2]catenane **18** represents the first example of an artificial molecular motor able to rotate in either direction, like  $F_1F_0$ -ATPase. Importantly in this system we can precisely identify what the working mechanism is. The [2]catenane **18** works by a particular type of energy ratchet named *flashing ratchet* where a Brownian particle is moved along an oscillating potential energy surface by sequentially raising and lowering each set of minima and maxima. Underlying the task performance of such Brownian ratchet or motor is the opportunity, given by the compartmentalization of the machine, to separately control (i) the thermodynamics and impetus for the net transport (balance-breaking reactions) and (ii) the ability to exchange and ratchet the substrate by lowering and raising kinetic barriers (linking/unlinking reactions).

### 1.4.2.3 A compartmentalized stimuli-responsive molecular shuttle.

The outcomes of exploiting a ratcheting mechanism in compartmentalized molecular machines were later discussed by Leigh, Kay and Chatterjee<sup>31</sup>. They started off by breaking down the behaviour of a classic stimuli-responsive molecular shuttle into chemical, physical and statistical descriptions in order to show that it can only act as a reversible molecular switch (section 1.3.2.3, Scheme 1.6) It therefore became apparent that in order to exploit a ratcheting mechanism, and be able to pump the substrate energetically uphill irreversibly, control over the kinetics for substrate transport also had to be introduced into the conventional molecular shuttle design.

Rotaxane **19** contains a fumaramide station (green) which can be isomerised to maleamide (blue) with UV light, a succinamide station (orange) and a TBDMS bulky group as a removable partition between the two binding sites (Figure 1.14).

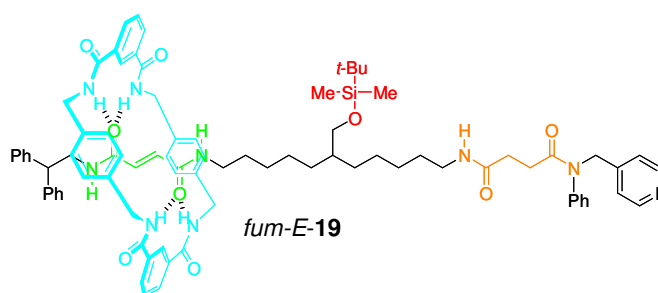
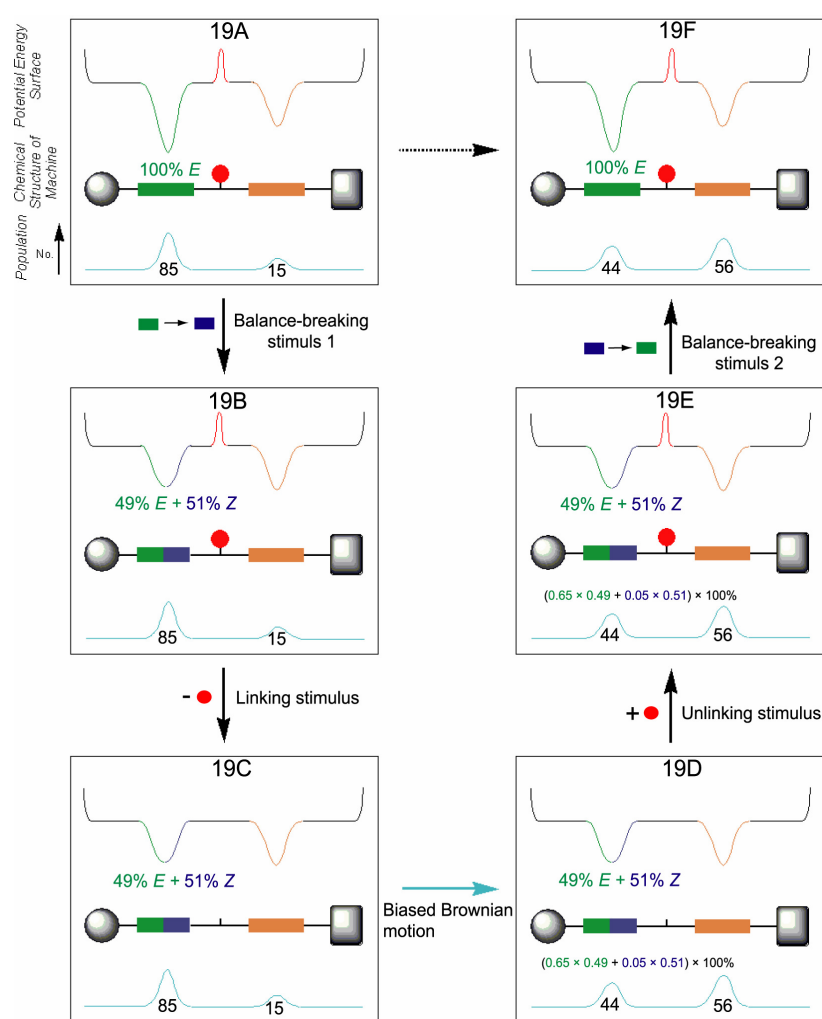


**Figure 1.14** Chemical structure of a compartmentalized stimuli-responsive molecular shuttle.

Similar to catenane **18** the machine can transport a substrate energetically uphill using the energy of the photon, via the olefin isomerization reactions in conjunction with the control over kinetics provided by the silyl ether. Four different stimuli are applied to govern in turn the thermodynamics and the kinetics for transport between the two stations: (i) irradiation at 312 nm (balance-breaking 1); (ii) removal of the barrier (linking); (iii) restoration of the barrier (unlinking), (iii) isomerization (balance-breaking 2). Therefore for a machine to do work repetitively two kinds of control are required<sup>33</sup>: a balance-breaking reaction to provoke an imbalance in the statistical distribution of a quantity (the thermodynamic impetus for the net transport); a linking/unlinking reaction to modulate the exchange of the substrate

between the two stations (kinetic control). Separating the two stations by the imposition of a barrier (i.e. to “compartmentalize” the machine) “ratchets” a net amount of macrocycle in one direction, allowing this task to be repetitively performed without reversing each transportation sequence. Ratcheting also allows the directional release of the substrate when the barrier is lowered; a property known as “escapement”.<sup>31, 33</sup> The machine-performance of rotaxane **19** has been represented in terms of the chemical structure, average potential energy surface of the thread and statistical distribution of the macrocycle along the thread (Scheme 1.8). The system starts statistically balanced and unlinked (**19A**).



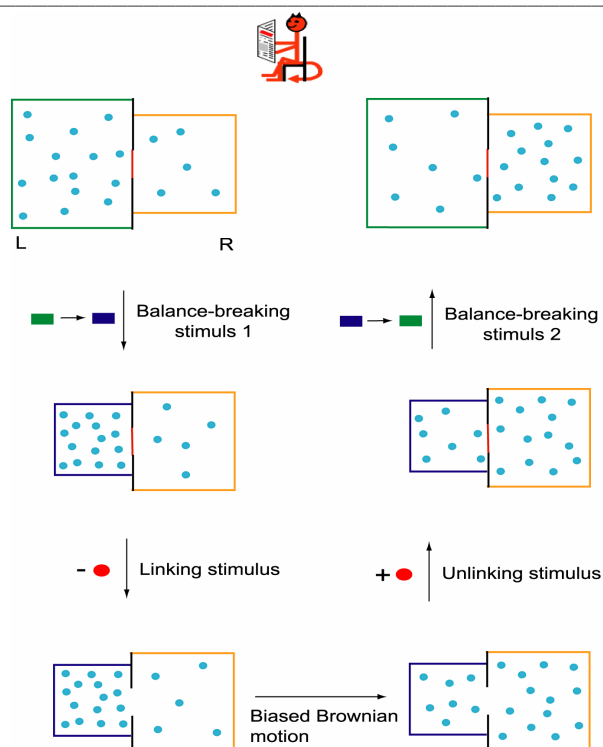
**Scheme 1.8** “Machine-performance” representation of a compartmentalized [2]rotaxane that acts as molecular energy ratchet.

A UV light irradiation isomerises the fumaramide station into maleamide (49:51 *E:Z*) creating the impetus for the net transport and making the system unbalanced but still unlinked (**19B**). Removal of the barrier allows the ring to exchange between the two stations, a property known as “escapement”. The system is now unbalanced and linked (**19C**). The ring moves to equilibrium by Brownian motion redistributing itself according to the new relative station binding affinities and making the system balanced and linked (**19D**). Raising the barrier ratchets the transported quantity; the system is balanced and unlinked (**19E**). Reisomerisation returns the thread to its initial chemical state but the barrier makes the transport irreversible in one direction preventing the ring from moving backward and the machine can be reset without undoing the task. The resulting system is unbalanced and unlinked (**19F**)

Through its operation rotaxane **19** establishes a thermodynamically unfavourable concentration gradient of macrocycles between the two compartments, exactly the function envisaged for the Maxwell’s pressure demon. Comparing the operation of **19** to a Maxwell’s demon like device (Scheme 1.9), however, shows that this result is achieved in very different ways by the two machines. In Scheme 1.9 the colours of the compartments, particles, and door correspond to those of **19**. The system is initially balanced; the Brownian particles are distributed between left (L) and right (R) in proportion to the sizes of the two compartments. A change in volume of the left-hand compartment makes the system statistically unbalanced. Opening the door allows the particles to redistribute themselves according to the new size ratio of the compartments. Closing the door ratchets the new distribution of particles. Resetting the machine to its original size then results in a concentration gradient of the Brownian particles across the two compartments.

As we can see, unlike in Maxwell’s pressure demon design, during the operation of **19** the position of the particle does not determine when or whether the door is open. Rotaxane **19** operates by an “energy ratchet”<sup>48, 33</sup> mechanism whereby the energy minima and maxima of the potential energy surface are varied irrespective of the particle’s location and therefore there is no role for an information-gathering mechanism.





**Scheme 1.9** Cartoon illustration of system **19** in terms of Maxwell's pressure demon design.

It is possible, however, to construct an alternative mechanism which *does* involve the communication of information regarding a Brownian particle's position to the machine. In such a mechanism the energy maxima (kinetic barriers to motion) would change according to the position of the particle in order to produce directed motion of the substrate. The remainder of this thesis concerns the design, synthesis and operation of a rotaxane-based molecular shuttle which is the first example of synthetic molecular that operates via an information ratchet mechanism in which the knowledge of a particle's position is used to control its transport away from equilibrium<sup>7, 48</sup>.

## 1.5 Summary

Nature uses molecular-sized motors and machines in virtually every important biological process and their extraordinary success is inspiring scientists to try to create synthetic devices that mimic the function of these amazing natural systems. However, it is far from obvious to see how to design such machines because mechanical behaviour at the molecular level, where everything is constantly moving under kinetic energy supplied by the heat of the surroundings and being buffeted by other atoms and molecules (Brownian motion), is very different to that which we observe in our everyday world.

Thanks to their interlocked architecture catenanes and rotaxanes are ideal candidates for use as molecular devices where translational movement is required. However despite their highest level of sophistication and the ability for some of them to perform useful tasks<sup>32</sup> all these systems remain simple two-state switches, the most basic and functionally limited type of machine mechanism<sup>49</sup> in which the ring distribution is always at, or relaxing towards, equilibrium so that the net transport of the substrate is reversibly undone every time the machine is reset. In contrast, biological motors and machines are able to drive chemical systems away from equilibrium.<sup>50</sup> Only few synthetic molecular machines have been made that can claim to do that.<sup>13a,14,18,31,33,43c</sup> Yet, although these structures are relatively diverse (they do not all use rotaxane architectures, for example), they all use similar mechanistic principles in their operation. In terms of catenanes and rotaxanes a step changing towards more sophisticated systems have been recently made by the Leigh group with the creation of “compartmentalized molecular-machines”, where variable kinetic barriers are inserted between the stations. In these systems an *energy input* controls the *thermodynamics* of the substrate motion providing the essential *driving force* for repeated net change in position (breaking ‘detailed balance’), while the presence of a controllable and temporary barrier controls the *kinetics* of the transport allowing driving the system away from equilibrium (energy ratchet mechanism), just like in the famous “thought machines”. The latest nanomachine developed during this PhD work, inspired by Maxwell’s Demon, operates using a new and entirely

different type of mechanism that involves *information* transfer between the substrate and the molecular machine (information ratchet mechanism).

## 1.6 References and notes

1. R. P. Feynman, *Saturday Rev.* **1960**, *43*, 47-54
2. For reviews about artificial molecular machines see: a) V. Balzani, A. Credi, F. M. Raymo, J. F. Stoddart, *Angew. Chem. Int. Ed. Engl.* **2000**, *39*, 3348-3391. b) J.-P. Sauvage *Molecular Machines and Motors*; Ed. Struct. Bonding (Berlin) **2001**, *99*.
3. a) R. Brown, *Philos. Mag.* **1828**, *4*, 171 – 173; b) R. Brown, *Edinb. New Philos. J.* **1828**, *5*, 358 – 371; c) R. Brown, *Philos. Mag.* **1829**, *6*, 161 – 166; Brown's accounts of these investigations are also reprinted in d) R. Brown in *The Miscellaneous Botanical Works of Robert Brown, Vol. 1* (Ed.: J. J. Bennett), Ray Society, London, **1866**, pp. 463 – 486; for a modern reconstruction of the original experiments, see: e) B. J. Ford, *Microscope* **1992**, *40*, 235 – 241.
4. A. Einstein, *Ann. Phys.* **1905**, *17*, 549 – 560; reprinted in *Einstein's Annalen Papers: The Complete Collection 1901– 1922* (Ed.: J. Renn), Wiley-VCH, Weinheim, **2005**, pp. 182 – 193.
5. J. Perrin, *Atoms* (English Translation: D. L. Hammick), 2<sup>nd</sup> English ed., Constable & Co., London, **1923**.
6. R. D. Astumian, *Sci. Am.*, July 2001, 57-64.
7. E. R. Kay, D. A. Leigh, F. Zerbetto, *Angew. Chem. Int. Ed.* **2007**, *46*, 72-191.
8. a) E. L. Eliel, S. H. Wilen, *Stereochemistry of Organic Compounds*, Wiley-Interscience, New York, **1994**. b) J. D. Kemp, K. S. Pitzer, *J. Chem. Phys.* **1936**, *4*, 749.
9. For examples of two- and three- blades propellers see: a) D. Gust, K. Mislow, *J. Am. Chem. Soc.* **1973**, *95*, 1535-1547. b) P. Finocchiaro, D. Gust, K. Mislow, *J. Am. Chem. Soc.* **1974**, *96*, 3198-3205. c) P. Finocchiaro, D. Gust, K. Mislow, *Top. Curr. Chem.* **1974**, *47*, 1-28. d) R. Glaser, J. F. Blount, K. Mislow, *J. Am. Chem. Soc.* **1980**, *102*, 277-278. e) S. E. Biali, D. A. Nugiel, Z. Rappoport, *J. Am. Chem. Soc.* **1989**, *111*, 846-847.
10. a) K. Mislow, *Acc. Chem. Res.* **1976**, *9*, 26-33. b) H. Iwamura, *J. Mol. Struct.* **1985**, *126*, 401-412.

11. For other examples of molecular bevel gears see: a) W. D. Hounshell, C. A. Johnson, A. Guenzi, F. Cozzi, K. Mislow, *Proc. Natl. Acad. Sci. USA* **1980**, 77, 6961-6973. b) F. Cozzi, A. Guenzi, C. A. Johnson, K. Mislow, W. D. Hounshell, J. F. Blount, *J. Am. Chem. Soc.* **1981**, 103, 957-960. c) C. A. Johnson, A. Guenzi, K. Mislow, *J. Am. Chem. Soc.* **1981**, 103, 6240-6244. d) N. Koga, Y. Kawada, H. Iwamura, *J. Am. Chem. Soc.* **1983**, 105, 5498-5502 e) Y. Kawada, H. Iwamura, *J. Am. Chem. Soc.* **1981**, 103, 958-962. f) H. Iwamura, T. Ito, H. Ito, K. Toriumi, Y. Kawada, E. Osawa, T. Fujiyoshi, C. Jaime, *J. Am. Chem. Soc.* **1984**, 106, 4712-4721.
12. T. R. Kelly, K. V. Bowyer, K. V. Bhaskar, A. Bebbington, A. Garcia, F. Lang, M. H. Kim, M. P. Jette, *J. Am. Chem. Soc.* **1994**, 116, 3657-3658.
13. a) T. R. Kelly, H. De Silva, R. A. Silva, *Nature*, **1999**, 401, 150-152. b) T. R. Kelly, H. De Silva, R. A. Silva, S. Jasmina, Y. J. Zhao, *J. Am. Chem. Soc.* **2000**, 122, 6935-6949.
14. N. Koumura, R. W. J. Zijlstra, R. A. van Delden, N. Harada, B. L. Feringa, *Nature*, **1999**, 401, 152-155.
15. N. Harada, N. Koumura, B. L. Feringa, *J. Am. Chem. Soc.* **1997**, 119, 7256-7264.
16. N. Koumura, E. M. Geertema, M. B. van Gelder, A. Meetsma, B. L. Feringa, *J. Am. Chem. Soc.* **2002**, 124, 5037-5051.
17. R. A. van Delden, N. Koumura, N. Harada, B. L. Feringa, *Proc. Natl. Acad. Sci. USA* **2002**, 99, 4945-4949.
18. Fletcher, S. P.; Dumur, F.; Pollard, M. M.; Feringa, B. L. *Science* **2005**, 310, 80-82.
19. a) G. Schill, *Catenanes, Rotaxanes and Knots*, Academic Press, New York, **1971**; b) D. M. Walba, *Tetrahedron* **1985**, 41, 3161 – 3212; c) D. B. Amabilino, J. F. Stoddart, *Chem. Rev.* **1995**, 95, 2725 – 2828; d) S. A. Nepogodiev, J. F. Stoddart, *Chem. Rev.* **1998**, 98, 1959 – 1976; e) D. A. Leigh, A. Murphy, *Chem. Ind.* **1999**, 178 – 183; f) G. A. Breault, C. A. Hunter, P. C. Mayers, *Tetrahedron* **1999**, 55, 5265 – 5293; g) *Molecular Catenanes Rotaxanes and Knots* (Eds.: J.-P. Sauvage, C. O. Dietrich- Buchecker), Wiley-VCH, Weinheim, **1999**.

20. a) V. Balzani, A. Credi, F. M. Raymo, J. F. Stoddart, *Angew. Chem.* **2000**, *112*, 3484-3530; *Angew. Chem. Int. Ed.* **2000**, *39*, 3348-3391; b) R. Ballardini, V. Balzani, A. Credi, M. T. Gandolfi, M. Venturi, *Acc. Chem. Res.* **2001**, **34**, 445-455; c) J.-P. Collin, C. Dietrich-Buchecker, P. Gavina, M. C. Jimenez-Molero and J.-P. Sauvage, *Acc. Chem. Res.*, **2001**, **34**, 447.
21. Myosin requires an actin track to move along: a) S. M. Block, *Cell* **1996**, *87*, 151 – 157; while kinesin progresses along the pathway provided by microtubule filaments: b) S. M. Block, *Cell* **1998**, *93*, 5 – 8; even ion pumps operate through precisely defined structural channels: c) J. C. Skou, *Angew. Chem.* **1998**, *110*, 2452 -2461; *Angew. Chem. Int. Ed.* **1998**, *37*, 2321 – 2328.
22. (a) Anelli, P. L.; Spencer, N.; Stoddart, J. F. *J. Am. Chem. Soc.* **1991**, *113*, 5131-5133. For the first example of an amide-based molecular shuttle see: (b) Lane, A. S.; Leigh, D. A.; Murphy, A. *J. Am. Chem. Soc.* **1997**, *119*, 11092-11093.
23. L. Onsager, *Phys. Rev.* **1931**, *37*, 405-426.
24. For examples of photochemically-responsive molecular shuttles see: (a) Benniston, A. C.; Harriman, A. *Angew. Chem. Int. Ed. Engl.* **1993**, *32*, 1459-1461. (b) Benniston, A. C.; Harriman, A.; Lynch, V. M. *Tetrahedron Lett.* **1994**, *35*, 1473-1476. (c) Benniston, A. C.; Harriman, A.; Lynch, V. M. *J. Am. Chem. Soc.* **1995**, *117*, 5275-5291. (d) Murakami, H.; Kawabuchi, A.; Kotoo, K.; Kunitake, M.; Nakashima, N. *J. Am. Chem. Soc.* **1997**, *119*, 7605-7606. (e) Armaroli, N.; Balzani, V.; Collin, J.-P.; Gaviña, P.; Sauvage, J.-P.; Ventura, B. *J. Am. Chem. Soc.* **1999**, *121*, 4397-4408. (f) Ashton, P. R.; Ballardini, R.; Balzani, V.; Credi, A.; Dress, K. R.; Ishow, E.; Kleverlaan, C. J.; Kocian, O.; Preece, J. A.; Spencer, N.; Stoddart, J. F.; Venturi, M.; Wenger, S. *Chem. Eur. J.* **2000**, *6*, 3558-3574. (g) Wurpel, G. W. H.; Brouwer, A. M.; van Stokkum, I. H. M.; Farran, A.; Leigh, D. A. *J. Am. Chem. Soc.* **2001**, *123*, 11327-11328. (h) Brouwer, A. M.; Frochot, C.; Gatti, F. G.; Leigh, D. A.; Mottier, L.; Paolucci, F.; Roffia, S.; Wurpel, G. W. H. *Science* **2001**, *291*, 2124-2128. (i) Stanier, C. A.; Alderman, S. J.; Claridge, T. D. W.; Anderson, H. L. *Angew. Chem. Int. Ed.* **2002**, *41*, 1769-1772. (j) Altieri, A.; Bottari, G.; Dehez, F.; Leigh, D. A.; Wong, J. K. Y.; Zerbetto, F. *Angew. Chem. Int. Ed.* **2003**, *42*, 2296-2300. (k)

- Abraham, W.; Grubert, L.; Grummt, U. W.; Buck, K. *Chem. Eur. J.* **2004**, *10*, 3562-3568.
25. For an example of entropy-driven shuttling see: Bottari, G.; Dehez, F.; Leigh, D. A.; Nash, P. J.; Pérez, E. M.; Wong, J. K. Y.; Zerbetto, F. *Angew. Chem. Int. Ed.* **2003**, *42*, 5886-5889.
26. For examples of electrochemically-responsive molecular shuttles see ref 23e and: (a) Bissell, R. A.; Córdova, E.; Kaifer, A. E.; Stoddart, J. F. *Nature* **1994**, *369*, 133-136. (b) Collin, J.-P.; Gaviña, P.; Sauvage, J.-P. *New J. Chem.* **1997**, 525-528. (c) Ballardini, R.; Balzani, V.; Dehaen, W.; Dell'Erba, A. E.; Raymo, F. M.; Stoddart, J. F.; Venturi, M. *Eur. J. Org. Chem.* **2000**, 591-602. (d) Ashton, P. R.; Ballardini, R.; Balzani, V.; Credi, A.; Dress, K. R.; Ishow, E.; Kleverlaan, C. J.; Kocian, O.; Preece, J. A.; Spencer, N.; Stoddart, J. F.; Venturi, M.; Wenger, S. *Chem. Eur. J.* **2000**, *6*, 3558-3574. (e) Altieri, A.; Gatti, F. G.; Kay, E. R.; Leigh, D. A.; Martel, D.; Paolucci, F.; Slawin, A. M. Z.; Wong, J. K. Y. *J. Am. Chem. Soc.* **2003**, *125*, 8644-8654. (f) Long, B.; Nikitin, K.; Fitzmaurice, D. *J. Am. Chem. Soc.* **2003**, *125*, 15490-15498. (g) Kihara, N.; Hashimoto, M.; Takata, T. *Org. Lett.* **2004**, *6*, 1693-1696. (h) Tseng, H.-R.; Vignon, S. A.; Celestre, P. C.; Perkins, J.; Jeppesen, J. O.; Di Fabio, A.; Ballardini, R.; Gandolfi, M. T.; Venturi, M.; Balzani, V.; Stoddart, J. F. *Chem. Eur. J.* **2004**, *10*, 155-172. (i) Flood, A. H.; Peters, A. J.; Vignon, S. A.; Steuerman, D. W.; Tseng, H.-R.; Kang, S.; Heath, J. R.; Stoddart, J. F. *Chem. Eur. J.* **2004**, *10*, 6558-6564. (j) Tseng, H.-R.; Wu, D. M.; Fang, N. X. L.; Zhang, X.; Stoddart, J. F. *ChemPhysChem* **2004**, *5*, 111-116. (k) Steuerman, D. W.; Tseng, H.-R.; Peters, A. J.; Flood, A. H.; Jeppesen, J. O.; Nielsen, K. A.; Stoddart, J. F.; Heath, J. R. *Angew. Chem. Int. Ed.* **2004**, *43*, 6486-6491. (l) Jeppesen, J. O.; Nygaard, S.; Vignon, S. A.; Stoddart, J. F. *Eur. J. Org. Chem.* **2005**, 196-220.
27. For examples of chemically-responsive molecular shuttles see ref 21b, 25h, 25l and: (a) Gong, C.; Gibson, H. W. *Angew. Chem., Int. Ed. Engl.* **1997**, *36*, 2331-2333. (b) Gong, C. G.; Glass, T. E.; Gibson, H. W. *Macromolecules* **1998**, *31*, 308-313. (c) Jiménez, M. C.; Dietrich-Buchecker, C.; Sauvage, J.-P. *Angew. Chem., Int. Ed.* **2000**, *39*, 3284-3287. (d) Lee, J. W.; Kim, K.; Kim, K. *Chem.*

- Commun.* **2001**, 1042-1043. (e) Jimenez-Molero, M. C.; Dietrich-Buchecker, C.; Sauvage, J.-P. *Chem. Eur. J.* **2002**, 8, 1456-1466. (f) Da Ross, T.; Guldi, D. M.; Farran Morales, A.; Leigh, D. A.; Prato, M.; Turco, R. *Org. Lett.* **2003**, 5, 689-691. (g) Tseng, H.-R.; Vignon, S. A.; Stoddart, J. F. *Angew. Chem. Int. Ed.* **2003**, 42, 1491-1495. (h) Laursen, B. W.; Nygaard, S.; Jeppesen, J. O.; Stoddart, J. F. *Org. Lett.* **2004**, 6, 4167-4170. (i) Huang, T. J.; Tseng, H.-R.; Sha, L.; Lu, W. X.; Brough, B.; Flood, A. H.; Yu, B.-D.; Celestre, P. C.; Chang, J. P.; Stoddart, J. F.; Ho, C.-M. *Nano Lett.* **2004**, 4, 2065-2071. (j) Leigh, D. A.; Pérez, E. M. *Chem. Commun.* **2004**, 2262-2263.
28. For examples of pH-responsive molecular shuttles see ref 25a and: (a) Martínez-Díaz, M.-V.; Spencer, N.; Stoddart, J. F. *Angew. Chem., Int. Ed. Engl.* **1997**, 36, 1904-1907. (b) Ashton, P. R.; Ballardini, R.; Balzani, V.; Baxter, I.; Credi, A.; Fyfe, M. C. T.; Gandolfi, M. T.; Gómez-López, M.; Martínez-Díaz, M.-V.; Piersanti, A.; Spencer, N.; Stoddart, J. F.; Venturi, M.; White, A. J. P.; Williams, D. J. *J. Am. Chem. Soc.* **1998**, 120, 11932-11942. (c) Elizarov, A. M.; Chiu, S.-H.; Stoddart, J. F. *J. Org. Chem.* **2002**, 67, 9175-9181. (d) Badjić, J. D.; Balzani, V.; Credi, A.; Silvi, S.; Stoddart, J. F. *Science* **2004**, 303, 1845-1849. (e) Keaveney, C. M.; Leigh, D. A. *Angew. Chem. Int. Ed.* **2004**, 43, 1222-1224.
29. For examples of molecular shuttles switched by alkali metal ion complexation, competitive binding or allosteric regulation, see: (a) Vignon, S. A.; Jarrosson, T.; Iijima, T.; Tseng, H.-R.; Sanders, J. K. M.; Stoddart, J. F. *J. Am. Chem. Soc.* **2004**, 126, 9884-9885. (b) Iijima, T.; Vignon, S. A.; Tseng, H.-R.; Jarrosson, T.; Sanders, J. K. M.; Marchioni, F.; Venturi, M.; Apostoli, E.; Balzani, V.; Stoddart, J. F. *Chem. Eur. J.* **2004**, 10, 6375-6392. (c) Marlin, D. S.; Gonzales, D.; Leigh, D. A.; Slawin, A. M. Z. *Angew. Chem. Int. Ed.* **2006**, 45, 1385-1390. (d) Marlin, D. S.; Gonzales, D.; Leigh, D. A.; Slawin, A. M. Z. *Angew. Chem. Int. Ed.* **2006**, 45, 77-83.
30. "Co-conformation" refers to the relative positions of the mechanically interlocked components with respect to each other, see: Fyfe, M. C. T.; Glink, P. T.; Menzer, S.; Stoddart, J. F.; White, A. J. P.; Williams, D. J. *Angew. Chem., Int. Ed. Engl.* **1997**, 36, 2068-2070.



31. M. N. Chatterjee, E R Kay, D. A. Leigh. *J. Am. Chem. Soc.* **2006**, *128*, 4058-4073.
32. Stimuli-induced shuttling has been used to control a number of different properties see: Fluorescence switching: (a) Pérez, E. M.; Dryden, D. T. F.; Leigh, D. A.; Teobaldi, G.; Zerbetto, F. *J. Am. Chem. Soc.* **2004**, *126*, 12210-12211. (b) Wang, Q.-C.; Qu, D.-H.; Ren, J.; Chen, K.; Tian, H. *Angew. Chem. Int. Ed.* **2004**, *43*, 2661-2665. (c) Qu, D.-H.; Wang, Q.-C.; Ren, J.; Tian, H. *Org. Lett.* **2004**, *6*, 2085-2088. (d) Qu, D. H.; Wang, Q. C.; Tian, H. *Mol. Cryst. Liq. Cryst.* **2005**, *430*, 59-65. (e) Leigh, D. A.; Morales, M. A. F.; Pérez, E. M.; Wong, J. K. Y.; Saiz, C. G.; Slawin, A. M. Z.; Carmichael, A. J.; Haddleton, D. M.; Brouwer, A. M.; Buma, W. J.; Wurpel, G. W. H.; León, S.; Zerbetto, F. *Angew. Chem. Int. Ed.* **2005**, *44*, 3062-3067. (f) Qu, D.-H.; Wang, Q.-C.; Tian, H. *Angew. Chem. Int. Ed.* **2005**, *44*, 5296-5299. Expression of chirality: (g) Bottari, G.; Leigh, D. A.; Pérez, E. M. *J. Am. Chem. Soc.* **2003**, *125*, 13360-13361. Conductivity of solid-state electronic junctions: (h) Collier, C. P.; Mattersteig, G.; Wong, E. W.; Luo, Y.; Beverly, K.; Sampaio, J.; Raymo, F. M.; Stoddart, J. F.; Heath, J. R. *Science* **2000**, *289*, 1172-1175. (i) Collier, C. P.; Jeppesen, J. O.; Luo, Y.; Perkins, J.; Wong, E. W.; Heath, J. R.; Stoddart, J. F. *J. Am. Chem. Soc.* **2001**, *123*, 12632-12641. (j) Luo, Y.; Collier, C. P.; Jeppesen, J. O.; Nielsen, K. A.; Delonno, E.; Ho, G.; Perkins, J.; Tseng, H.-R.; Yamamoto, T.; Stoddart, J. F.; Heath, J. R. *ChemPhysChem* **2002**, *3*, 519-525. (k) Diehl, M. R.; Steuerman, D. W.; Tseng, H.-R.; Vignon, S. A.; Star, A.; Celestre, P. C.; Stoddart, J. F.; Heath, J. R. *ChemPhysChem* **2003**, *4*, 1335-1339. Conductivity at electrode interfaces: (l) Willner, I.; Pardo-Yissar, V.; Katz, E.; Ranjit, K. T. *J. Electroanal. Chem.* **2001**, *497*, 172-177. (m) Sheeney-Haj-Ichia, L.; Willner, I. *J. Phys. Chem. B* **2002**, *106*, 13094-13097. (n) Katz, E.; Sheeney-Haj-Ichia, L.; Willner, I. *Angew. Chem. Int. Ed.* **2004**, *43*, 3292-3300. (o) Katz, E.; Lioubashevsky, O.; Willner, I. *J. Am. Chem. Soc.* **2004**, *126*, 15520-15532. Exertion of a mechanical force on a macroscopic object: (p) Huang, T. J.; Brough, B.; Ho, C.-M.; Liu, Y.; Flood, A. H.; Bonvallet, P. A.; Tseng, H.-R.; Stoddart, J. F.; Baller, M.; Magonov, S. *Appl. Phys. Lett.* **2004**, *85*, 5391-5393. (q) Liu, Y.; Flood, A. H.; Bonvallett, P. A.; Vignon, S. A.;

- Northrop, B. H.; Tseng, H.-R.; Jeppesen, J. O.; Huang, T. J.; Brough, B.; Baller, M.; Magonov, S.; Solares, S. D.; Goddard, W. A.; Ho, C.-M.; Stoddart, J. F. *J. Am. Chem. Soc.* **2005**, *127*, 9745-9759. Access to a nanopore: (r) Nguyen, T. D.; Tseng, H.-R.; Celestre, P. C.; Flood, A. H.; Liu, Y.; Stoddart, J. F.; Zink, J. I. *Proc. Natl. Acad. Sci. U.S.A.* **2005**, *102*, 10029-10034. Surface wettability: ref 32<sup>o</sup> and (s) Berná, J.; Leigh, D. A.; Lubomska, M.; Mendoza, S. M.; Pérez, E. M.; Rudolf, P.; Teobaldi, G.; Zerbetto, F. *Nature Mater.* **2005**, *4*, 704-710. The latter also demonstrates the macroscopic transport of a droplet of liquid across a surface using stimuli-responsive molecular shuttles.
33. Hernández, J. V.; Kay, E. R.; Leigh, D. A. *Science* **2004**, *306*, 1532-1537.
  34. R. Clausius, “On a Modified Form of the Second Theorem in the Mechanical Theory of Heat,” *Phil. Mag.* *12* (1856), 86.
  35. For reprints of key papers and commentary on some of the main issues regarding Maxwell’s demon, see: *Maxwell's Demon 2. Entropy, classical and quantum information, computing*; Leff, H. S. Rex, A. F., Eds.; Institute of Physics Publishing: Bristol, U.K., 2003.
  36. The first (a) private and (b) public written discussions of the ‘temperature demon’ were: (a) Maxwell, J. C. *Letter to P. G. Tait, 11 December 1867*. Quoted in Knott, C. G. *Life and Scientific Work of Peter Guthrie Tait*; Cambridge University Press: London, 1911; pp 213-214. (b) Maxwell, J. C. *Theory of Heat*; Longmans, Green and Co.: London, 1871; Chapter 12. (c) Maxwell introduced the idea of a ‘pressure demon’ in a later (undated) letter to Tait, also quoted in Knott, C. G. *Life and Scientific Work of Peter Guthrie Tait*; Cambridge University Press: London, 1911; pp 214-215 and ref (35). A pressure demon operates in a system linked to a constant-temperature reservoir with the sole effect of using energy transferred as heat from that reservoir to do work (see Szilard’s engine, Figure 1.10 and ref 40). This is in conflict with the Kelvin-Planck form of the Second Law, whereas the temperature demon challenges the Clausius definition.
  37. W. Thomson, *Nature* **1874**, *9*, 441-444.
  38. Landauer, R. 1961 Irreversibility and heat generation in the computing process. *IBM J Res. Develop.* **5**, 183-191.

39. Bennet, C. H., The thermodynamics of computation- a review, *Int. J. Theor. Phys.* **21**, 905-940 (1982); Bennet, C. H. and Landauer, R., The fundamental physical limits of computation, *Sci. Am.* **253**, 48-56 (July 1985); Bennet, C. H., Information physics in cartoons, *Superlattices and Microstructures* **23**, 367-372 (1998).
40. Szilard, L. *Z. f. Physik* **1929**, 53, 840-856.
41. von Smoluchowski, M. *Physik. Z.* **1912**, 13, 1069-1080.
42. Feynman, R. P.; Leighton, R. B.; Sands, M. *The Feynman Lectures on Physics*; Addison-Wesley: Reading, MA, 1963; Vol. 1, Chapter 46.
43. For the realization of Feynman's ratchet-and-pawl in molecular form see (a) Kelly, T. R.; Tellitu, I.; Sestelo, J. P. *Angew. Chem., Int. Ed. Engl.* **1997**, 36, 1866-1868. For non-adiabatic molecular versions which unidirectionally rotate (b) see ref 13<sup>a</sup>, (c) Leigh, D. A.; Wong, J. K. Y.; Dehez, F.; Zerbetto, F. *Nature* **2003**, 424, 174-179. (d) see ref. 33
44. A. Yildiz, M. Tomishige, R.D. Vale and P. R. Selvin, *Science*, **2004**, 303, 676-679.
45. K. Kitamura, M. Tokunaga, A. H. Iwane, T. Yanagida *Nature*, **1999**, 397, 129–134.
46. For an introduction to Brownian motors see: (a) Astumian, R. D. *Sci. Am.* **2001**, 285 (1), 56-64. (b) Astumian, R. D.; Hänggi, P. *Phys. Today* **2002**, 55 (11), 33-39.
47. For reviews of Brownian ratchet mechanisms see: (a) Hänggi, P.; Bartussek, R. In *Nonlinear Physics of Complex Systems – Current Status and Future Trends*; Parisi, J., Müller, S. C., Zimmermann, W., Eds.; Lecture Notes in Physics, Vol. 476; Springer: Berlin, 1996; pp 294-308. (b) Astumian, R. D. *Science* **1997**, 276, 917-922. (c) Jülicher, F.; Ajdari, A.; Prost, J. *Rev. Mod. Phys.* **1997**, 69, 1269-1281. (d) Special issue on 'The constructive role of noise in fluctuation driven transport and stochastic resonance' *Chaos* **1998**, 8, 533-664. (e) Reimann, P. *Phys. Rep.* **2002**, 361, 57-265. (f) Reimann, P.; Hänggi, P. *Appl. Phys. A* **2002**, 75, 169-178. (g) Parrondo, J. M. R.; De Cisneros, B. J. *Appl. Phys. A* **2002**, 75, 179-191. (h) Gabrys, B. J.; Pesz, K.; Bartkiewicz, S. J.

- 
- Physica A* **2004**, 336, 112-122. (i) Linke, H.; Downton, M. T.; Zuckermann, M. *J. Chaos* **2005**, 15, 026111.
48. a) Astumian, R. D.; Derényi, I. *Eur. Biophys. J.* **1998**, 27, 474-489; b) J. M. R. Parrondo, B. J. De Cisneros, *Appl. Phys. A* **2002**, 75, 179 – 191.
49. (a) E. R. Kay, D. A. Leigh *Nature* **2006**, 440, 286-287. (b) E. R. Kay, D. A. Leigh and F. Zerbetto *Angew. Chem. Int. Ed.* **2007**, 46, 72-191.
50. *Molecular Motors*; Schliwa, M., Ed.; Wiley-VCH, Weinheim, 2003.

## *Chapter Two*

## Exercising demons: How to drive a chemical system away from equilibrium

An abbreviated version of this chapter has been published as

“A molecular information ratchet”.

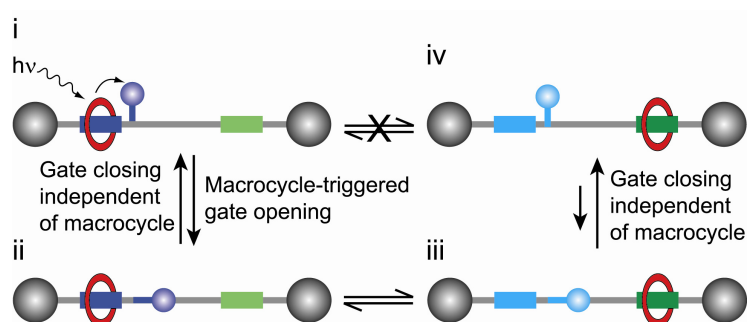
V. Serreli, C.-F. Lee, E. R. Kay and D.A. Leigh, *Nature* **445**, 523-527 (2007).

### Acknowledgements

The following people are gratefully acknowledged for their contributions to this chapter: Dr. C.-F. Lee for support in the synthesis and photochemistry of models compounds; Dr. E. R. Kay and Prof. D. A. Leigh for discussion of the results in terms of kinetics and thermodynamics; Dr. P. J. Camp for the free energy calculation.

## Synopsis

*Motor proteins are highly efficient at converting energy into directed molecular-level motion and driving chemical systems away from thermodynamic equilibrium. But even though these natural systems have inspired the design of many interesting synthetic machine-like molecules, the current generations of artificial nanomachines operate almost exclusively by moving towards thermodynamic equilibrium, not away from it. Here we show that asymmetry in the location of the macrocycle in a rotaxane can be used to cause an input of light energy to alter the kinetics of the shuttling of the ring between two binding sites. For an ensemble of such molecular machines, the macrocycle distribution is directionally driven away from equilibrium without ever changing the relative binding affinities of the macrocycle for the different parts of the thread.*



*A ‘gate’ unit divides the thread component of a [2]rotaxane into two compartments. When ‘closed’, the gate prevents motion of the macrocycle between the two compartments (i and iv). In one compartment the macrocycle is held close to the gate by a suitable binding site (i). The macrocycle can ‘signal’ its proximity to the gate by a distance-dependent photo-induced energy transfer (ET) that results in opening of the gate (i→ii). This allows the macrocycle to move freely between the two compartments (ii↔iii). A second process that closes the gate independent of the macrocycle position (ii→i and iii→iv) will result in trapping of the rings in the second compartment (iv).*

*Our observations demonstrate that synthetic molecular machines can be designed that operate via an information ratchet mechanism in which knowledge of a particle's position is used to control its transport away from equilibrium.*

*The selective transport of particles between two compartments by Brownian motion in this way bears similarities to the hypothetical task performed without an energy input by a demon in Maxwell's famous thought experiments.*



## 2.1. Introduction.

### 2.1.1 Driving Chemical Systems Away from Equilibrium.

The fundamental processes associated with life – such as homeostasis, growth and motility – intrinsically require the maintenance of complex molecular systems in states that are far from equilibrium<sup>1</sup>. For any given set of initial conditions, a chemical system will approach a unique equilibrium state. At this state, not only must the concentrations of all chemical species be invariant, but the Principle of Detailed Balance<sup>2</sup> requires that each and every transition occurring between species must be balanced, so that no flux can appear at the steady state. This means that at equilibrium no directional processes of any sort can occur, even across asymmetric potential-energy surfaces or around closed cycles.<sup>3</sup>

In order to move away from equilibrium, a perturbation of the system is required. For example, a change in external conditions, or the selective addition or removal of particular chemical species. Considering a simple equilibrium between two species, **A** and **B** (Figure 2.1a), selective removal of **B** would move the system away from equilibrium. However, the nonequilibrium state cannot be maintained unless removal proceeds continuously at a rate faster than **B** is replenished. Nature has evolved a sophisticated array of mechanisms for achieving such effects, based on the interconnection of chemical reactions in metabolic pathways and the physical compartmentalization of chemical processes into vesicles, organelles, cells, and organs, in conjunction with the selective transport of species between these compartments<sup>1, 4</sup>. Yet, these processes must function continuously and progressively and the energy for generating such directional electrochemical gradients must ultimately be derived from intrinsically nondirectional energy sources such as solar energy or the oxidation of fuels<sup>1, 4a</sup>.

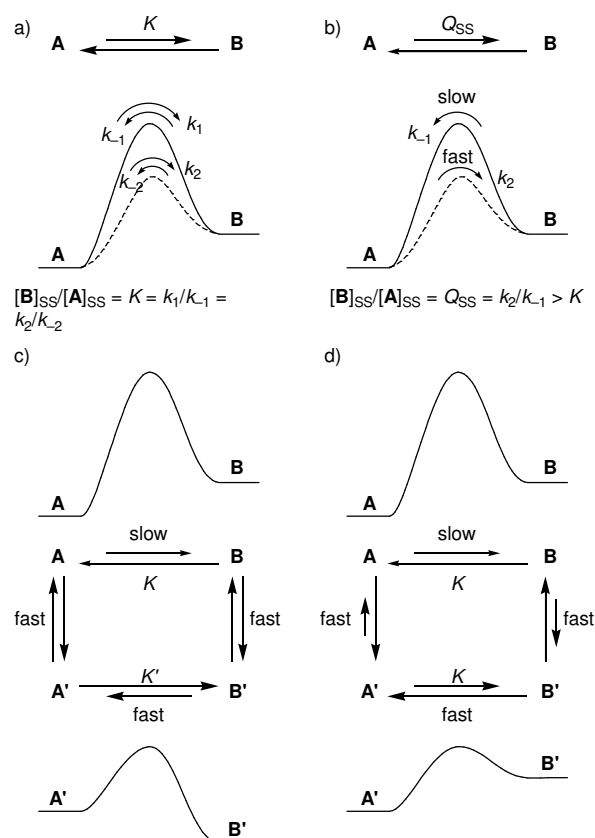


**Figure 2.1** Driving a chemical system away from equilibrium. a) Standard description of a reversible chemical reaction between two species **A** and **B** via non-catalyzed (solid line) and catalyzed (dashed line) mechanisms. b) Hypothetical chemical construct in which transitions between **A** and **B** occur via different reaction pathways through different transition states, depending on the direction of transformation, resulting in a nonequilibrium steady-state ratio of species. c) Four-state model for a system with time-dependent transition rates. Switching between the upper (slowly interconverting) and lower (quickly interconverting) pairs of states occurs randomly but must be driven by a nonequilibrium chemical reaction. This is the basic element of an *energy ratchet* mechanism, described in terms of chemical kinetics. d) Four-state model for a system with state-dependent transition rates. Switching between the upper (slowly interconverting) and lower (quickly interconverting) pairs of states occurs with probabilities dependent on the chemical state (**A** or **B**; **A'** or **B'**) but must be driven by a nonequilibrium chemical reaction. Note that the value of the equilibrium constant in the two equilibrating pairs remains unchanged in this example. This is the basic element of an *information ratchet* mechanism, described in terms of chemical kinetics. Hybrid mechanisms adopting elements of both schemes are also possible.

The myriad enzymes that nature possesses act as highly specific catalysts for biochemical reactions. Yet, by the common definition of a catalyst, most of these systems stabilize a transition state, thus lowering the activation energies for reaction in both directions by an equal amount, precluding any effect on the position of equilibrium (Figure 2.1a). However, a small subset – energy-transducing enzymes – are able to directly couple the catalyzed reaction to an energy source, so as to produce a nonequilibrium product distribution. In simplistic terms, it might be arranged for the ‘catalyzed’ pathway introduced in Figure 1a to operate in only one direction, so that transitions from **A** to **B** to occur via a faster mechanism than those from **B** to **A** (Figure 2.1b). The result would be a nonequilibrium ratio of **A** and **B**.

The situation illustrated in Figure 2.1b is not possible for an elementary reaction with a single transition state. A minimalist model<sup>5</sup> for achieving such a scheme requires two pathways exhibiting different kinetics for exchange between the chemical states. For example if **A** and **B** exchange slowly, some change (e.g. catalyst binding, chemical modification, application of an electric field, etc.) could give a related pair of states (**A'** and **B'**) for which exchange is rapid. Alternation between these two pairs so as to generate a nonequilibrium steady-state ratio can be achieved in one of two ways (Figures 2.1c and 2.1d). In Figure 2.1c, switching between the upper (slow) and lower (fast) regimes occurs regularly or randomly, but is concomitant with a change in equilibrium constant between the equilibrating species.<sup>6</sup> If such fluctuations are an equilibrium process (e.g. if **A'** and **B'** are simply catalyst-bound **A** and **B**), the Principle of Detailed Balance requires that the only effect is that **A'** and **B'** provide an alternative pathway for equilibration of **A** and **B**, as would be expected under classic catalysis kinetics. However, if the transitions between upper and lower schemes are *driven* by a nonequilibrium chemical process, then the relative positions of the energy levels mean that transitions from the slow to the fast mechanism occur with greater probability from **A** and from fast to slow exchanging states more often from **B'**. The result is a cyclic flux of species from **A** through **A'** then **B'**, **B** and finally, slowly back to **A**. Central to being able to harness such a cyclic flux (which might be by accumulation of **B**, or passing species in this state onto another state, other than **A**) is a suitably slow equilibration step in the mechanism. In the language

of molecular machines this is the crucial ‘ratcheting’ step<sup>7</sup> required by all molecular motors (see Chapter 1).

Alternatively, switching between the fast and slow exchange reactions may occur dependent on state (Figure 2.1d). For example, if some interaction (e.g. an allosteric interaction) means that the transition from upper to lower reaction pathway occurs preferentially from **A** rather than **B** and, vice versa, **B'** reacts faster to give **B** than **A'** does to give **A**, again a cyclic flux will be generated, this time without changing the relative energy levels. Once again, the Principle of Detailed Balance must be satisfied, requiring that the information-triggered switching steps involve dissipation of energy.<sup>8</sup>

### 2.1.2 Driving Chemical Systems Away from Equilibrium using Molecular-Level Motion.

Molecular-level motions can be described as thermally activated transitions between states, just as readily as can other chemical transformations. The above chemical-kinetic arguments can therefore be applied when states **A** and **B** are, for example, two thermally exchanging conformations, co-conformations<sup>9</sup> or relative positions within a chemical system. Figure 2.1c illustrates in terms of chemical kinetics the “*energy ratchet*” mechanism for driving a system away from equilibrium that has been used to successfully describe the operation of ion pumps<sup>6</sup> and motor proteins<sup>10</sup> as well as being the basis of how the few synthetic molecular motors already reported<sup>11</sup> work (Chapter 1). On the other hand, Figure 2.1d embodies the basic principles of a fundamentally different mechanism – an “*information ratchet*”. Using information about the position of Brownian particles in order to direct their motion is a concept that dates back to the 19<sup>th</sup> century and James Clerk Maxwell’s famous ‘demon’ thought experiment<sup>12</sup> (see section 1.4.1.1 for details). However, despite intense theoretical interest in other implications of the demon, this concept has not been widely explored as a working Brownian ratchet mechanism and has never been applied to a synthetic molecular system.

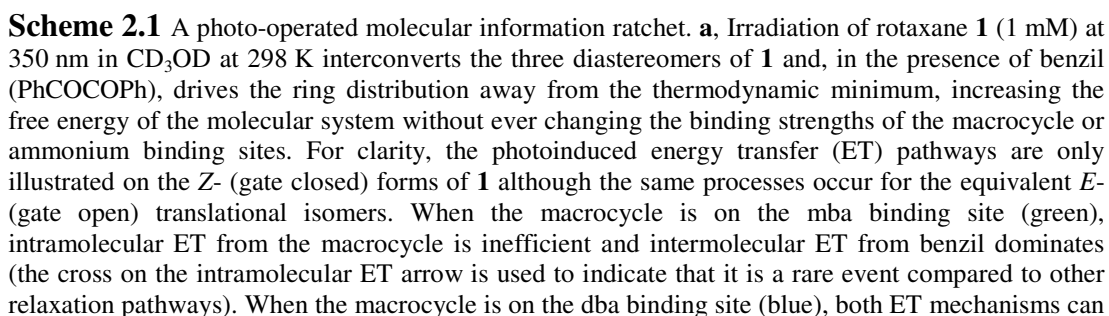
Maxwell originally conceived his celebrated thought experiment to illustrate the statistical nature of the second law of thermodynamics. But modern synthetic chemistry allows us to consider his idea from a very different perspective: rather than test the second law by attempting to reduce entropy in an isolated system, how can information transfer between a particle and a ‘gatekeeper’ be accomplished non-adiabatically to form a mechanism for a working Brownian motion nanomachine?

In Chapter 1 we saw the utility of catenane and rotaxane structures for exploring mechanisms for the control of molecular-level motion. In this chapter I discuss the design, development, operation and implications of rotaxane **1** which uses the mechanism illustrated in Figure 2.1d and which is the first example of a synthetic molecular machine to operate by an information ratchet mechanism.

### 2.1.3 Design of a Non-Adiabatic Molecular Maxwellian Pressure Demon.

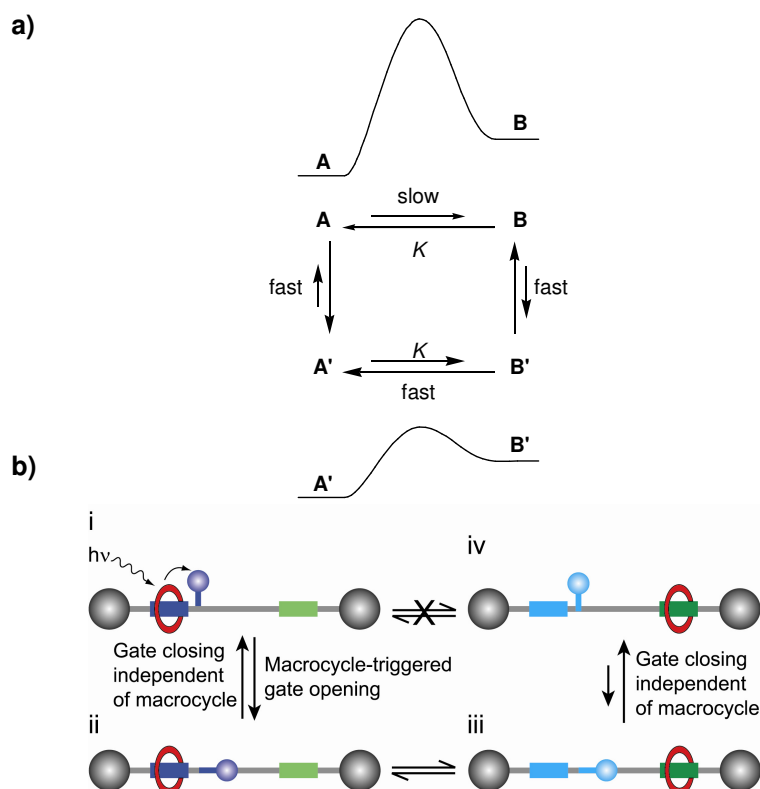
Let us consider the key features required to create a molecular machine operating via the mechanism shown in Figure 2.1d and therefore performing the task envisaged for Maxwell’s pressure demon. Maxwell’s device for sorting many Brownian particles can be compared to an ensemble of ‘compartmentalized’ rotaxane-based shuttles<sup>7</sup> in which an information-transfer process opens and closes a gate between the two compartments so as to control the movement of a macrocycle between the two sides. In the current system, photochemistry was chosen as the means to effect the opening and closing steps.

Rotaxane **1** (Scheme 2.1) was developed to exhibit these design criteria. The molecule consists of a dibenzo-24-crown-8-based macrocycle mechanically locked onto a linear thread by bulky 3,5-di-*t*-butylphenyl groups situated at either end. An  $\alpha$ -methyl stilbene unit in the thread divides the molecule into two compartments, and is able to act as a gate because the *Z*-isomer provides a non-traversable steric barrier for a dibenzo-24-crown-8 macrocycle.<sup>13</sup> The *E*-stilbene isomer on the other hand allows free thermal motion of the same ring along the full length of the thread.



operate efficiently. The amount of benzil present determines the relative contributions of the two ET pathways and thus the nanomachine's effectiveness in pumping the macrocycle distribution away from equilibrium (see Fig 7). The mechanism requires the shuttling of the ring between the two ammonium groups in *E*-**1** to be slow with respect to the lifetime of the macrocycle-sensitizer triplet excited state. The Greek and italicized lettering are the proton assignments for the  $^1\text{H}$  NMR spectra shown in Figs 6 and 7. **b**, Cartoon illustration of the operation of **1** in terms of a non-adiabatic Maxwellian pressure demon<sup>12</sup>. See text for details.

Directional movement of the macrocycle requires a process that operates preferentially in one of the two compartments whereby the gate is opened due to the proximity of the macrocycle (Scheme 2.2a, i→ii), combined with another process for closing the gate, which operates independent of the ring position (Scheme 2.2a, ii→i and iii→iv).



**Scheme 2.2** a) Chemical kinetic description of an *information ratchet* mechanism for a system with state-dependent transition rates. Switching between the upper (slowly interconverting) and lower (quickly interconverting) pairs of states occurs with probabilities dependent on the chemical state (**A** or **B**; **A'** or **B'**) but must be driven by a nonequilibrium chemical reaction (section 2.1.1). b) Design of a molecular information ratchet. A 'gate' unit divides the thread component of a [2]rotaxane into two compartments. When 'closed', the gate prevents motion of the macrocycle between the two compartments (i and iv). In one compartment the macrocycle is held close to the gate by a suitable binding site (i). The macrocycle can 'signal' its proximity to the gate by a distance-dependent photo-induced energy transfer (ET) that results in opening of the gate (i→ii). This allows the macrocycle to

move freely between the two compartments (iii $\rightleftharpoons$ iv). A second process that closes the gate independent of the macrocycle position (ii $\rightarrow$ i and iii $\rightarrow$ iv) will result in trapping of the rings in the second compartment (iv).

## 2.2. Experimental Results.

In this section I describe the photochemical studies carried out on the model compounds which have also help to understand individually the role of each photochemical unit on the sensitized photoisomerization and their contribution to the whole information ratchet mechanism of rotaxane **1**. Then I will discuss the photochemical behaviour and operation of rotaxane **1** (Scheme 2.1).

### 2.2.1 Photochemical studies on the model compounds.

In order to select the photoactive units required to perform the information-triggered gate opening and closing processes, a number of model studies were carried out. The photochemical behavior of uncharged  $\alpha$ -methyl stilbene derivative **2** under both direct and sensitized irradiation was first studied (Figure 2.2). Direct irradiation (350 nm, CH<sub>2</sub>Cl<sub>2</sub>)<sup>15</sup> gave a photostationary state (PSS) ratio of 55:45 *Z:E* after nearly 40 minutes (Figure 2.2a). Irradiation of the same compound in the presence of 1 equivalent benzil (Figure 2.2b) proved to be a faster process, reaching a PSS of 72:28 *Z:E* in under 10 minutes. This is in close agreement with literature values for the benzil-sensitized photoisomerization of unsubstituted  $\alpha$ -methyl stilbene.<sup>16</sup> A benzoyl substituent can be readily incorporated into a dibenzo-24-crown-8 macrocycle (**3**), conferring on it the properties of a benzophenone triplet sensitizer. Using 1 equivalent of macrocycle **3** as sensitizer (Figure 2.2c) resulted in similar kinetics to



the benzil-sensitized reaction, but with a lower PSS ratio of 58:42 *Z:E* after 5 minutes. This is in agreement with literature values for unsubstituted benzophenone and  $\alpha$ -methyl stilbene.<sup>16</sup>

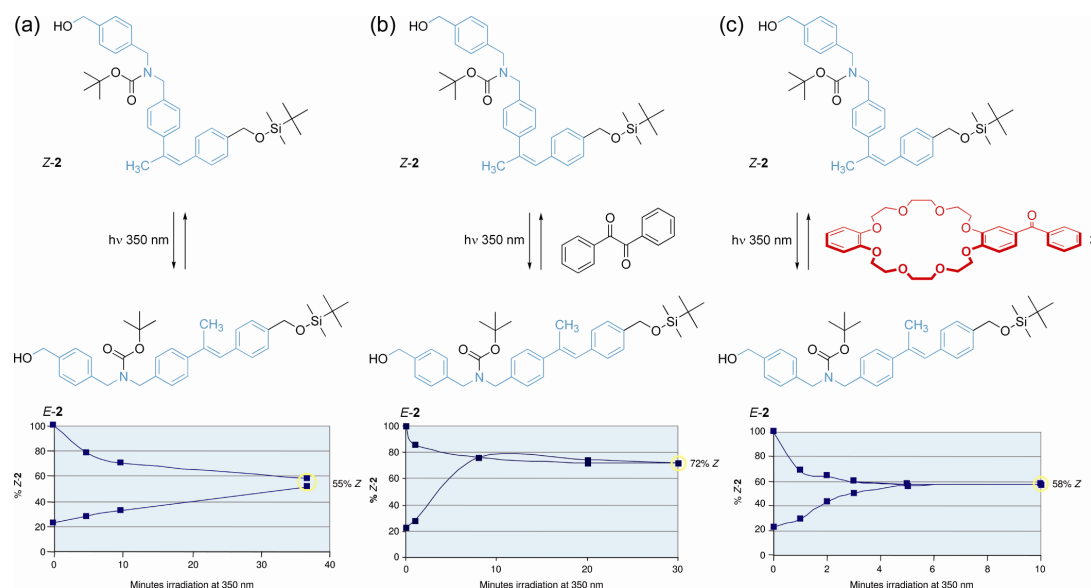


**Figure 2.2** Summary of photochemistry experiments on model  $\alpha$ -methyl stilbene derivative **2**. All experiments were carried out by irradiating 1 mM solutions in  $\text{CH}_2\text{Cl}_2$  at 298 K with light at 350 nm. a) Direct irradiation of gate model **2**. b) Photoisomerization of gate model **2**, sensitized by benzil (1:1 molar ratio). c) Photoisomerization of gate model **2**, sensitized by benzophenone-derivatised crown ether macrocycle **3** (1:1 molar ratio). The error in the measured diastereomer ratios is  $\pm 2\%$ .

In order to investigate the behavior of interlocked systems, single-station rotaxanes **E-4** and **E-5** were prepared. The isomerization of pristine **E-4** in the presence of 0, 1 and 5 equivalents benzil is shown in Figure 2.3a. Comparing with Figures 2.2a and 2.2b, it can be seen that the presence of the macrocycle and the ammonium center have negligible effect on both the kinetics and PSS ratios of either the direct or

sensitized processes. Irradiation of model rotaxane *E*-**5** (Figure 2.3b) results in an intramolecular benzophenone-sensitized process, giving a similar photostationary state (55:45 *Z:E*) to the intermolecular experiment with the same sensitizer (Figure 2.2c), but in a much shorter time (< 1 minute). It may be concluded that benzil can act in an intermolecular fashion to produce a high proportion of *Z*-stilbene, allowing the gate to be closed independent of macrocycle position. The macrocyclic benzophenone sensitizer **3** on the other hand gives a relatively high proportion of ‘gate open’ *E*-stilbene, and when used in an intramolecular fashion results in rapid ‘opening’ of the gate when sitting on a binding site adjacent to the stilbene. Furthermore, isomerization due to direct photon absorption under these conditions is inefficient.

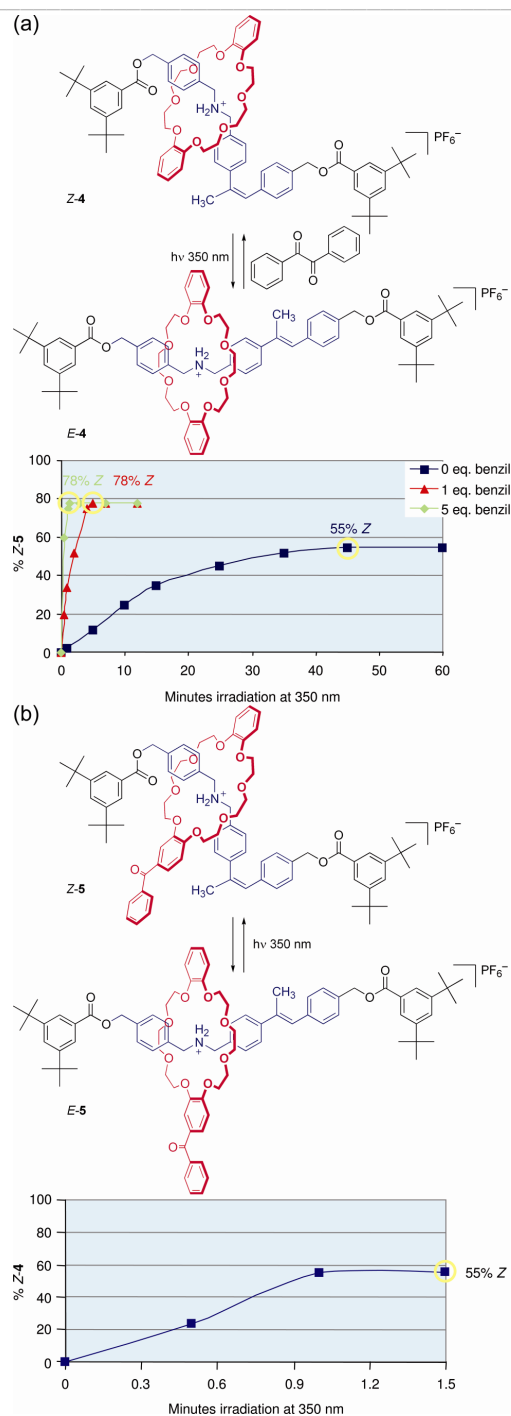


**Figure 2.3** Summary of photochemistry experiments on single-station model [2]rotaxanes. All experiments were carried out by irradiating 1 mM solutions in  $\text{CH}_2\text{Cl}_2$  at 298 K with light at 350 nm. a) Irradiation of model rotaxane *E-4*, in the absence and presence (1 and 5 equivalents) of benzil. b) Photoisomerization of rotaxane *E-5* – intramolecular sensitization by benzophenone. The error in the measured diastereomer ratios is  $\pm 2\%$ .

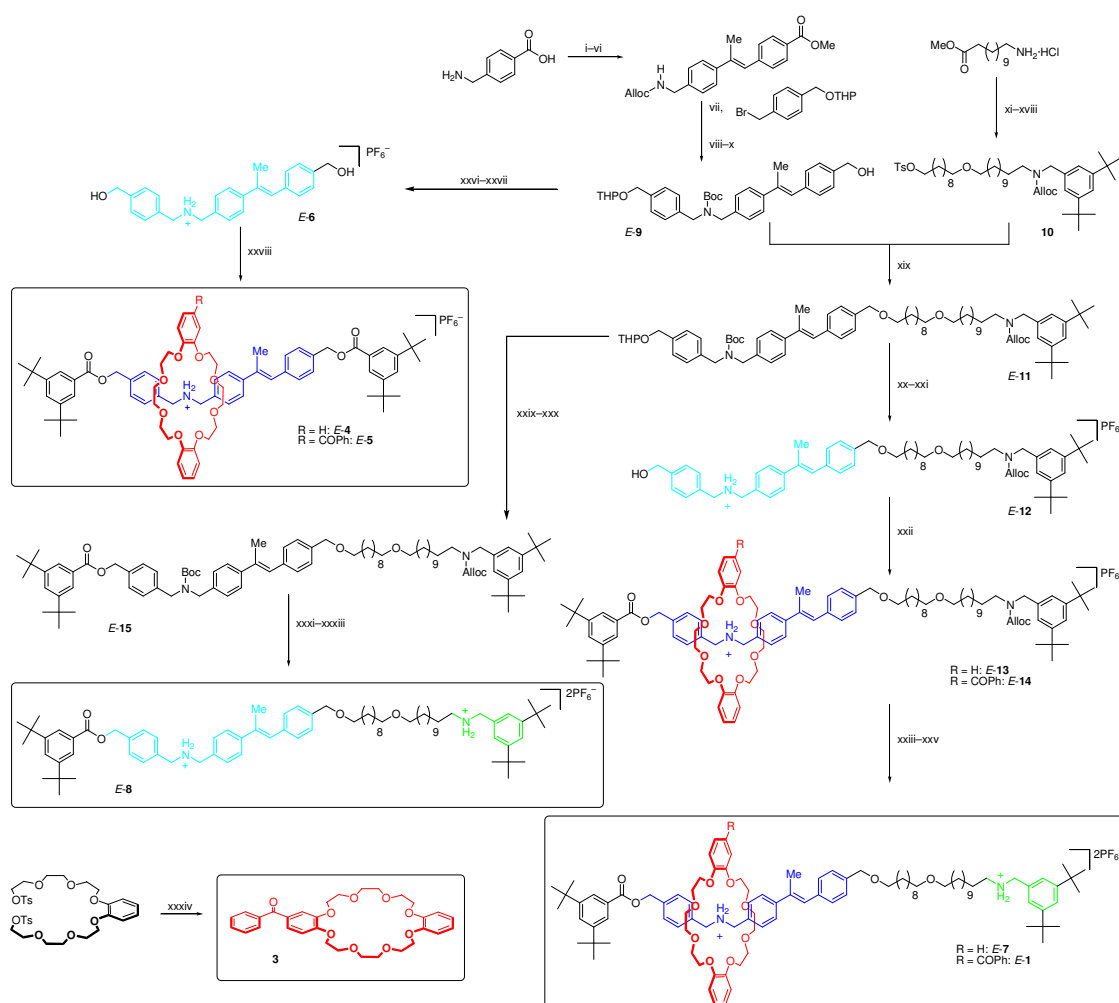
## 2.2.2 Photochemistry behavior of rotaxane 1.

## *Chapter Three*

## Experimental Part

### 3.1. Synthesis

The synthesis of rotaxane **E-1** (25 steps in the longest linear sequence), **E-4**, **E-5**, **E-7**, macrocycle **3** and thread **E-8** is worthy of some comment. In the following paragraphs I discussed experimental details of the full synthetic route, summarized in Scheme 3.1. In order to maintain consistency with the numbering used in Chapter 2 I marked with S those intermediate compounds skipped in the scheme below.

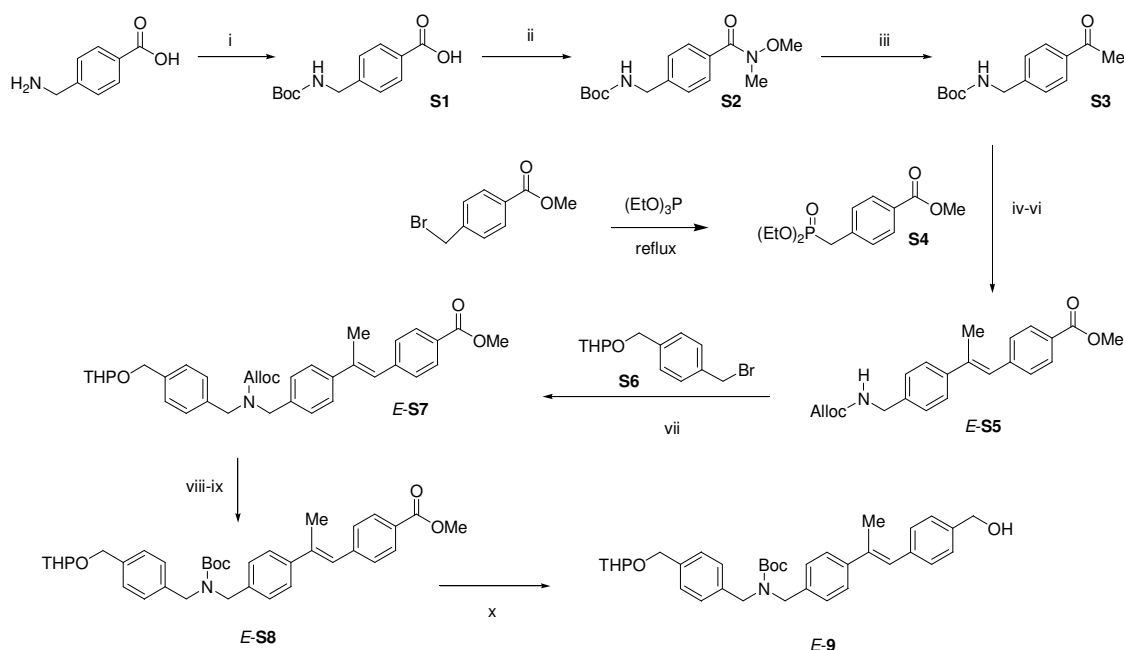


**Scheme 3.1** Synthesis of rotaxanes **E-1**, **E-4**, **E-5**, **E-7**, macrocycle **3** and thread **E-8**<sup>a</sup>

<sup>a</sup> Reaction conditions (unless otherwise stated, reactions were carried out at room temperature): i) Di-*tert*-butyl dicarbonate (Boc<sub>2</sub>O), NaOH, THF/H<sub>2</sub>O (1:1), 0 °C to rt, 40 min, 81%. ii) MeNHOMe, Et<sub>3</sub>N, 1-(3-dimethylaminopropyl)-3-ethylcarbodiimide hydrochloride (EDCI·HCl), CH<sub>2</sub>Cl<sub>2</sub>, 16 h, 97%. iii) MeMgBr (3.0 M in Et<sub>2</sub>O), THF, 0 °C to rt, 15 h, 88%. iv) Diethyl-(4-methoxycarbonylbenzyl)-phosphonate, NaH, THF, 0 °C, 1 h, 91% (*cis:trans* ~2:1). v) CF<sub>3</sub>CO<sub>2</sub>H, CH<sub>2</sub>Cl<sub>2</sub>, 20 h. vi) Allyl chloroformate, NaHCO<sub>3</sub>, THF/H<sub>2</sub>O (1:1), 0 °C to rt, 16 h, 65% (2 steps, based on *trans* isomer). vii)

NaH, DMF, 0 °C, 15 min, 85%. viii) PhSiH<sub>3</sub>, cat. Pd(PPh<sub>3</sub>)<sub>4</sub>, CH<sub>2</sub>Cl<sub>2</sub>, 1 h, 92%. ix) (Boc)<sub>2</sub>O, CH<sub>2</sub>Cl<sub>2</sub>, 2 h, 91%. x) Diisobutylaluminium hydride (DIBAL-H), THF, 0 °C, 4 h, 88%. xi) 3,5-Di-*tert*-butylbenzoic acid, Et<sub>3</sub>N, EDCI·HCl, CH<sub>2</sub>Cl<sub>2</sub>, 48 h, quant. xii) LiAlH<sub>4</sub>, THF, reflux, 2 h, 95%. xiii) Boc<sub>2</sub>O, CH<sub>2</sub>Cl<sub>2</sub>, 2 h, 91%. xiv) BnO(CH<sub>2</sub>)<sub>10</sub>OTf, proton sponge, CH<sub>2</sub>Cl<sub>2</sub>, reflux, 48 h, 85%. xv) H<sub>2</sub>, 10% Pd/C, THF, 16 h, 92%. xvi) CF<sub>3</sub>CO<sub>2</sub>H, CH<sub>2</sub>Cl<sub>2</sub>, 20 h. xvii) Allyl chloroformate, NaHCO<sub>3</sub>, THF/H<sub>2</sub>O (1:1), 0 °C to rt, 16 h, 62% (two steps). xviii) *p*-Toluenesulfonyl chloride (TsCl), Et<sub>3</sub>N, CH<sub>2</sub>Cl<sub>2</sub>, 16 h, 54%. xix) NaH, DMF, 48 h, 78%. xx) HCl (1.0 M in Et<sub>2</sub>O), MeOH, 18 h. xxi) NH<sub>4</sub>PF<sub>6</sub>, acetone/H<sub>2</sub>O (1:1), 1 h, 85% (two steps). xxii) 3,5-Di-*tert*-butylbenzoic anhydride, dibenzo-24-crown-8 or **3**, cat. PBU<sub>3</sub>, CH<sub>2</sub>Cl<sub>2</sub>, 16 h, *E*-**13** 86%; *E*-**14** 91%. xxiii) PhSiH<sub>3</sub>, cat. Pd(PPh<sub>3</sub>)<sub>4</sub>, CH<sub>2</sub>Cl<sub>2</sub>, 2 h. xxiv) HCl (1.0 M in Et<sub>2</sub>O), CH<sub>2</sub>Cl<sub>2</sub>, 10 min. xxv) NH<sub>4</sub>PF<sub>6</sub>, acetone/H<sub>2</sub>O (1:1), 1 h, *E*-**7** 58%; *E*-**1** 67% (three steps). xxvi) HCl (1 M in Et<sub>2</sub>O), CH<sub>2</sub>Cl<sub>2</sub>, 16 h. xxvii) NH<sub>4</sub>PF<sub>6</sub>, acetone/H<sub>2</sub>O (1:1), 1 h, 79% (two steps). xxviii) 3,5-Di-*tert*-butylbenzoic anhydride, dibenzo-24-crown-8 or **3**, cat. PBU<sub>3</sub>, CH<sub>2</sub>Cl<sub>2</sub>/CH<sub>3</sub>CN (1:1), 16 h, *E*-**4** 55%; *E*-**5** 69%. xxix) Pyridinium *p*-toluenesulfonate, EtOH, 60 °C, 7 h, 97%. xxx) 3,5-Di-*tert*-butylbenzoyl chloride, Et<sub>3</sub>N, CH<sub>2</sub>Cl<sub>2</sub>, 1 h, 77%. xxxi) PhSiH<sub>3</sub>, cat. Pd(PPh<sub>3</sub>)<sub>4</sub>, CH<sub>2</sub>Cl<sub>2</sub>, 1 h, 67%. xxxii) HCl (1.0 M in Et<sub>2</sub>O), CH<sub>2</sub>Cl<sub>2</sub>, 10 h. xxxiii) NH<sub>4</sub>PF<sub>6</sub>, acetone/H<sub>2</sub>O (1:1), 1 h, 89% (two steps). xxxiv) 3,4-Dihydroxybenzophenone, Cs<sub>2</sub>CO<sub>3</sub>, THF, reflux, 5 days, 54%.

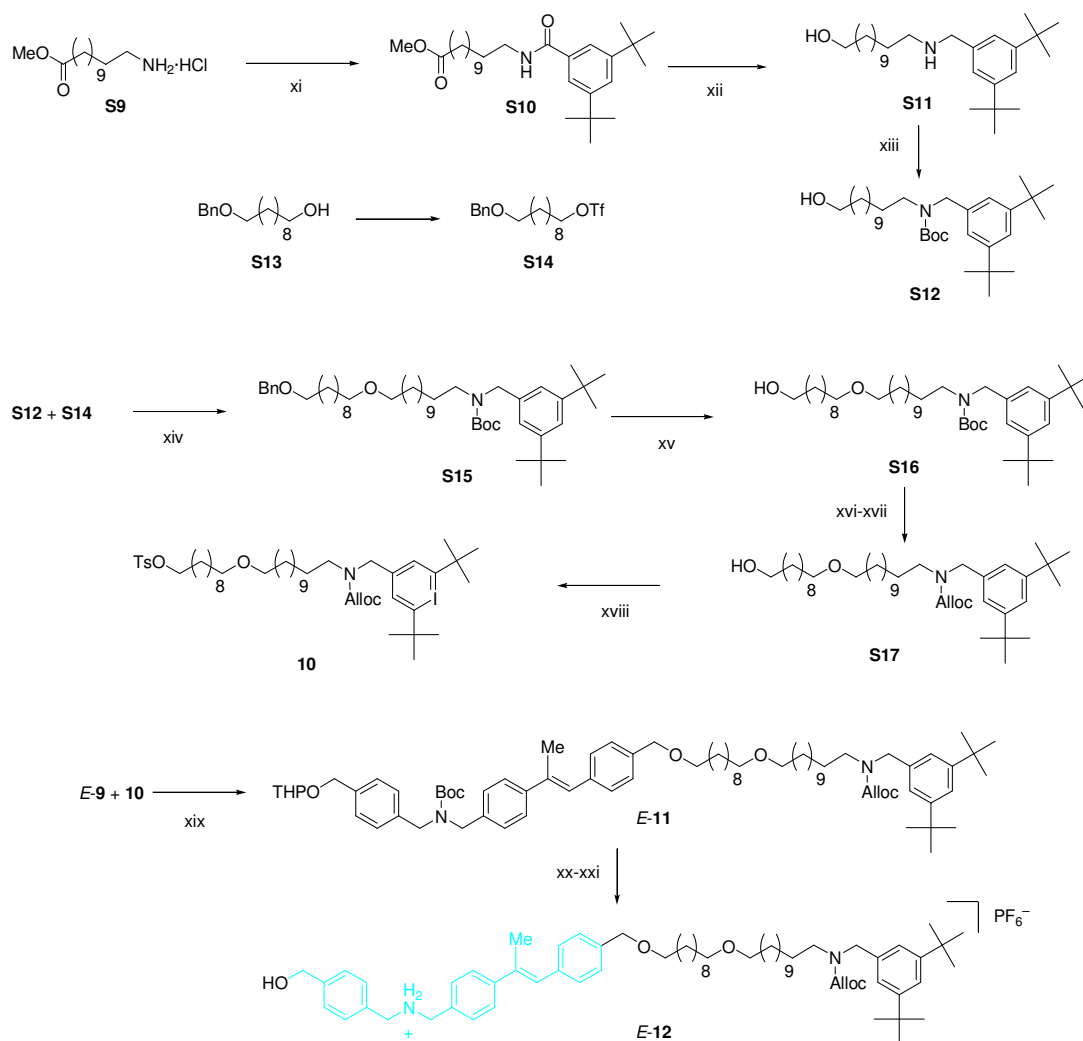
The synthesis of stilbene gate (Scheme 3.2) started from a commercially available *p*-aminomethyl benzoic acid, which was protected with di-*tert*-butylpyrocarbonate (Boc)<sub>2</sub>O to give **S1** (step i, 81%) and subsequently activated to Weinreb amide **S2** (step ii, 97%). The subsequent Grignard reaction with methyl magnesium bromide in dry THF affords the methyl ketone derivative **S3** (step iii, 88%). Next olefination in Wadsworth-Emmons conditions with the phosphonate derivative **S4**<sup>1</sup> (step iv, 91%) gives the  $\alpha$ -methyl stilbene gate with rather poor stereoselectivity (typically ca. 2:1 *Z/E*). After a protecting group manipulation (steps v-vi, 65%), the *trans* isomer *E*-**S5** could be isolated by recrystallization, while the *cis*-enriched mother liquors could be recycled by photochemical isomerization (350 nm, CH<sub>2</sub>Cl<sub>2</sub>, 30 min).<sup>2</sup> Alkylation on the carbamate nitrogen with 2-(4-Bromomethyl-benzyloxy)-tetrahydro-pyran **S6**<sup>3,4</sup> (step vii, 85%) gives **S7** as precursor of the *dba*-station. A second protecting group manipulation (steps viii-ix, 91%) is done to restore the Boc-group in *E*-**S9**<sup>5</sup> and to selectively differentiate the *dba*-station from the Alloc-protected *mba*-station in view of the final rotaxanation. Ester reduction with DIBAL-H (steps x, 88%) provided the selectively protected unit *E*-**9**.



**Scheme 3.2** Synthesis of the  $\alpha$ -methyl stilbene gate **E-9**.

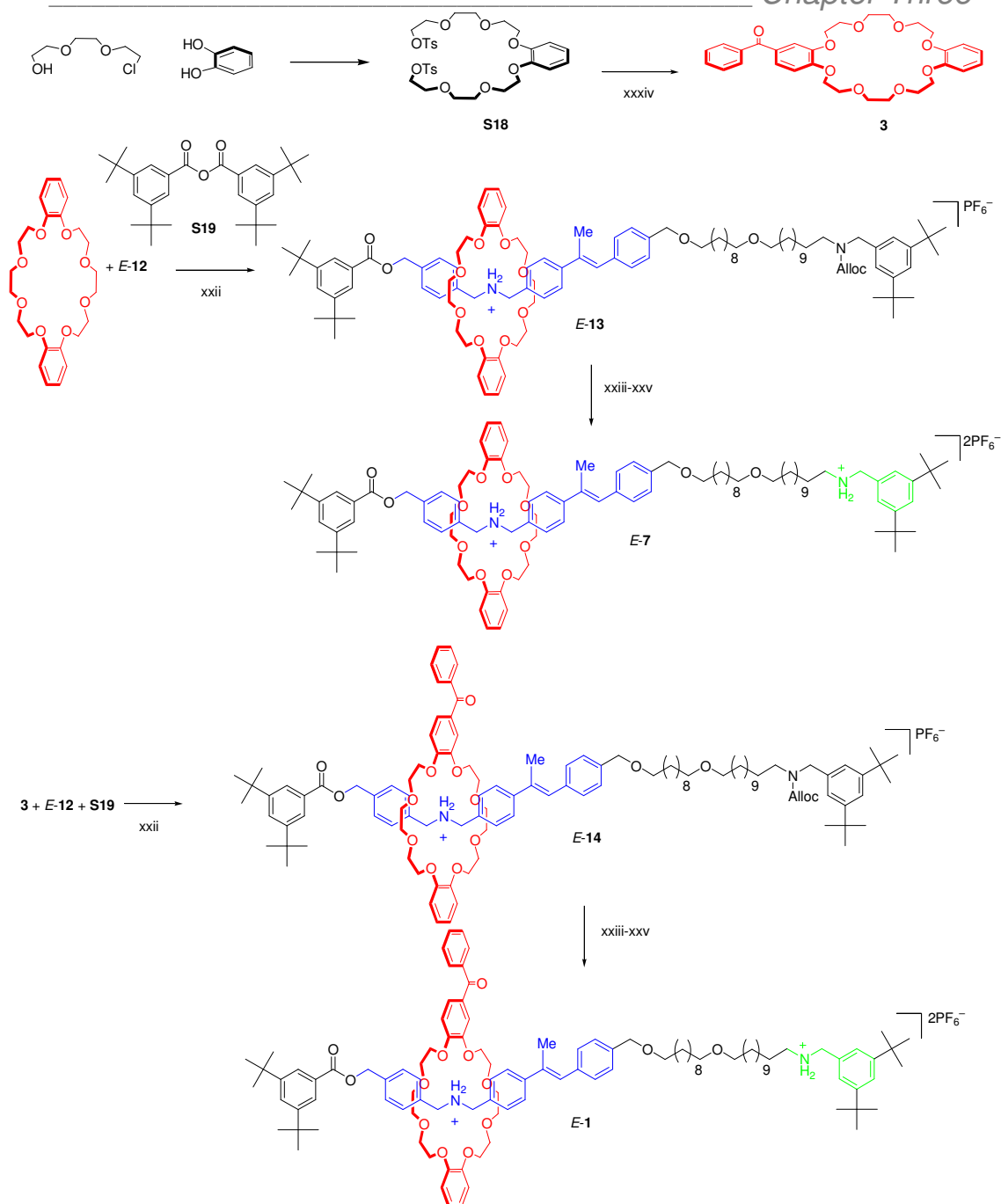
The synthesis of the thread **S10** containing the stopper and the precursor of the *mba*-station (Scheme 3.3) was prepared by coupling the amino-dodecanoic acid **S9** with a commercially available 3,5-Di-*tert*-butylbenzoic acid in EDCI·HCl (step xi, quantitative yield). Successive reaction with 5 eq. of LiAlH<sub>4</sub> in dry THF at reflux allowed to concomitantly reducing the ester group to alcohol and the secondary amide to amine (compound **S11**, step xii, 95%). Nitrogen protection of the *mba*-station with di-*tert*-butyl dicarbonate afforded **S12** (step xiii, 91%) to be used for next chain elongation. Activation of the alcohol **S13**<sup>6</sup> with trifluoromethanesulfonic anhydride (compound **S14**, step xvi), followed by alkylation with **S12** and proton sponge at reflux afforded **S15** in good yield (step xiv, 85%) vs. the respective tosylate (yield 51%), mesilate (yield 48%) and bromide derivatives (elimination reaction occurred in 75% yield). Selective benzyl-deprotection by catalytic hydrogenation (compound **S16**, step xv, 92%) and successive protecting group manipulation (step xvi-xvii, 62%) provided the alcohol **S17** with the *mba*-station Alloc-protected for next coupling with the gate.





**Scheme 3.3** Synthetic sequence for the preparation of precursor *E*-12.

Activation of the benzylic alcohol of *E*-9 (either as tosylate, triflate and bromide) proved surprisingly difficult so *E*-9 was employed as the nucleophile in ether formation with the linear portion of the thread **10** previously activated to tosylate (step xviii, 54%) giving *E*-11 (step xix, 78%). Alcohol and selective Boc-deprotection under acidic conditions followed by anion exchange (steps xx–xxi, 85%) then afforded monoammonium thread precursor *E*-12. The macrocycle ring **3** (Scheme 3.4) was prepared by alkylation of the catechol in DMF and  $K_2CO_3$ , successive activation of the alcoholic groups to tosylate **S18**<sup>7</sup> and cyclization with 3,4-Dihydroxybenzophenone (step xxxiv, 54%).

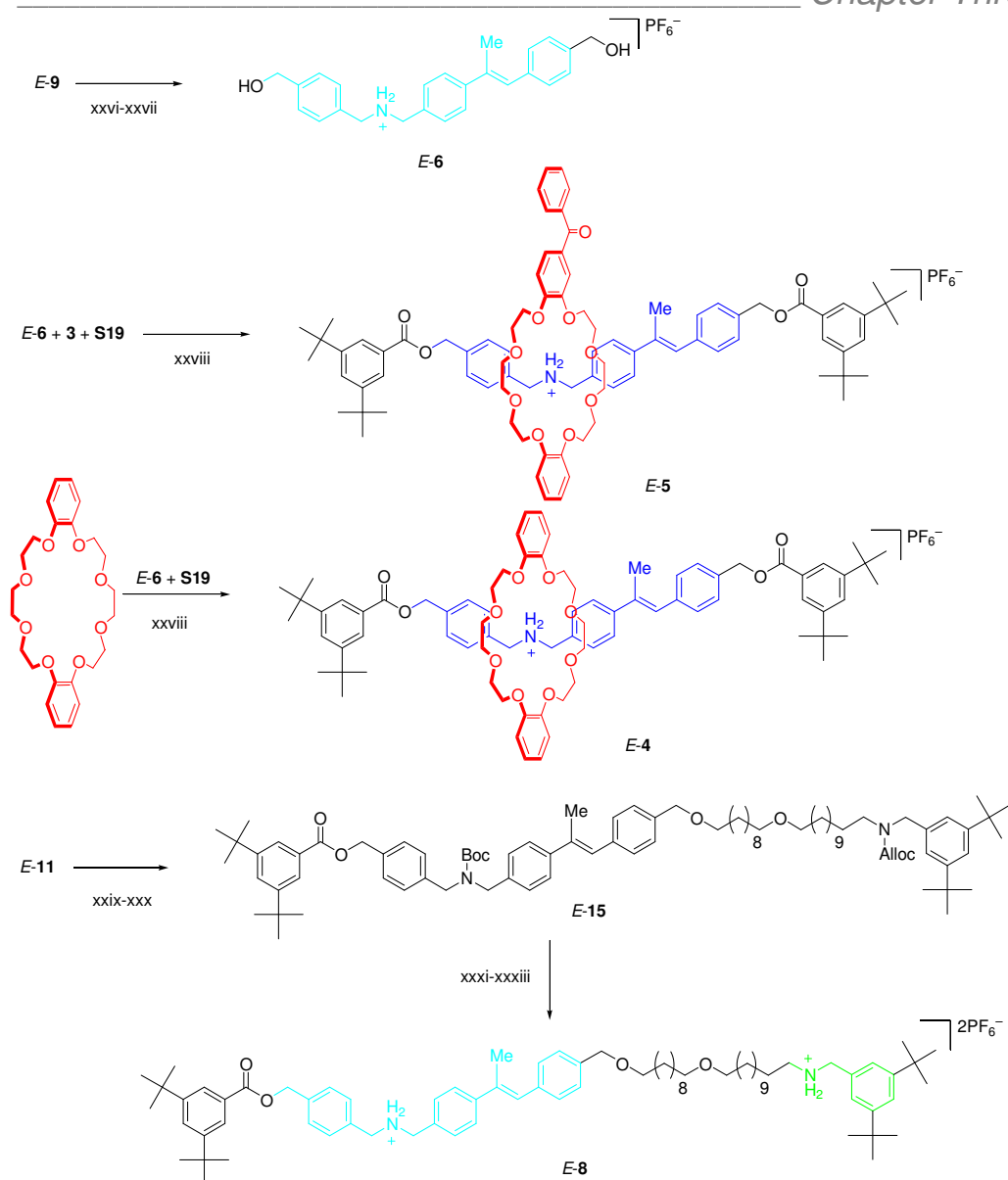


**Scheme 3.4** Synthetic sequence for the preparation of macrocycle **3** and rotaxanes **E-1** and **E-7**.

Rotaxane formation by threading and stoppering of **E-12** (step xxii) was accomplished under the mild phosphine-catalyzed acylation conditions developed by Takata and co-workers.<sup>8</sup> Stoppering in the presence of commercially available

dibenzo-24-crown-8 or of the bespoke 4-benzoyl-24-crown-8 (**3**) readily afforded rotaxanes *E-13* and *E-14* (86% and 91% respectively). A final Alloc-deprotection, salt formation and counterion exchange afforded the diammonium rotaxanes *E-7* and *E-1* (step xxiii-xxv, *E-7* 58% and *E-1* 67%).

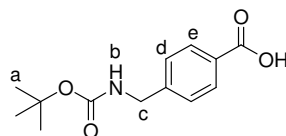
A similar rotaxane-forming protocol (Scheme 3.5) was applied in a bis-stoppering preparation of model rotaxanes *E-4* and *E-5* (step xxvii, 55% and 69%, respectively). The synthesis started from a diol precursor *E-6* obtained from *E-9* by simultaneous alcohol and nitrogen deprotection in acid chloride conditions and successive counterion exchange (step xxvi-xxvii, 79%). For the preparation of the non-interlocked thread, it was found that stoppering of *E-12* was less efficient, perhaps due to *N*-acylation in the absence of the protecting macrocycle, so the synthesis of thread molecule *E-8* proceeded most easily by selective removal of the remaining oxygen protection in *E-11* with pyridinium *p*-toluenesulfonate in EtOH (step xxix, 97%) followed by ester formation under standard acid chloride conditions to give *E-15* (step xxx, 77%), then sequential removal of both carbamate functionalities before acidification and counterion exchange (steps xxxi-xxxiii, 89%).



**Scheme 3.5** Synthesis of model rotaxanes *E-4*, *E-5* and thread *E-8*.

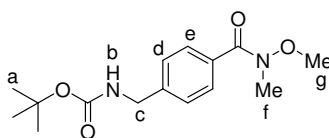
### 3.2. Experimental procedures.

#### 4-(*tert*-Butoxycarbonylamino methyl) benzoic acid (**S1**)



To a solution of 4-(aminomethyl)benzoic acid (10.0 g, 64.9 mmol), NaOH (65.5 mL, 1.0 M in water, 65.5 mmol) and water (60 mL) in tetrahydrofuran (120 mL) was added di-*tert*-butyl dicarbonate (16.4 g, 75.2 mmol) at 0 °C. The reaction mixture was stirred at room temperature for 40 min and then concentrated under reduced pressure. The residue was diluted with water (60 mL) and extracted with ethyl acetate (3 × 20 mL). The organic extracts were concentrated under reduced pressure. The product was purified by flash chromatography (SiO<sub>2</sub>, CH<sub>2</sub>Cl<sub>2</sub>:methanol 97:3) to give **S1** as a colorless solid (13.3 g, 52.5 mmol, 81%): mp. 169-170 °C; <sup>1</sup>H NMR (CDCl<sub>3</sub>, 400 MHz) δ 1.47 (s, 9 H, H<sub>a</sub>), 4.35 (d, *J* = 5.5 Hz, 2 H, H<sub>c</sub>), 4.92 (br s, 1 H, H<sub>b</sub>), 7.37 (d, *J* = 8.1 Hz, 2 H, H<sub>d</sub>), 8.05 (d, *J* = 8.1 Hz, 2 H, H<sub>e</sub>); <sup>13</sup>C NMR (CDCl<sub>3</sub>, 100 MHz) δ 28.4, 44.3, 45.4, 79.9, 127.2, 128.3, 130.5, 145.1, 171.0; HRMS (FAB, 3-NOBA matrix): *m/z* = 252.1239 [(M+H)<sup>+</sup>], (anal. calcd. for C<sub>13</sub>H<sub>18</sub>NO<sub>4</sub>: 252.1236).

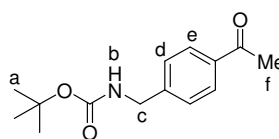
#### [4-(Methoxy methyl carbamoyl) benzyl] carbamic acid-*tert* butyl ester (**S2**)



To a solution of **S1** (10.0 g, 39.8 mmol) in CH<sub>2</sub>Cl<sub>2</sub> (400 mL) was added 1-(3-dimethylaminopropyl)-3-ethyl carbodiimide hydrochloride (EDCI·HCl) (15.0 g, 79.6 mmol) followed by triethylamine (6.71 mL, 47.8 mmol). The reaction was cooled to 0 °C, *N,O*-dimethylhydroxylamine hydrochloride (3.92 g, 40.2 mmol) was added. The solution was stirred for 2 days at room temperature then diluted with water (50 mL),

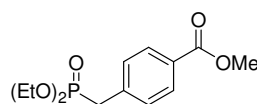
washed with HCl (1.0 M, 3 × 200 mL) and water (100 mL) then concentrated under reduced pressure to give **S2** as a yellow oil (11.4 g, 38.6 mmol, 97%):  $^1\text{H}$  NMR ( $\text{CDCl}_3$ , 400 MHz)  $\delta$  1.47 (s, 9 H,  $\text{H}_a$ ), 3.35 (s, 3 H,  $\text{H}_f$ ), 3.55 (s, 3 H,  $\text{H}_g$ ), 4.35 (d,  $J$  = 5.5 Hz, 2 H,  $\text{H}_c$ ), 4.92 (br s, 1 H,  $\text{H}_b$ ), 7.31 (d,  $J$  = 8.2 Hz, 2 H,  $\text{H}_d$ ), 7.65 (d,  $J$  = 8.2 Hz, 2 H,  $\text{H}_e$ );  $^{13}\text{C}$  NMR ( $\text{CDCl}_3$ , 100 MHz)  $\delta$  28.3, 33.6, 44.2, 60.9, 79.5, 126.7, 128.4, 132.8, 141.6, 157.8, 169.5; HRMS (FAB, 3-NOBA matrix):  $m/z$  = 295.1657  $[(\text{M}+\text{H})^+]$ , (anal. calcd. for  $\text{C}_{15}\text{H}_{23}\text{N}_2\text{O}_4$ : 295.1658).

**(4-Acetyl benzyl) carbamic acid *tert*-butyl ester (**S3**)**



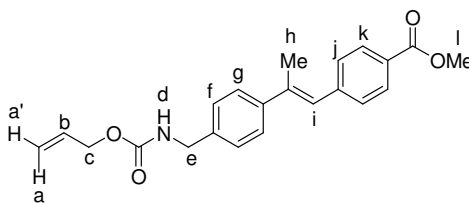
To a solution of **S2** (9.70 g, 33.0 mmol) in dry tetrahydrofuran (330 mL) was added methyl magnesium bromide (33.0 mL, 3.0 M in diethyl ether, 99 mmol) dropwise at 0 °C. The solution was stirred for 2 h then quenched with saturated aqueous  $\text{NH}_4\text{Cl}$  (50 mL). The reaction mixture was extracted with diethyl ether (3 × 100 mL) and the organic extracts were washed with brine (sat., 2 × 30 mL), dried ( $\text{MgSO}_4$ ) and concentrated under reduced pressure to give **S3** as a colorless oil (7.23 g, 29.0 mmol, 88%):  $^1\text{H}$  NMR ( $\text{CDCl}_3$ , 400 MHz)  $\delta$  1.47 (s, 9 H,  $\text{H}_a$ ), 2.59 (s, 3 H,  $\text{H}_f$ ), 4.35 (d,  $J$  = 5.5 Hz, 2 H,  $\text{H}_c$ ), 4.92 (br s, 1 H,  $\text{H}_b$ ), 7.37 (d,  $J$  = 8.2 Hz, 2 H,  $\text{H}_d$ ), 7.92 (d, 2 H,  $J$  = 8.2 Hz,  $\text{H}_e$ );  $^{13}\text{C}$  NMR ( $\text{CDCl}_3$ , 100 MHz):  $\delta$  26.6, 28.3, 44.2, 79.7, 127.3, 128.6, 136.1, 144.5, 155.9, 197.7; HRMS (FAB, 3-NOBA matrix):  $m/z$  = 250.1441  $[(\text{M}+\text{H})^+]$  (anal. calcd. for  $\text{C}_{14}\text{H}_{20}\text{NO}_3$ : 250.1443).

**Diethyl (4-methoxycarbonylbenzyl) phosphonate (**S4**)<sup>1</sup>**



**S4** was prepared as described by Kitazume, Lin, Takeda and Yamazaki.<sup>1</sup>

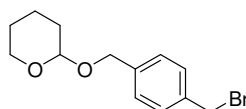
**4-[(*E*)-2-[4-(Allyloxycarbonylamino methyl) phenyl] propenyl] benzoic acid methyl ester (*E*-S5)**



To a suspension of NaH (60% w/w in oil, 1.88 g, 47.1 mmol) in tetrahydrofuran (350 mL) was added **S4** (6.74 g, 23.6 mmol) at 0 °C. After stirring for 10 min, a solution of **S3** (5.87 g, 23.6 mmol) in tetrahydrofuran (150 mL) was added dropwise. The mixture was stirred for 2 h then quenched with saturated aqueous NH<sub>4</sub>Cl solution (20 mL) at 0 °C. The reaction mixture was extracted with diethyl ether (3 × 100 mL) and the organic extracts were washed with brine (sat., 2 × 30 mL), dried (MgSO<sub>4</sub>) and concentrated under reduced pressure. The product was purified by flash chromatography (SiO<sub>2</sub>, hexane:diethyl ether 1:3) to give the product as a mixture of diastereoisomers (*Z*:*E* 2:1) in 91% yield. This material (1.00 g, 2.62 mmol, *Z*:*E* 2:1) was dissolved in CH<sub>2</sub>Cl<sub>2</sub> (40 mL). Trifluoroacetic acid (4.00 mL, 54.0 mmol) was added and the mixture stirred for 16 h. The solvent was removed under reduced pressure, the crude material was re-dissolved in tetrahydrofuran (50 mL) and NaHCO<sub>3</sub> (2.20 g, 26.2 mmol) in water (50 mL) was added. Allyl chloroformate (0.300 mL, 2.88 mmol) was then added at 0 °C. The reaction mixture was stirred for 16 h then extracted with ethyl acetate (3 × 30 mL). The organic extracts were washed with water and brine, then dried (MgSO<sub>4</sub>). Solvent was removed under reduced pressure. Recrystallization from ethyl acetate/hexane afforded pure *E*-**S5** as a colorless solid (210 mg, 65% based on *E* isomer): mp. 98-100 °C; <sup>1</sup>H NMR (400 MHz, CDCl<sub>3</sub>) δ 2.29 (s, 3 H, H<sub>h</sub>), 3.93 (s, 3 H, H<sub>l</sub>), 4.40 (d, *J* = 6 Hz, 2 H, H<sub>e</sub>), 4.61 (d, *J* = 5.6 Hz, 2 H, H<sub>c</sub>), 5.07 (s, 1 H, H<sub>d</sub>), 5.24 (d, *J* = 10.0 Hz, 1 H, H<sub>a</sub>), 5.32 (d, *J* = 17.0 Hz, 1 H, H<sub>a'</sub>), 5.80-6.00 (m, 1 H, H<sub>b</sub>), 6.83 (s, 1 H, H<sub>i</sub>), 7.31 (d, *J* = 8.0 Hz, 2 H, H<sub>f</sub>), 7.42 (d, *J* = 7.7 Hz, 2 H, H<sub>j</sub>), 7.49 (d, *J* = 8.0 Hz, 2 H, H<sub>g</sub>), 8.04 (d, *J* = 7.7 Hz, 2 H, H<sub>k</sub>); <sup>13</sup>C NMR (100 MHz, CDCl<sub>3</sub>) δ 17.6, 44.7, 52.0, 65.7, 117.7, 126.3 (×2), 126.8, 127.5, 127.9, 129.0, 129.4, 132.7, 137.7, 139.0, 142.7, 142.8, 166.9; HRMS (EI): *m/z* = 365.1624 [*M*<sup>+</sup>] (anal. calcd. for C<sub>22</sub>H<sub>23</sub>NO<sub>4</sub>: 365.1627).

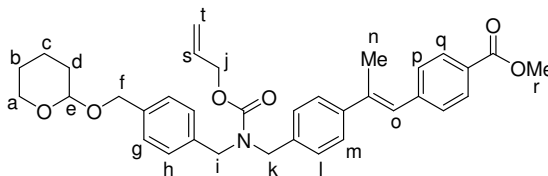
The *Z*-enriched mother liquors were evaporated under reduced pressure, re-dissolved in CH<sub>2</sub>Cl<sub>2</sub> and placed in a quartz vessel. This solution was then de-gassed by bubbling with nitrogen for 15 min prior to irradiation (350 nm) for 30 min to generate more *trans* product. This material was again purified by recrystallization, as described above.

**2-(4-Bromomethyl benzyloxy) tetrahydro pyran (S6)<sup>3, 4</sup>**



**S6** was prepared in two steps from methyl (4-bromomethyl) benzoate as described by Allard, Delaunay and Cousseau,<sup>3</sup> and Klopsch, Franke and Schlüter.<sup>4</sup>

**4-[(*E*)-2-[4-({Allyloxycarbonyl-[4-(tetrahydro-pyran-2-yloxymethyl) benzyl] amino} methyl) phenyl] propenyl] benzoic acid methyl ester (*E*-S7)**

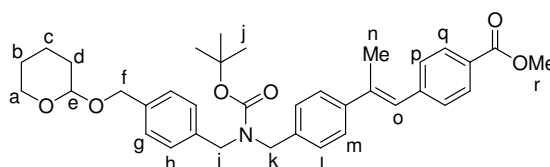


To a solution of *E*-**S5** (120 mg, 0.329 mmol) in *N,N*-dimethylformamide (5 mL), was added NaH (60% w/w in oil, 19.7 mg, 0.494 mmol). The reaction was stirred for 15 min, then a solution of **S6** (141 mg, 0.494 mmol) in *N,N*-dimethylformamide (2 mL) was added at 0 °C. Stirring was continued at this temperature for 1 h, followed by a further 1 h at room temperature. The reaction was quenched with saturated aqueous NH<sub>4</sub>Cl (10 mL). The mixture was extracted with ethyl acetate (3 × 20 mL) and organic extracts were washed with water and brine, then dried (MgSO<sub>4</sub>) and concentrated under reduced pressure. The crude material was purified by flash chromatography (SiO<sub>2</sub>, hexane:ethyl acetate 9:1) to afford *E*-**S7** as a colorless oil (159 mg, 0.279 mmol, 85%): <sup>1</sup>H NMR (400 MHz, CDCl<sub>3</sub>) δ 1.68-1.86 (m, 6 H, H<sub>b</sub>, c, f),



2.29 (s, 3 H,  $H_n$ ), 3.50-3.53 (m, 1 H,  $H_a$ ), 3.80-4.00 (m, 4 H,  $H_{a,r}$ ), 4.35-4.60 (m, 5 H,  $H_{e,i,k}$ ), 4.72 (br s, 2 H,  $H_i$ ), 4.80 (d,  $J = 12.0$  Hz, 2 H,  $H_d$ ), 5.15-5.40 (m, 2 H,  $H_t$ ), 5.85-6.10 (m, 1 H,  $H_s$ ), 6.85 (s, 1 H,  $H_o$ ), 7.10-7.30 (m, 4 H,  $H_{g,h}$ ), 7.35 (d,  $J = 8.2$  Hz, 2 H,  $H_m$ ), 7.43 (d,  $J = 8.0$  Hz, 2 H,  $H_p$ ), 7.49 (d,  $J = 8.2$  Hz, 2 H,  $H_l$ ), 8.04 (d,  $J = 8.0$  Hz, 2 H,  $H_q$ );  $^{13}\text{C}$  NMR ( $\text{CDCl}_3$ , 100 MHz)  $\delta$  17.6, 19.3, 25.4, 30.5, 48.6, 49.0, 52.0, 62.1, 66.3, 68.4, 97.7, 117.5, 126.2 ( $\times 2$ ), 126.7, 127.5, 128.1, 129.0, 129.4, 132.8, 136.4, 136.6, 137.5, 139.0, 139.1, 142.6, 142.9, 156.4, 166.9; HRMS (FAB, 3-NOBA matrix):  $m/z = 570.2843$  [ $(\text{M}+\text{H})^+$ ] (anal. calcd. for  $\text{C}_{35}\text{H}_{40}\text{NO}_6$ : 570.2856).

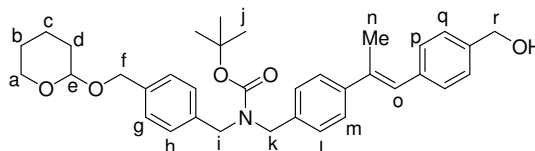
**4-[(*E*)-2-[4-[(*tert*-Butoxycarbonyl-[4-(tetrahydro-pyran-2-ylloxymethyl)-benzyl]-amino)-methyl]-phenyl]-propenyl]-benzoic acid methyl ester (*E*-S8)**



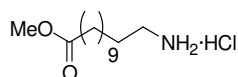
Phenylsilane (0.260 mL, 2.13 mmol) and a solution of tetrakis(triphenylphosphine) palladium(0) (78 mg, 0.071 mmol) in dry  $\text{CH}_2\text{Cl}_2$  (20 mL) were added to a solution of *E*-S7 (405 mg, 0.711 mmol) in dry  $\text{CH}_2\text{Cl}_2$  (20 mL). The mixture was stirred for 1 h then concentrated under reduced pressure. The resulting crude brown material was purified by flash chromatography ( $\text{SiO}_2$ ,  $\text{CH}_2\text{Cl}_2$ :methanol 9:1) to afford the free amine which was dissolved in  $\text{CH}_2\text{Cl}_2$  (15 mL). Di-*tert*-butyl dicarbonate (199 mg, 0.913 mmol) was added and the reaction was stirred for 1 h. The mixture was washed with water, dried ( $\text{MgSO}_4$ ) and the solvent removed under reduced pressure to afford *E*-S8 (278 mg, 0.475 mmol, 67%):  $^1\text{H}$  NMR ( $\text{CDCl}_3$ , 400 MHz)  $\delta$  1.47 (s, 9 H,  $H_j$ ), 1.68-1.71 (m, 2 H,  $H_f$ ), 1.72-1.75 (m, 2 H,  $H_b$ ), 1.82-1.86 (m, 2 H,  $H_c$ ), 2.29 (s, 3 H,  $H_n$ ), 3.52-3.54 (m, 1 H,  $H_a$ ), 3.80-4.00 (m, 4 H,  $H_{a,r}$ ), 4.38-4.44 (m, 4 H,  $H_{i,k}$ ), 4.54 (d,  $J = 12.0$  Hz, 1 H,  $H_e$ ), 4.70 (t,  $J = 3.5$  Hz, 1 H,  $H_d$ ), 4.80 (d,  $J = 12.0$  Hz, 1 H,  $H_d$ ), 6.85 (s, 1 H,  $H_o$ ), 7.20-7.23 (m, 4 H,  $H_{g,h}$ ), 7.29 (d,  $J = 8.2$  Hz, 2 H,  $H_m$ ), 7.35 (d,  $J = 8.3$  Hz, 2 H,  $H_p$ ), 7.51 (d,  $J = 8.2$  Hz, 2 H,  $H_l$ ), 8.04 (d,  $J = 8.3$  Hz, 2 H,  $H_q$ );  $^{13}\text{C}$  NMR ( $\text{CDCl}_3$ , 100 MHz)  $\delta$  14.3, 17.6, 19.4, 25.4, 28.4, 30.5, 48.5, 48.6, 48.9, 49.0, 52.1, 60.9, 62.1, 68.5, 80.1, 97.7, 126.1, 126.6, 127.4, 128.0, 129.0, 129.4, 137.3,

142.4, 143.0, 155.9, 166.5, 166.9; HRMS (FAB, 3-NOBA matrix):  $m/z$  = 586.3168  $[(M+H)^+]$  (anal. calcd. for  $C_{36}H_{44}NO_6$ : 586.3169).

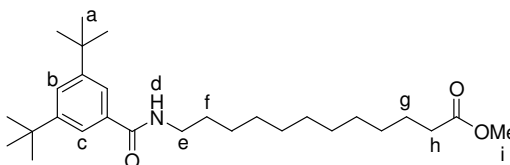
**{4-[(*E*)-2-(4-Hydroxymethyl phenyl)-1-methyl vinyl] benzyl}-[4-(tetrahydro pyran-2-yloxymethyl) benzyl] carbamic acid *tert*-butyl ester (*E*-9)**



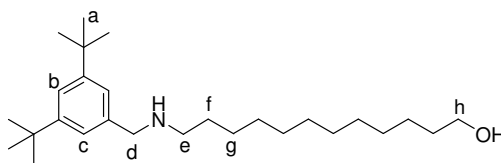
To a solution of *E*-**S8** (800 mg, 1.37 mmol) in dry tetrahydrofuran (80 mL) was added diisobutylaluminium hydride (1.5 M in toluene, 3.65 mL, 5.48 mmol) dropwise over 10 min at  $-78$  °C. The reaction was stirred at this temperature for 3 h then a further 16 h at room temperature. The reaction was cooled to  $0$  °C and citric acid (10% aq., 30 mL) was added, followed by diethyl ether (50 mL). The resulting colorless precipitate was removed by filtration under reduced pressure. The filtrate was washed with saturated aqueous  $NaHCO_3$  ( $3 \times 100$  mL), brine (sat.,  $2 \times 100$  mL), dried ( $MgSO_4$ ) then concentrated under reduced pressure to give *E*-**9** as a colorless oil (672 mg, 1.20 mmol, 88%):  $^1H$  NMR ( $CDCl_3$ , 400 MHz)  $\delta$  1.52 (s, 9 H,  $H_j$ ), 1.68-1.71 (m, 2 H,  $H_f$ ), 1.72-1.75 (m, 2 H,  $H_b$ ), 1.82-1.86 (m, 2 H,  $H_c$ ), 2.29 (s, 3 H,  $H_n$ ), 3.52-3.54 (m, 1 H,  $H_a$ ), 3.93-3.99 (m, 1H,  $H_a$ ), 4.38-4.44 (m, 4 H,  $H_{i,k}$ ), 4.54 (d,  $J = 12.0$  Hz, 1 H,  $H_e$ ), 4.70 (s, 3 H,  $H_{d,r}$ ), 4.8 (d,  $J = 12.0$  Hz, 1 H,  $H_d$ ), 6.85 (s, 1 H,  $H_o$ ), 7.20-7.23 (m, 4 H,  $H_{g,m}$ ), 7.36 (d,  $J = 7.9$  Hz, 2 H,  $H_h$ ), 7.39-7.41 (m, 4 H,  $H_{p,q}$ ), 7.51 (d,  $J = 8.2$  Hz, 2 H,  $H_l$ );  $^{13}C$  NMR ( $CDCl_3$ , 100 MHz)  $\delta$  17.4, 19.3, 25.4, 28.4, 30.5, 48.4, 48.6, 48.8, 49.0, 62.1, 65.2, 68.5, 80.1, 97.7, 126.1 ( $\times 2$ ), 126.9, 127.1, 127.4, 128.0 ( $\times 2$ ), 129.3, 137.3, 137.7, 139.0, 155.9, 157.6; HRMS (FAB, 3-NOBA matrix):  $m/z$  = 557.3141  $[(M+H)^+]$  (anal. calcd. for  $C_{35}H_{43}NO_5$ : 557.3141).

**12-Amino dodecanoic acid methyl ester hydrochloride (S9)<sup>5</sup>**

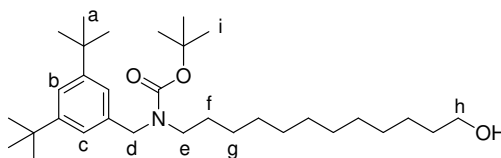
**S9** was prepared as described by Jakobsen, Denmeade, Isaacs, Gady, Olsen and Christensen.<sup>5</sup>

**12-(3,5-Di-*tert*-butyl benzoylamino) dodecanoic acid methyl ester (S10)**

To a solution of 3,5-di-*tert*-butyl benzoic acid (500 mg, 2.34 mmol) in CH<sub>2</sub>Cl<sub>2</sub> (20 mL) was added **S9** (540 mg, 2.13 mmol) and triethylamine (0.660 mL, 4.74 mmol). The resulting suspension was cooled to 0 °C and EDCI·HCl (806 mg, 4.26 mmol) was added. The mixture was stirred at room temperature for 48 h then washed with HCl (1.0 M, 3 × 100 mL), water (2 × 100 mL), brine (sat., 50 mL) and dried (MgSO<sub>4</sub>). The solvent was removed under reduced pressure and the residue was purified by flash chromatography (SiO<sub>2</sub>, CH<sub>2</sub>Cl<sub>2</sub>:methanol 9:1) to obtain **S10** as a colorless oil (1.04 g, 2.34 mmol, 100%): <sup>1</sup>H NMR (CDCl<sub>3</sub>, 400 MHz) δ 1.27-1.34 (m, 32 H, alkyl CH<sub>2</sub> + H<sub>a</sub>), 1.60-1.62 (m, 4 H, H<sub>f</sub>, g), 2.29 (t, *J* = 7.6 Hz, 2 H, H<sub>h</sub>), 3.44 (q, *J* = 6.8 Hz, 2 H, H<sub>e</sub>), 3.66 (s, 3 H, H<sub>i</sub>), 6.14 (br s, 1 H, H<sub>d</sub>), 7.55 (s, 1 H, H<sub>b</sub>), 7.56 (s, 2 H, H<sub>c</sub>); <sup>13</sup>C NMR (CDCl<sub>3</sub>, 100 MHz) δ 24.9, 27.0, 29.1, 29.2, 29.3, 29.40, 29.46, 29.47, 29.7, 31.3, 34.0, 34.9, 40.1, 51.9, 120.9, 125.4, 134.5, 151.1, 168.6, 174.3; HRMS (FAB, 3-NOBA matrix): *m/z* = 446.3623 [(M+H)<sup>+</sup>] (anal. calcd. for C<sub>28</sub>H<sub>48</sub>NO<sub>3</sub>: 446.3634).

**12-(3,5-Di-*tert*-butyl benzylamino) dodecan-1-ol (S11)**

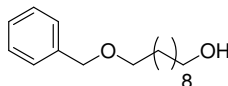
To a solution of **S10** (460 mg, 1.03 mmol) in dry tetrahydrofuran (30 mL) was added  $\text{LiAlH}_4$  (1.0 M in tetrahydrofuran, 7.22 mL, 7.22 mmol). The mixture was stirred under reflux for 16 h, then cooled to 0 °C and quenched by slow addition of aqueous NaOH (1.0 M, 5 mL) followed by water (5 mL). The resulting mixture was extracted with ethyl acetate (3 × 50 mL). The organic phase was washed with brine (sat., 2 × 20 mL), dried ( $\text{MgSO}_4$ ) and concentrated under reduced pressure to give **S11** as a colorless oil (395 mg, 0.980 mmol, 95%):  $^1\text{H}$  NMR ( $\text{CDCl}_3$ , 400 MHz)  $\delta$  1.27-1.34 (m, 34 H, alkyl  $\text{CH}_2$  +  $\text{H}_a$ ), 1.60-1.62 (m, 4 H,  $\text{H}_{f,g}$ ), 2.65 (t,  $J = 6.8$  Hz, 2 H,  $\text{H}_e$ ), 3.64 (t,  $J = 7.2$  Hz, 2 H,  $\text{H}_h$ ), 3.77 (s, 2 H,  $\text{H}_d$ ), 7.15 (s, 2 H,  $\text{H}_c$ ), 7.31 (s, 1 H,  $\text{H}_b$ );  $^{13}\text{C}$  NMR ( $\text{CDCl}_3$ , 100 MHz)  $\delta$  25.7, 26.2, 26.6, 28.9, 29.2, 29.3, 29.4 (×2), 31.2, 32.7, 34.7, 46.7, 51.7, 62.6, 64.6, 122.7, 123.8, 131.0, 151.5; HRMS (FAB, 3-NOBA matrix):  $m/z = 404.3892$  [ $(\text{M}+\text{H})^+$ ] (anal. calcd. for  $\text{C}_{27}\text{H}_{50}\text{NO}$ : 404.3891).

**(3,5-Di-*tert*-butyl benzyl)-(12-hydroxy dodecyl) carbamic acid -*tert*-butyl ester (S12)**

To a solution of **S11** (520 mg, 1.29 mmol) in  $\text{CH}_2\text{Cl}_2$  (30 mL) was added di-*tert*-butyl dicarbonate (285 mg, 1.31 mmol). The reaction was stirred for 1 h then washed with water and brine (sat., 2 × 100 mL), dried ( $\text{MgSO}_4$ ) and concentrated under reduced pressure to afford the product **S12** as a sticky oil (591 mg, 1.17 mmol, 91%):  $^1\text{H}$  NMR ( $\text{CDCl}_3$ , 400 MHz)  $\delta$  1.19-1.4 (m, 43 H, alkyl  $\text{CH}_2$  +  $\text{H}_a, i$ ), 1.60-1.62 (m, 4 H,  $\text{H}_{f,g}$ ), 3.09-3.2 (m, 2 H,  $\text{H}_e$ ), 3.64 (t,  $J = 7.2$  Hz, 2 H,  $\text{H}_h$ ), 4.41 (br d, 2 H,  $\text{H}_d$ ), 7.05 (s, 2 H,  $\text{H}_c$ ), 7.28 (s, 1 H,  $\text{H}_b$ );  $^{13}\text{C}$  NMR ( $\text{CDCl}_3$ , 100 MHz)  $\delta$  21.0, 25.7, 25.8, 26.8,

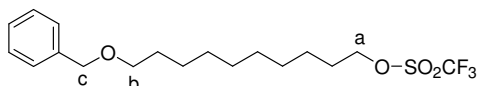
27.3, 28.4, 29.4, 29.5, 31.4, 32.7, 34.7, 46.5, 46.7, 50.3, 51.0, 62.9, 64.6, 79.2, 120.9, 121.4, 121.7, 150.7; HRMS (FAB, 3-NOBA matrix):  $m/z = 504.4405$   $[(M+H)^+]$  (anal. calcd. for  $C_{32}H_{58}NO_3$ : 504.4417).

### 10-Benzyloxy decan-1-ol (**S13**)<sup>5</sup>



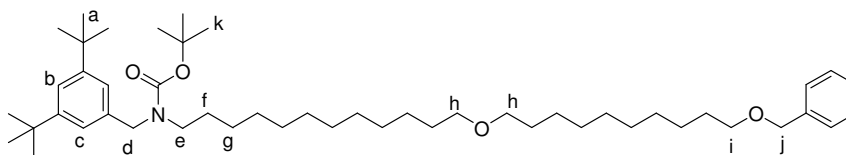
**S13** was prepared as described by Naito, Kawahara, Maruta, Maeda and Sasaki.<sup>5</sup>

### Trifluoro methanesulfonic acid 10-benzyloxy decyl ester (**S14**)



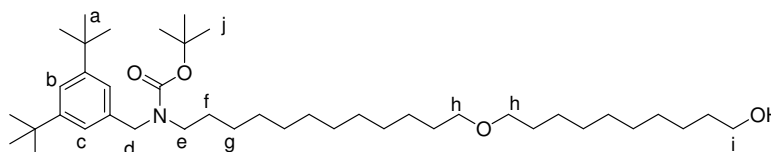
To a solution of **S13** (2.70 g, 10.2 mmol) in  $CH_2Cl_2$  (20 mL) at  $-20\text{ }^{\circ}C$  was added pyridine (1.10 mL, 14.0 mmol) followed by trifluoromethanesulfonic anhydride (2.40 mL, 14.0 mmol). A colorless precipitate immediately appeared. The reaction was stirred for 2 h at room temperature then water (30 mL) was added. The mixture was extracted with  $CH_2Cl_2$  (200 mL) and the organic phase was washed with brine (sat.,  $2 \times 100$  mL), dried ( $MgSO_4$ ) and concentrated under reduced pressure to give **S14** as a colorless oil (3.37 g, 8.51 mmol, 85%):  $^1H$  NMR (400 MHz,  $CDCl_3$ )  $\delta$  0.80-1.65 (m, 16 H, alkyl  $CH_2$ ), 3.50 (t,  $J = 6.6$  Hz, 2 H,  $H_b$ ), 4.50-4.58 (m, 4 H,  $H_{a, c}$ ), 7.42-7.26 (m, 5 H,  $H_{Ar}$ ). Compound **S14** decomposes gradually upon standing and did not give a satisfactory  $^{13}C$  spectrum. It was used directly without further purification.

**[12-(10-Benzyloxy decyloxy) dodecyl]-(3,5-di-*tert*-butyl-benzyl) carbamic acid - *tert*-butyl ester (S15)**



To a mixture of **S14** (1.16 g, 2.92 mmol), **S12** (818 mg, 1.62 mmol) in CH<sub>2</sub>Cl<sub>2</sub> (300 mL) was added proton-sponge (625 mg, 2.92 mmol). The reaction was refluxed for 78 h. The organic phase was washed with saturated aqueous NaHCO<sub>3</sub> and water, then dried (MgSO<sub>4</sub>) and concentrated under reduced pressure. The product was purified by flash chromatography (SiO<sub>2</sub>, hexane:ethyl acetate 8:1) to afford **S15** as a colorless oil (1.86 g, 2.48 mmol, 85%): <sup>1</sup>H NMR (CDCl<sub>3</sub>, 400 MHz) δ 1.19-1.4 (m, 59 H, alkyl CH<sub>2</sub> + H<sub>a, k</sub>), 1.60-1.62 (m, 4 H, H<sub>f, g</sub>), 3.09-3.21 (m, 2 H, H<sub>e</sub>), 3.38 (t, *J* = 6.6 Hz, 4H, H<sub>h</sub>), 3.64 (t, *J* = 7.2 Hz, 2 H, H<sub>i</sub>), 4.35 (s, 2 H, H<sub>j</sub>), 4.41 (br d, 2 H, H<sub>d</sub>), 7.05 (s, 2 H, H<sub>c</sub>), 7.28 (s, 1 H, CH<sub>b</sub>), 7.29 (s, 5 H, H<sub>Ph</sub>); <sup>13</sup>C NMR (CDCl<sub>3</sub>, 100 MHz) δ 26.2, 26.9, 27.4, 27.9, 28.5, 29.44, 29.46, 29.50, 29.51, 29.6, 29.8, 31.4 (×2), 34.7, 46.52, 46.56, 46.7, 50.3, 50.5, 50.6, 50.7 (×2), 51.0, 70.5, 71.0, 72.8, 79.2 (×2), 120.9, 121.4, 121.8, 127.4, 127.6, 128.3 (×2), 138.7, 150.7; HRMS (FAB, 3-NOBA matrix): *m/z* = 748.6241 [(M<sup>+</sup>)] (anal. calcd. for C<sub>49</sub>H<sub>82</sub>NO<sub>4</sub>: 748.6244).

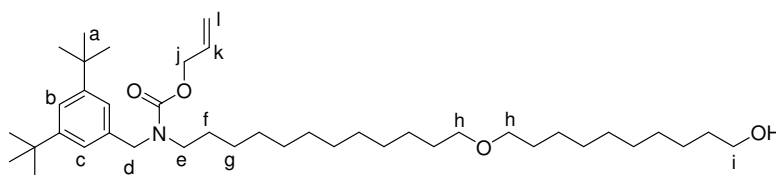
**(3,5-Di-*tert*-butyl benzyl)-[12-(10-hydroxy decyloxy) dodecyl] carbamic acid - *tert*-butyl ester (S16)**



To a solution of **S15** (360 mg, 0.481 mmol) in tetrahydrofuran (10 mL) was added 10% Pd/C (200 mg). The suspension was stirred for 16 h under an atmosphere of H<sub>2</sub> (balloon), then filtered through a short plug of silica gel. The solvent was removed under reduced pressure and the residue was purified by flash chromatography (SiO<sub>2</sub>, hexane:ethyl acetate 4:1) to afford **S16** as a colorless oil (292 mg, 0.443 mmol, 92%): <sup>1</sup>H NMR (CDCl<sub>3</sub>, 400 MHz) δ 1.19-1.40 (m, 59 H, alkyl CH<sub>2</sub> + H<sub>a, j</sub>), 1.60-1.62 (m, 4

H, H<sub>f, g</sub>), 3.09-3.2 (m, 2 H, H<sub>e</sub>), 3.38 (t,  $J = 6.6$  Hz, 4 H, H<sub>h</sub>), 3.64 (t,  $J = 6.7$  Hz, 2 H, H<sub>i</sub>), 4.41 (br d, 2 H, H<sub>d</sub>), 7.05 (s, 2 H, H<sub>c</sub>), 7.28 (s, 1 H, H<sub>b</sub>); <sup>13</sup>C NMR (CDCl<sub>3</sub>, 100 MHz)  $\delta$  25.7, 26.16 ( $\times 2$ ), 26.17 ( $\times 2$ ), 28.5 ( $\times 2$ ), 29.3 ( $\times 2$ ), 29.40 ( $\times 2$ ), 29.45, 29.50 ( $\times 2$ ), 29.52, 29.6 ( $\times 2$ ), 29.68, 29.8 ( $\times 2$ ), 31.5 ( $\times 2$ ), 32.8, 34.8, 63.1, 70.6, 71.0, 120.9 ( $\times 2$ ), 121.4, 121.8, 150.7; HRMS (FAB, 3-NOBA matrix):  $m/z = 660.5944$  [(M+H)<sup>+</sup>] (anal. calcd. for C<sub>42</sub>H<sub>78</sub>NO<sub>4</sub>: 660.5931).

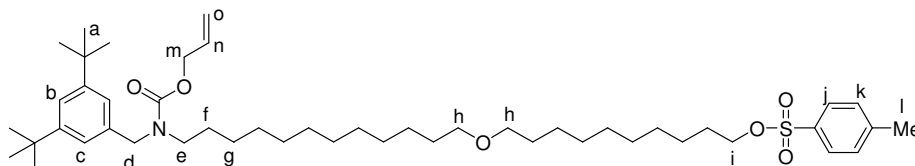
**(3,5-Di-*tert*-butyl benzyl)-[12-(10-hydroxy decyloxy) dodecyl] carbamic acid allyl ester (S17)**



To a solution of **S16** (2.00 g, 3.03 mmol) in CH<sub>2</sub>Cl<sub>2</sub> (45 mL), was added trifluoroacetic acid (5.00 mL, 65.0 mmol). The reaction was stirred for 20 h then volatile components were removed under reduced pressure. The crude material was dissolved in CH<sub>2</sub>Cl<sub>2</sub> (50 mL) and K<sub>2</sub>CO<sub>3</sub> (10.0 g, 72.0 mmol) in water (50 mL) was introduced. The reaction was stirred vigorously for 30 min and extracted with CH<sub>2</sub>Cl<sub>2</sub> (3  $\times$  30 mL). The organic layer was dried (MgSO<sub>4</sub>) and concentrated under reduced pressure to afford the free amine (1.57 g, 2.80 mmol). This material was re-dissolved in tetrahydrofuran (20 mL) and NaHCO<sub>3</sub> (707 mg, 8.41 mmol) in water (20 mL) was added, followed by allyl chloroformate (0.330 mL, 3.08 mmol). The mixture was stirred for 16 h at room temperature, then extracted with ethyl acetate (3  $\times$  30 mL). The organic phase was washed with brine (sat., 2  $\times$  50 mL), dried (MgSO<sub>4</sub>) and concentrated under reduced pressure. The crude material was purified by flash chromatography (SiO<sub>2</sub>, hexane:ethyl acetate 4:1) to afford **S17** as a colorless oil (1.20 g, 1.88 mmol, 62%): <sup>1</sup>H NMR (400 MHz, CDCl<sub>3</sub>)  $\delta$  1.10-1.40 (m, 46 H, alkyl CH<sub>2</sub> + H<sub>a</sub>), 1.40-1.60 (m, 8 H, alkyl CH<sub>2</sub>), 3.10-3.30 (m, 2 H, H<sub>e</sub>), 3.39 (t,  $J = 6.8$  Hz, 4 H, H<sub>h</sub>), 3.63 (t,  $J = 6.8$  Hz, 2 H, H<sub>i</sub>), 4.47 (br d, 2 H, H<sub>d</sub>), 4.64 (s, 2 H, H<sub>j</sub>), 5.10-5.40 (m, 2 H, H<sub>i</sub>), 5.80-6.10 (m, 1 H, H<sub>k</sub>), 7.06 (br d, 2 H, H<sub>c</sub>), 7.31 (d,  $J = 1.6$  Hz, 1 H, H<sub>b</sub>); <sup>13</sup>C NMR (100 MHz, CDCl<sub>3</sub>)  $\delta$  25.7, 26.1, 26.8, 27.6, 28.0, 29.3, 29.4, 29.43, 29.48,

29.50 (×2), 29.55, 29.56, 29.7 (×2), 31.4, 32.7, 34.7, 46.0, 47.1, 50.5, 50.8, 62.9, 65.8, 70.9, 70.91, 117.3, 121.1, 121.5, 122.0, 133.1, 137.1, 150.8; HRMS (FAB, 3-NOBA matrix):  $m/z$  = 644.5618 [(M+H)<sup>+</sup>] (anal. calcd. for C<sub>41</sub>H<sub>74</sub>NO<sub>4</sub>: 644.5610).

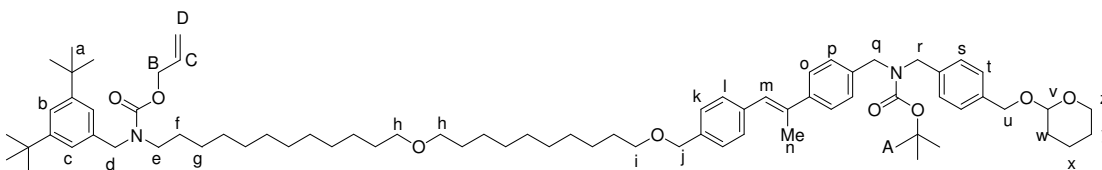
**Toluene-4-sulfonic acid 10-{12-[allyloxycarbonyl-(3,5-di-*tert*-butyl benzyl) amino] dodecyloxy} decyl ester (10)**



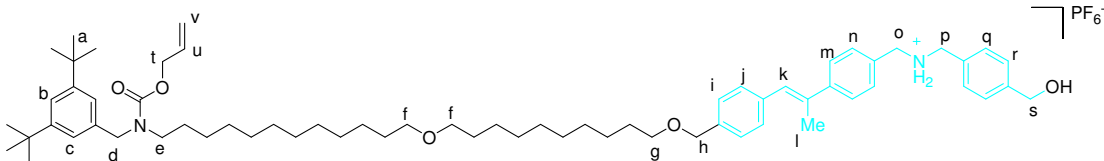
To a solution of **S17** (1.30 g, 2.02 mmol) in CH<sub>2</sub>Cl<sub>2</sub> (30 mL) at room temperature was added triethylamine (0.60 mL, 4.04 mmol) and *p*-toluenesulfonyl chloride (500 mg, 2.62 mmol). The reaction was stirred for 16 h then diluted with CH<sub>2</sub>Cl<sub>2</sub> (50 mL), washed with saturated aqueous NaHCO<sub>3</sub> (2 × 50 mL), brine (sat., 2 × 50 mL) and dried (MgSO<sub>4</sub>). Solvent was removed under reduced pressure and the residue purified by flash chromatography (SiO<sub>2</sub>, hexane:ethyl acetate 9:1) to afford **10** as a colorless sticky oil (870 mg, 1.09 mmol, 54%): <sup>1</sup>H NMR (400 MHz, CDCl<sub>3</sub>) δ 1.10-1.40 (m, 46 H, alkyl CH<sub>2</sub> + H<sub>a</sub>), 1.40-1.70 (m, 8 H, alkyl CH<sub>2</sub>), 2.45 (s, 3 H, H<sub>l</sub>), 3.10-3.30 (m, 2 H, H<sub>e</sub>), 3.38 (t, *J* = 6.4 Hz, 4 H, H<sub>h</sub>), 4.01 (t, *J* = 6.4 Hz, 2 H, H<sub>i</sub>), 4.47 (br d, 2 H, H<sub>d</sub>), 4.64 (br s, 2 H, H<sub>m</sub>), 5.10-5.40 (m, 2 H, H<sub>o</sub>), 5.80-6.10 (m, 1 H, H<sub>n</sub>), 7.06 (br d, 2 H, H<sub>c</sub>), 7.31 (t, *J* = 1.8 Hz, 1 H, H<sub>b</sub>), 7.34 (d, *J* = 8.2 Hz, 2 H, H<sub>k</sub>), 7.79 (d, *J* = 8.2 Hz, 2 H, H<sub>j</sub>); <sup>13</sup>C NMR (100 MHz, CDCl<sub>3</sub>) δ 21.6, 25.3, 26.13, 26.17, 26.8, 27.7, 28.0, 28.8, 28.9, 29.3, 29.4, 29.5, 29.53, 29.56 (×2), 29.74, 29.75, 31.4, 34.7, 46.0, 47.1, 50.5, 50.8, 65.8, 70.7, 70.9, 71.0, 117.2, 121.1, 121.5, 122.0, 127.8, 129.7, 133.2, 133.3, 137.0, 144.6, 150.8; HRMS (FAB, 3-NOBA matrix):  $m/z$  = 798.5676 [(M+H)<sup>+</sup>] (anal. calcd. for C<sub>48</sub>H<sub>80</sub>NO<sub>6</sub>S: 798.5706).



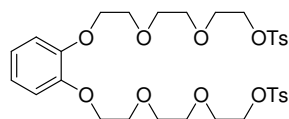
**{12-[10-(4-((*E*)-2-[4-((*tert*-Butoxycarbonyl-[4-(tetrahydro pyran-2-yloxymethyl)-benzyl] amino) methyl) phenyl] propenyl) benzyloxy) decyloxy] dodecyl}-(3,5-di-*tert*-butyl-benzyl) carbamic acid allyl ester (*E*-11)**



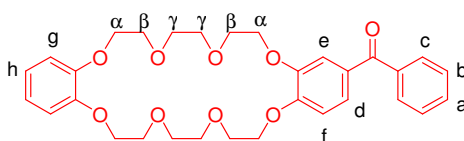
To a solution of *E*-9 (700 mg, 1.26 mmol) in *N,N*-dimethylformamide (100 mL) at 0 °C was added NaH (60% w/w in oil, 66.0 mg, 1.64 mmol) followed by **10** (1.00 g, 1.26 mmol). The suspension was stirred for 16 h at room temperature, then poured into water (10 mL). The reaction was extracted with ethyl acetate (3 × 20 mL) and the organic phase was washed with water and brine (sat., 2 × 100 mL), then dried (MgSO<sub>4</sub>) and concentrated under reduced pressure. Flash chromatography (SiO<sub>2</sub>, hexane:ethyl acetate 8:1) afforded *E*-11 as a colorless oil (1.16 g, 0.981 mmol, 78%): <sup>1</sup>H NMR (CDCl<sub>3</sub>, 400 MHz) δ 1.54-1.23 (m, 63 H, alkyl CH<sub>2</sub> + H<sub>A, a</sub>), 1.71-1.68 (m, 2 H, H<sub>u</sub>), 1.72-1.75 (m, 2 H, H<sub>y</sub>), 1.82-1.86 (m, 2 H, H<sub>x</sub>), 2.29 (s, 3 H, H<sub>n</sub>), 3.10-3.30 (m, 2 H, H<sub>e</sub>), 3.39 (t, *J* = 6.8 Hz, 4 H, H<sub>h</sub>), 3.49 (t, *J* = 6.8 Hz, 2 H, H<sub>i</sub>), 3.52-3.54 (m, 1 H, H<sub>z</sub>), 3.93-3.99 (m, 1 H, H<sub>z</sub>), 4.38 (br s, 2 H, H<sub>b</sub>), 4.44 (br s, 2 H, H<sub>c</sub>), 4.47 (br d, 2 H, H<sub>d</sub>), 4.52 (s, 3 H, H<sub>v, j</sub>), 4.64 (s, 2 H, H<sub>B</sub>), 4.74 (t, *J* = 3.4 Hz, 1 H, H<sub>w</sub>), 4.80 (d, *J* = 12.0 Hz, 1 H, H<sub>w</sub>), 5.10-5.40 (m, 2 H, H<sub>D</sub>), 5.80-6.10 (m, 1 H, H<sub>C</sub>), 6.85 (s, 1 H, H<sub>g</sub>), 7.05 (br d, 2 H, H<sub>c</sub>), 7.26-7.20 (m, 4 H, H<sub>o, t</sub>), 7.34-7.31 (m, 7 H, H<sub>k, l, s, b</sub>), 7.48 (d, *J* = 8.2 Hz, 2 H, H<sub>p</sub>); <sup>13</sup>C NMR (CDCl<sub>3</sub>, 100 MHz) δ 17.5, 19.3, 22.7, 25.5, 26.2, 26.8, 27.7, 28.5 (×2), 28.9, 29.4, 29.5, 29.5, 29.6, 29.7, 29.8, 30.0, 30.6, 31.4 (×2), 32.6, 34.8, 45.2, 46.1, 47.2, 48.6, 49.0, 50.6, 50.9, 62.1, 65.8, 68.6, 70.6, 71.0, 72.7, 77.3, 80.1, 97.8, 121.2 (×2), 121.5, 122.1, 126.1 (×2), 127.4, 127.5 (×2), 128.1 (×2), 129.1 (×2), 133.2 (×2), 136.9, 137.0, 137.3, 137.5, 142.9, 150.9, 156.0; HRMS (FAB, 3-NOBA matrix): *m/z* = 1183.7270 [(M+H)<sup>+</sup>] (anal. calcd. for C<sub>76</sub>H<sub>115</sub>N<sub>2</sub>O<sub>8</sub>: 1183.7269).

Thread (*E*-12)

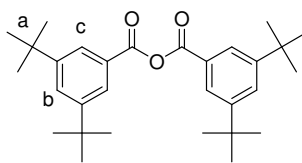
To a solution of *E*-11 (284 mg, 0.240 mmol) in methanol (10 mL), was added HCl (2.0 mL, 1.0 M in diethyl ether, 2.0 mmol). The mixture was allowed to stir for 18 h at room temperature before volatile components were removed under reduced pressure. The crude material was then dissolved in acetone (25 mL) and  $\text{NH}_4\text{PF}_6$  (3.00 g, 18.4 mmol) in water (25 mL) was added. The mixture was stirred for 1 h then concentrated under reduced pressure, diluted with water (50 mL) and extracted with  $\text{CHCl}_3$  ( $3 \times 20$  mL). The organic extracts were concentrated to obtain *E*-12 as a colorless oil (233 mg, 0.203 mmol, 85%):  $^1\text{H}$  NMR (400 MHz,  $\text{CDCl}_3$ )  $\delta$  1.10-1.40 (m, 46 H, alkyl  $\text{CH}_2$  +  $\text{H}_a$ ), 1.45-1.70 (m, 8 H, alkyl  $\text{CH}_2$ ), 2.24 (s, 3 H,  $\text{H}_i$ ), 3.10-3.30 (m, 2 H,  $\text{H}_e$ ), 3.38 (t,  $J = 6.6$  Hz, 4 H,  $\text{H}_f$ ), 3.48 (t,  $J = 6.8$  Hz, 2 H,  $\text{H}_g$ ), 4.06 (s, 2 H,  $\text{H}_o$ ), 4.16 (s, 2 H,  $\text{H}_p$ ), 4.46 (s, 2 H,  $\text{H}_s$ ), 4.50 (s, 2 H,  $\text{H}_h$ ), 4.52 (s, 2 H,  $\text{H}_d$ ), 4.61 (d,  $J = 5.2$  Hz, 2 H,  $\text{H}_t$ ), 5.10-5.40 (m, 2 H,  $\text{H}_v$ ), 5.80-6.10 (m, 1 H,  $\text{H}_u$ ), 6.84 (s, 1 H,  $\text{H}_k$ ), 7.05 (d,  $J = 7.6$  Hz, 2 H,  $\text{H}_{\text{Ph}}$ ), 7.18 (d,  $J = 8.0$  Hz, 2 H,  $\text{H}_{\text{Ph}}$ ), 7.28-7.38 (m, 7 H,  $\text{H}_{\text{Ph}}$ ), 7.45 (d,  $J = 8.0$  Hz, 2 H,  $\text{H}_{\text{Ph}}$ ), 7.56 (d,  $J = 8.0$  Hz, 2 H,  $\text{H}_{\text{Ph}}$ );  $^{13}\text{C}$  NMR (100 MHz,  $\text{CDCl}_3$ )  $\delta$  17.3, 26.2 ( $\times 2$ ), 26.8, 27.7, 28.0, 29.3, 29.4, 29.47 ( $\times 2$ ), 29.49, 29.5 ( $\times 2$ ), 29.6, 29.7, 29.8 ( $\times 2$ ), 31.4, 34.7, 45.2, 46.2, 47.1, 50.6, 50.80, 50.84, 51.2, 64.2, 65.9, 70.7, 70.9, 72.6, 116.8, 117.2, 121.2, 121.5, 121.9, 126.8, 127.5, 127.7, 128.2, 128.6, 129.0, 129.1, 130.1, 130.14, 133.1, 136.1, 137.0, 137.2, 142.3, 145.5, 150.9; HRMS (FAB, 3-NOBA matrix):  $m/z = 999.7553$  [ $(\text{M}-\text{PF}_6)^+$ ] (anal. calcd. for  $\text{C}_{66}\text{H}_{99}\text{N}_2\text{O}_5$ : 999.7554).

**1,2-Bis(2-{2-[2-(2-*p*-tolylsulfonyloxy)ethoxy]ethoxy}ethoxy)benzene (S18)<sup>7</sup>**

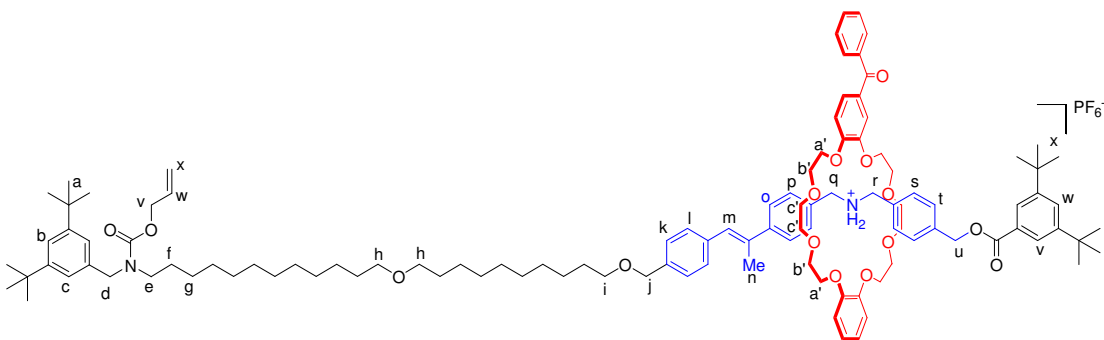
**S18** was prepared as described by Cantrill, Youn, Stoddart and Williams.<sup>7</sup>

**4-Benzoyl-24-crown-8 (3)**

A solution of 3,4-dihydroxybenzophenone (2.62 g, 12.2 mmol) in dry tetrahydrofuran (55 mL) was added to a suspension of cesium carbonate (5.43 g, 16.7 mmol) in dry tetrahydrofuran (25 mL) over 30 min while the temperature was raised to reflux. After a further 15 min at reflux, a solution of **S18** (3.80 g, 5.56 mmol) in dry tetrahydrofuran (30 mL) was added and the reaction mixture was heated at reflux for 5 days. After cooling to room temperature, the suspension was filtered, the solid washed with tetrahydrofuran and the combined filtrates concentrated under reduced pressure. The resulting brown residue was partitioned between CH<sub>2</sub>Cl<sub>2</sub> (50 mL) and water (30 mL). The aqueous phase was extracted once more with CH<sub>2</sub>Cl<sub>2</sub> (50 mL) and the organic extracts were washed with brine (sat., 2 × 50 mL), dried (MgSO<sub>4</sub>) and concentrated under reduced pressure. The product was purified by flash chromatography (SiO<sub>2</sub>, neat ethyl acetate) to give **3** as a yellow solid (1.67 g, 3.02 mmol, 54%): mp. 80-82 °C; <sup>1</sup>H NMR (CDCl<sub>3</sub>, 400 MHz) δ 3.82-3.87 (m, 8 H, H<sub>γ</sub>), 3.90-3.98 (m, 8 H, H<sub>β</sub>), 4.13-4.24 (m, 8 H, H<sub>α</sub>), 6.84-6.92 (m, 5 H, H<sub>e, g, h</sub>), 7.36 (d, *J* = 1.8 Hz, 1 H, H<sub>d</sub>), 7.43-7.49 (m, 3 H, H<sub>a, b</sub>), 7.53-7.59 (m, 1 H, H<sub>f</sub>), 7.74 (d, *J* = 7.1 Hz, 2 H, H<sub>c</sub>); <sup>13</sup>C NMR (CDCl<sub>3</sub>, 100 MHz): δ 69.32, 69.39, 69.4, 69.5, 69.6, 69.7, 69.9 (× 2), 71.30, 71.31, 71.4, 71.5, 111.4, 113.9, 114.4, 121.35, 121.38, 125.6, 128.1, 129.7 (× 2), 130.3, 131.9, 138.2, 148.5, 148.8, 148.9, 152.8, 195.5; HRMS (FAB, 3-NOBA matrix): *m/z* = 552.2359 [M<sup>+</sup>], (anal. calcd. for C<sub>31</sub>H<sub>36</sub>O<sub>9</sub>: 552.2360).

**3,5-Di-*tert*-butylbenzoic anhydride (S19)**

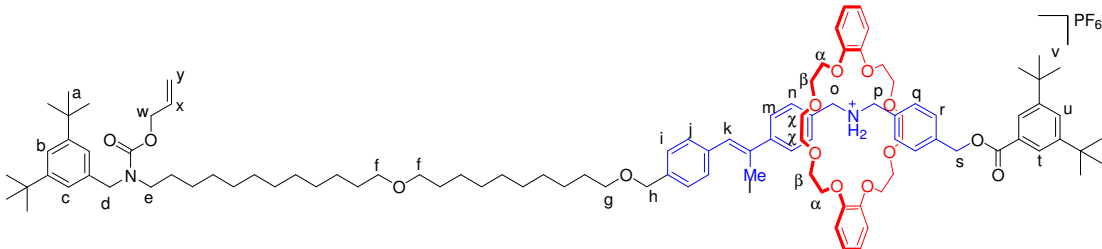
To a solution of 3,5-di-*tert*-butylbenzoic acid (2.52 g, 10.8 mmol) in  $\text{CH}_2\text{Cl}_2$  (30 mL) was added 1,3-dicyclohexylcarbodiimide (1.22 g, 5.91 mmol). The reaction was stirred for 2 h at room temperature then filtered through a short plug of celite. The solvent was removed under reduced pressure and the residue was purified by flash chromatography ( $\text{SiO}_2$ , hexane:ethyl acetate 4:1) to afford **S19** as a colorless solid (1.96 g, 4.35 mmol, 81%): mp. 122-123 °C;  $^1\text{H}$  NMR (400 MHz,  $\text{CDCl}_3$ )  $\delta$  1.37 (s, 36 H,  $\text{H}_a$ ), 7.74 (t,  $J = 1.9$  Hz, 2 H,  $\text{H}_b$ ), 8.03 (d,  $J = 1.9$  Hz, 4 H,  $\text{H}_c$ );  $^{13}\text{C}$  NMR (100 MHz,  $\text{CDCl}_3$ )  $\delta$  31.3, 35.0, 124.7, 128.5, 128.7, 151.6, 162.9.

**[2]Rotaxane (E-14)**

To a solution of *E*-**12** (100 mg, 0.0873 mmol), **3** (58.0 mg, 0.105 mmol) and **S19** (39.3 mg, 0.0873 mmol) in  $\text{CH}_2\text{Cl}_2$  (5 mL) was added tributyl phosphine (4.00  $\mu\text{L}$ , 0.0162 mmol). The reaction mixture was stirred at room temperature for 16 h and then concentrated under reduced pressure. Flash chromatography ( $\text{SiO}_2$ ,  $\text{CH}_2\text{Cl}_2$ :methanol 97:3) afforded *E*-**14** as a colorless sticky oil (152 mg, 0.0794 mmol, 91%):  $^1\text{H}$  NMR (400 MHz,  $\text{CDCl}_3$ )  $\delta$  1.15-1.40 (m, 64 H, alkyl  $\text{CH}_2$  +  $\text{H}_a$ ,  $\text{H}_v$ ), 1.45-1.70 (m, 8 H, alkyl  $\text{CH}_2$ ), 2.16 (s, 3 H,  $\text{H}_l$ ), 3.10-3.35 (m, 2 H,  $\text{H}_e$ ), 3.39 (t,  $J = 6.8$  Hz,

4 H,  $H_f$ ), 3.48 (t,  $J = 6.8$  Hz, 2 H,  $H_g$ ), 3.50-3.70 (m, 8 H,  $H_\gamma$ ), 3.70-3.95 (m, 8 H,  $H_\beta$ ), 3.95-4.30 (m, 8 H,  $H_\alpha$ ), 4.47 (br d, 2 H,  $H_d$ ), 4.50 (s, 2 H,  $H_h$ ), 4.60-4.75 (m, 6 H,  $H_{o,p,w}$ ), 5.10-5.45 (m, 4 H,  $H_{s,y}$ ), 5.85-6.05 (m, 1 H,  $H_x$ ), 6.65-6.75 (m, 3 H,  $H_{k, catechol}$ ), 6.75-6.90 (m, 3 H,  $H_{catechol}$ ), 7.06 (br d, 2 H,  $H_{Ph}$ ), 7.20-7.38 (m, 13 H,  $H_{Ph}$ ), 7.41 (d,  $J = 7.6$  Hz, 2 H,  $H_{Ph}$ ), 7.45-7.60 (m, 2 H,  $H_{Ph}$ ), 7.60-7.75 (m, 4 H,  $H_{Ph}$ ), 7.90 (d,  $J = 2.0$  Hz, 2 H,  $H_{Ph}$ );  $^{13}C$  NMR (100 MHz,  $CDCl_3$ )  $\delta$  17.2, 26.15 ( $\times 2$ ), 26.18 ( $\times 2$ ), 26.8 ( $\times 2$ ), 27.7, 28.0, 29.4 ( $\times 2$ ), 29.48 ( $\times 2$ ), 29.5 ( $\times 2$ ), 29.65, 29.7 ( $\times 2$ ), 31.3 ( $\times 2$ ), 31.4 ( $\times 2$ ), 34.7, 34.9 ( $\times 2$ ), 45.2, 46.0, 47.1, 50.5, 50.8, 52.20, 52.24, 65.6, 65.8, 67.8, 68.1, 68.4, 70.0, 70.1, 70.2, 70.6, 70.7, 70.8, 70.9, 72.6, 111.1, 112.2, 112.3, 113.0, 121.1, 121.47, 121.5, 121.6, 122.0, 123.8, 126.0 ( $\times 2$ ), 126.1, 126.5, 127.4, 127.5, 128.1, 128.2, 128.9, 129.1, 129.2, 129.6, 130.0, 130.4, 130.6, 131.4, 132.0, 133.1, 133.3, 135.9, 136.9, 137.0, 137.1, 137.7, 137.74, 144.5, 146.9, 147.5, 150.8, 151.1, 151.5, 166.9, 195.2; HRMS (FAB, 3-NOBA matrix):  $m/z = 1770.1540$  [ $(M+H-PF_6)^+$ ] (anal. calcd. for  $^{12}C_{112}^{13}C_1H_{156}N_2O_{15}$ : 1770.1539).

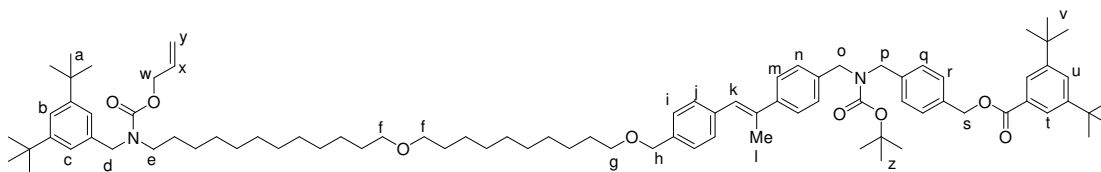
## [2]Rotaxane (*E*-13)



To a solution of *E*-12 (128 mg, 0.112 mmol), dibenzo-24-crown-8 (59.0 mg, 0.132 mmol) and **S19** (50.4 mg, 0.112 mmol) in  $CH_2Cl_2$  (8 mL) was added tributyl phosphine (5.50  $\mu$ L, 0.0223 mmol). The reaction mixture was stirred at room temperature for 16 h and then concentrated under reduced pressure. Flash chromatography ( $SiO_2$ ,  $CH_2Cl_2$ :methanol 97:3) afforded *E*-13 as a colorless sticky oil (175 mg, 0.0967 mmol, 86%):  $^1H$  NMR (400 MHz,  $CDCl_3$ )  $\delta$  1.10-1.45 (m, 64 H, alkyl  $CH_2 + H_{a,v}$ ), 1.45-1.70 (m, 8 H, alkyl  $CH_2$ ), 2.20 (s, 3 H,  $H_l$ ), 3.12-3.28 (m, 2 H,  $H_e$ ), 3.38 (t,  $J = 6.6$  Hz, 4 H,  $H_f$ ), 3.44-3.55 (m, 10 H,  $H_g, \gamma$ ), 3.70-4.00 (m, 8 H,  $H_\beta$ ),

4.05-4.20 (m, 8 H, H<sub>a</sub>), 4.47 (d,  $J = 8.8$  Hz, 2 H, H<sub>d</sub>), 4.51 (s, 2 H, H<sub>h</sub>), 4.55-4.70 (m, 6 H, H<sub>o, p, w</sub>), 5.10-5.40 (m, 4 H, H<sub>s, y</sub>), 5.85-6.05 (m, 1 H, H<sub>x</sub>), 6.70-6.95 (m, 9 H, H<sub>k</sub>, catechol), 7.06 (br d, 2 H, H<sub>Ph</sub>), 7.25-7.50 (m, 11 H, H<sub>Ph</sub>), 7.55-7.80 (m, 3 H, H<sub>Ph</sub>), 7.91 (d,  $J = 2.0$  Hz, 2 H, H<sub>Ph</sub>); <sup>13</sup>C NMR (100 MHz, CDCl<sub>3</sub>)  $\delta$  17.3, 26.18, 26.19, 26.8, 27.7, 28.0, 29.5 ( $\times 2$ ), 29.55 ( $\times 2$ ), 29.57 ( $\times 2$ ), 29.59 ( $\times 2$ ), 29.8 ( $\times 2$ ), 31.3 ( $\times 2$ ), 31.4 ( $\times 2$ ), 34.8, 34.9 ( $\times 2$ ), 46.1, 47.1, 50.6, 50.8, 52.2, 65.7, 65.8, 68.0, 70.2, 70.6, 70.7, 71.0, 72.6, 112.6, 121.1, 121.5, 121.7, 122.0, 123.8, 126.0 ( $\times 2$ ), 127.4, 127.5 ( $\times 2$ ), 128.1, 128.2, 129.07, 129.1, 129.3, 129.4, 130.2, 131.4, 136.1, 137.1, 137.2, 137.6, 144.6, 147.3, 150.8, 151.2, 157.7, 166.9; HRMS (FAB, 3-NOBA matrix):  $m/z = 1665.1202$  [(M-PF<sub>6</sub>)<sup>+</sup>] (anal. calcd. for <sup>12</sup>C<sub>104</sub><sup>13</sup>C<sub>1</sub>H<sub>151</sub>N<sub>2</sub>O<sub>14</sub>: 1665.1199).

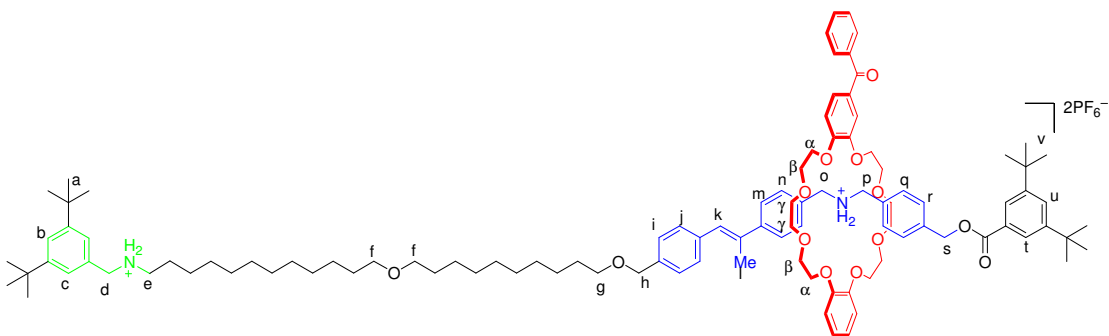
**3,5-Di-*tert*-butyl benzoic acid 4-[[[(4-{(E)-2-[4-(10-{12-[allyloxycarbonyl-(3,5-di-*tert*-butyl benzyl) amino] dodecyloxy} decyloxymethyl) phenyl]-1-methyl vinyl} benzyl)-*tert*-butoxycarbonyl amino] methyl} benzyl ester (*E*-15)**



A solution of *E*-**11** (500 mg, 0.423 mmol) and pyridinium *p*-toluenesulfonate (10.0 mg, 0.0398 mmol) in ethanol (50 mL) was stirred at 60 °C for 7 h. After this time, the solvent was evaporated under reduced pressure and the residue was chromatographed on silica (hexane:diethyl ether 3:7) to afford the alcohol product as a sticky yellow oil (452 mg, 0.411 mmol, 97%): <sup>1</sup>H NMR (CDCl<sub>3</sub>, 400 MHz)  $\delta$  1.66-1.23 (m, 63 H), 2.29 (s, 3 H), 3.10-3.30 (m, 2 H), 3.39 (t,  $J = 6.8$  Hz, 4 H), 3.49 (t,  $J = 6.8$  Hz, 2 H), 4.38 (br s, 2 H), 4.44 (br s, 2 H), 4.47 (br d, 2 H), 4.51 (s, 2 H), 4.52 (s, 2 H), 4.64 (s, 2 H), 5.10-5.40 (m, 2 H), 5.80-6.10 (m, 1 H), 6.85 (s, 1 H), 7.05 (br d, 2 H), 7.26-7.20 (m, 4 H), 7.34-7.31 (m, 7 H), 7.48 (d,  $J = 8.2$ , 2 H). This material (65.0 mg, 0.0591 mmol) and triethylamine (16.4  $\mu$ L, 0.118 mmol) were dissolved in CH<sub>2</sub>Cl<sub>2</sub> (5 mL) and 3,5-di-*tert*-butylbenzoyl chloride (18.0 mg, 0.0714 mmol) was added. The mixture was stirred for 1 h at room temperature, before volatile components were removed under reduced pressure. The resulting crude material was purified by flash

chromatography (SiO<sub>2</sub>, CH<sub>2</sub>Cl<sub>2</sub>:methanol 9:1) to afford *E*-**15** as a colorless sticky oil (60.0 mg, 45.6 nmol, 77%): <sup>1</sup>H NMR (400 MHz, CDCl<sub>3</sub>) δ 1.10-1.45 (m, 73 H, alkyl CH<sub>2</sub> + H<sub>a, v, z</sub>), 1.45-1.70 (m, 8 H, alkyl CH<sub>2</sub>), 2.28 (s, 3 H, H<sub>i</sub>), 3.12-3.30 (m, 2 H, H<sub>e</sub>), 3.39 (t, *J* = 6.8 Hz, 4 H, H<sub>f</sub>), 3.49 (t, *J* = 6.6 Hz, 2 H, H<sub>g</sub>), 4.25-4.50 (m, 6 H, H<sub>d, o, p</sub>), 4.52 (s, 2 H, H<sub>h</sub>), 4.65 (s, 2 H, H<sub>w</sub>), 5.10-5.38 (m, 2 H, H<sub>y</sub>), 5.38 (s, 2 H, H<sub>s</sub>), 5.85-6.05 (m, 1 H, H<sub>x</sub>), 6.84 (s, 1 H, H<sub>k</sub>), 7.06 (br d, 2 H, H<sub>c</sub>), 7.10-7.30 (m, 4 H, H<sub>Ph</sub>), 7.32 (t, *J* = 2.0 Hz, 1 H, H<sub>b</sub>), 7.35 (s, 4 H, H<sub>Ph</sub>), 7.44 (d, *J* = 8.4 Hz, 2 H, H<sub>r</sub>), 7.49 (d, *J* = 8.4 Hz, 2 H, H<sub>q</sub>), 7.64 (t, *J* = 1.9 Hz, 1 H, H<sub>u</sub>), 7.94 (d, *J* = 1.9 Hz, 2 H, H<sub>t</sub>); <sup>13</sup>C NMR (100 MHz, CDCl<sub>3</sub>) δ 17.4, 26.2 (×2), 26.8, 28.4 (×2), 29.49, 29.51, 29.55 (×2), 29.58 (×2), 29.59 (×2), 29.8 (×2), 31.35 (×2), 31.4 (×2), 34.8, 34.9, 46.1, 47.1, 48.6, 48.0, 50.6, 50.8, 65.8, 66.2, 70.6, 71.0 (×2), 72.7, 80.2, 116.8, 117.2, 121.1, 121.5, 122.1, 123.9, 124.3, 126.1, 127.3, 127.4, 127.5, 128.0, 128.1, 128.3, 129.1 (×2), 129.4, 133.2, 133.3, 135.4, 136.9, 137.5, 142.9, 150.7, 151.0, 156.0, 167.1; HRMS (FAB, 3-NOBA matrix): *m/z* = 1313.9426 [(M-H)<sup>+</sup>] (anal. calcd. for C<sub>86</sub>H<sub>125</sub>N<sub>2</sub>O<sub>8</sub>: 1313.9436).

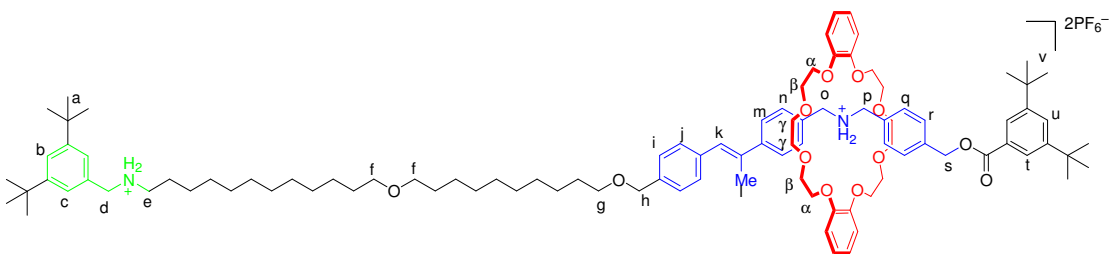
## [2]Rotaxane *E*-1



Phenylsilane (19 mg, 0.17 mmol) and a solution of tetrakis(triphenylphosphine) palladium(0) (6.0 mg, 5.2 nmol) in dry CH<sub>2</sub>Cl<sub>2</sub> (10 mL) were added under nitrogen to a solution of compound *E*-**14** (65 mg, 0.034 mmol) in dry CH<sub>2</sub>Cl<sub>2</sub> (10 mL). The mixture was stirred for 2 h, then the reaction was concentrated under reduced pressure. The resulting crude brown material was purified by flash chromatography (SiO<sub>2</sub>, CH<sub>2</sub>Cl<sub>2</sub>:methanol 9:1) to afford the free amine (48 mg, 0.026 mmol, 76%). This material was then dissolved in CH<sub>2</sub>Cl<sub>2</sub> (5 mL) and HCl (0.26 mL, 1.0 M in

diethyl ether, 0.26 mmol) was added. The mixture was stirred for 10 min then the solvent was removed under reduced pressure and the crude material re-dissolved in acetone (15 mL).  $\text{NH}_4\text{PF}_6$  (1.5 g, 9.2 mmol) in water (10 mL) was added and the mixture was stirred for a further 1 h. Volatile components were removed under reduced pressure then the residue was diluted with water (20 mL) and extracted with  $\text{CHCl}_3$  ( $3 \times 20$  mL). The organic extracts were concentrated to furnish **E-1** as a sticky colorless oil (45 mg, 23 nmol, 88%):  $^1\text{H}$  NMR (400 MHz,  $\text{CD}_3\text{OD}$ )  $\delta$  1.10-1.35 (m, 64 H, alkyl  $\text{CH}_2$  +  $\text{H}_{a,v}$ ), 1.35-1.70 (m, 8 H, alkyl  $\text{CH}_2$ ), [2.06 (s),  $\text{H}_{l(\text{ring near to the gate})}$ ; 2.20 (s),  $\text{H}_{l(\text{ring far from the gate})}$ ; 3 H], [2.98 (t,  $J = 7.8$  Hz),  $\text{H}_{e(\text{ring near to the gate})}$ ; 3.25 (t,  $J = 7.8$  Hz),  $\text{H}_{e(\text{ring far from the gate})}$ ; 2 H], 3.34 (t,  $J = 6.4$  Hz, 4 H,  $\text{H}_f$ ), 3.44 (t,  $J = 6.4$  Hz, 2 H,  $\text{H}_g$ ), 3.50-3.70 (m, 8 H,  $\text{H}_y$ ), 3.70-3.95 (m, 8 H,  $\text{H}_\beta$ ), 3.39-4.27 (m, 8 H,  $\text{H}_a$ ), 4.43 (s, 2 H,  $\text{H}_h$ ), 4.67 (s, 2 H,  $\text{H}_d$ ), 4.73 (br s, 4 H,  $\text{H}_{o,p}$ ), [5.21 (s),  $\text{H}_{s(\text{ring near to the gate})}$ ; 5.36 (s),  $\text{H}_{s(\text{ring far from the gate})}$ ; 2 H], 6.60-7.00 (m, 8 H,  $\text{H}_k$ , catechol), 7.00-7.75 (m, 21 H,  $\text{H}_{\text{Ph}}$ ), 7.80-7.90 (m, 2 H,  $\text{H}_i$ );  $^{13}\text{C}$  NMR (100 MHz,  $\text{CDCl}_3$ )  $\delta$  24.3, 27.1, 27.3 ( $\times 2$ ), 27.6, 30.5, 30.55, 30.6, 30.7, 30.72, 30.78 ( $\times 2$ ), 31.76, 31.79, 31.8, 31.9, 35.8, 35.9, 51.7, 51.8, 52.9, 67.0, 69.5 ( $\times 2$ ), 69.53 ( $\times 2$ ), 69.6, 71.2, 71.4, 71.5 ( $\times 2$ ), 71.8 ( $\times 4$ ), 71.90 ( $\times 4$ ), 71.93 ( $\times 4$ ), 73.6, 122.9, 124.65, 124.7 ( $\times 2$ ), 125.2 ( $\times 2$ ), 125.4, 127.7, 127.8, 128.7, 128.8, 129.42, 129.45, 129.72, 129.78, 129.5, 130.0 ( $\times 2$ ), 130.1 ( $\times 2$ ), 130.3, 130.7, 131.17, 131.2, 131.22, 131.3, 131.4, 131.9, 131.96, 132.1, 132.93, 133.0 ( $\times 2$ ), 133.1 ( $\times 2$ ), 133.8 ( $\times 2$ ), 133.83 ( $\times 2$ ), 159.1; HRMS (FAB, 3-NOBA matrix):  $m/z$  = 1685.1251 [ $(\text{M}-\text{H}-2\text{PF}_6)^+$ ] (anal. calcd. for  $^{12}\text{C}_{107}^{13}\text{C}_1\text{H}_{151}\text{N}_2\text{O}_{13}$ : 1685.1250).

## [2]Rotaxane **E-7**

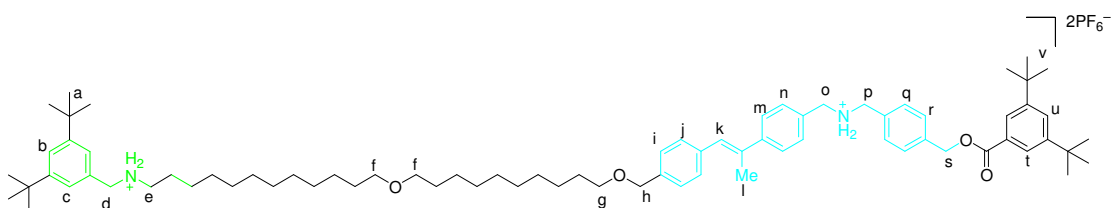


Phenylsilane (25 mg, 0.22 mmol) and a solution of tetrakis(triphenylphosphine)



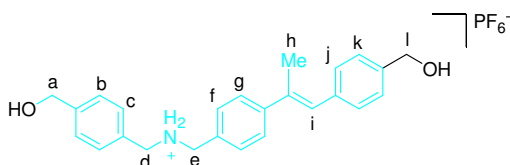
palladium(0) (6.0 mg, 5.2 nmol) in dry  $\text{CH}_2\text{Cl}_2$  (3 mL) were added under nitrogen to a solution of compound *E-13* (100 mg, 0.055 mmol) in dry  $\text{CH}_2\text{Cl}_2$  (10 mL). The mixture was stirred for 1 h, then the reaction was concentrated under reduced pressure. The resulting crude brown material was purified by flash chromatography ( $\text{SiO}_2$ ,  $\text{CH}_2\text{Cl}_2$ :methanol 9:1) to afford the free amine. This material was then dissolved in  $\text{CH}_2\text{Cl}_2$  (5 mL) and HCl (0.50 mL, 1.0 M in diethyl ether, 0.50 mmol) was added. The mixture was stirred for 10 min then the solvent was removed under reduced pressure and the crude material re-dissolved in acetone (10 mL).  $\text{NH}_4\text{PF}_6$  (2.0 g, 18 mmol) in water (10 mL) was added and the mixture was stirred for a further 1 h. Volatile components were removed under reduced pressure then the residue was diluted with water (10 mL) and extracted with  $\text{CHCl}_3$  ( $3 \times 20$  mL). The organic extracts were concentrated to furnish *E-7* as a colorless sticky oil (60 mg, 32 nmol, 58%):  $^1\text{H}$  NMR (600 MHz,  $\text{CD}_3\text{OD}$ )  $\delta$  1.10-1.40 (m, 64 H, alkyl  $\text{CH}_2$  +  $\text{H}_a$ ,  $\nu$ ), 1.40-1.70 (m, 8 H, alkyl  $\text{CH}_2$ ), [2.14 (s),  $\text{H}_{\text{l(ring near to the gate)}}$ ]; 2.22 (s),  $\text{H}_{\text{l(ring far from the gate)}}$ ; 3 H], [2.98 (t,  $J = 12.3$  Hz),  $\text{H}_{\text{e(ring near to the gate)}}$ ]; 3.20 (t,  $J = 12.0$  Hz),  $\text{H}_{\text{e(ring far from the gate)}}$ ; 2 H], 3.30-3.65 (m, 14 H,  $\text{H}_{\text{f, g, } \gamma}$ ), 3.66-3.86 (m, 8 H,  $\text{H}_{\beta}$ ), 4.00-4.25 (m, 8 H,  $\text{H}_{\alpha}$ ), 4.45 (s, 2 H,  $\text{H}_{\text{h}}$ ), 4.68 (s, 2 H,  $\text{H}_{\text{d}}$ ), 4.69 (s, 4 H,  $\text{H}_{\text{o, p}}$ ), [5.21 (s),  $\text{H}_{\text{s(ring near to the gate)}}$ ]; 5.37 (s),  $\text{H}_{\text{s(ring far from the gate)}}$ ; 2 H], 6.70-6.82 (m, 5 H,  $\text{H}_{\text{k, catechol}}$ ), 6.84-6.92 (m, 2 H,  $\text{H}_{\text{catechol}}$ ), 6.93-7.00 (m, 2 H,  $\text{H}_{\text{catechol}}$ ), 7.16-7.72 (m, 16 H,  $\text{H}_{\text{Ph}}$ ), 7.80-7.90 (m, 2 H,  $\text{H}_{\text{Ph}}$ );  $^{13}\text{C}$  NMR (100 MHz,  $\text{CDCl}_3$ )  $\delta$  17.7, 27.3, 30.50, 30.55, 30.57, 30.60, 30.68, 30.7, 30.73, 30.78, 31.77, 31.80, 31.83, 31.9 ( $\times 2$ ), 35.9 ( $\times 2$ ), 50.1, 51.7, 51.8, 52.9, 53.3, 53.9, 67.0, 69.2, 69.5, 71.4 ( $\times 2$ ), 71.5 ( $\times 2$ ), 71.8 ( $\times 2$ ), 71.9, 71.94, 73.6, 113.6 ( $\times 2$ ), 114.0 ( $\times 2$ ), 122.5, 122.9, 124.67, 124.7, 124.8, 125.2, 125.7, 127.1, 127.8, 128.8, 130.0, 130.1, 130.3, 130.6, 130.9, 131.2, 131.4, 133.0, 133.1, 133.8, 148.9, 152.7; HRMS (FAB, 3-NOBA matrix):  $m/z = 1580.0932$  [ $(\text{M}-2\text{H}-2\text{PF}_6)^+$ ] (anal. calcd. for  $^{12}\text{C}_{100}^{13}\text{C}_1\text{H}_{146}\text{N}_2\text{O}_{12}$ : 1580.0909).

## Thread E-8



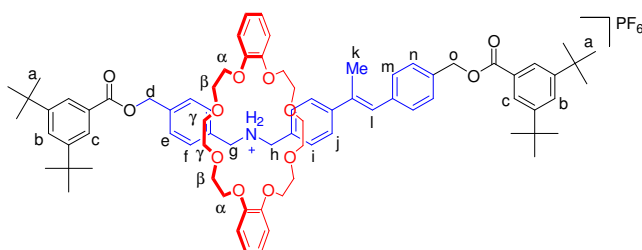
Phenylsilane (9.0 mg, 0.083 mmol) and a solution of tetrakis(triphenylphosphine) palladium(0) (3.0 mg, 2.6 nmol) in dry CH<sub>2</sub>Cl<sub>2</sub> (10 mL) were added under nitrogen to a solution of compound *E-15* (35 mg, 0.027 mmol) in dry CH<sub>2</sub>Cl<sub>2</sub> (10 mL). The mixture was stirred for 1 h, during which time the light yellow solution turned brown. Volatile components were removed under reduced pressure to afford a crude material that was purified by flash chromatography (SiO<sub>2</sub>, CH<sub>2</sub>Cl<sub>2</sub>:methanol 9:1) to afford the free amine as an oil (23 mg, 0.018 mmol, 67%). This material was then dissolved in CH<sub>2</sub>Cl<sub>2</sub> (8 mL) and HCl (2.0 mL, 1.0 M in diethyl ether, 2.0 mmol) added. The mixture was stirred for 10 h at room temperature then concentrated under reduced pressure. The crude material was re-dissolved in acetone (10 mL) then NH<sub>4</sub>PF<sub>6</sub> (2.0 g, 12 mmol) in water (10 mL) was added. The mixture was stirred for a further 1 h then concentrated to furnish *E-8* as a colorless sticky oil (22 mg, 0.016 mmol, 89%): <sup>1</sup>H NMR (400 MHz, CD<sub>3</sub>OD) δ 1.10-1.40 (m, 64 H, alkyl CH<sub>2</sub> + H<sub>a</sub>, v), 1.40-1.70 (m, 8 H, alkyl CH<sub>2</sub>), 2.19 (s, 3 H, H<sub>i</sub>), 2.94 (t, *J* = 8.0 Hz, 2 H, H<sub>e</sub>), 3.34 (t, *J* = 6.6 Hz, 4 H, H<sub>f</sub>), 3.44 (t, *J* = 6.6 Hz, 2 H, H<sub>g</sub>), 3.99 (br s, 4 H, H<sub>o</sub>, p), 4.08 (s, 2 H, H<sub>d</sub>), 4.44 (s, 2 H, H<sub>h</sub>), 5.33 (s, 2 H, H<sub>s</sub>), 6.82 (s, 1 H, H<sub>k</sub>), 7.29 (s, 6 H, H<sub>Ph</sub>), 7.36 (d, *J* = 8.4 Hz, 2 H, H<sub>Ph</sub>), 7.41 (d, *J* = 8.4 Hz, 2 H, H<sub>Ph</sub>), 7.44-7.50 (m, 3 H, H<sub>Ph</sub>), 7.52 (d, *J* = 8.4 Hz, 2 H, H<sub>Ph</sub>), 7.66 (t, *J* = 2.0 Hz, 1 H, H<sub>u</sub>), 7.84 (d, *J* = 2.0 Hz, 2 H, H<sub>t</sub>); <sup>13</sup>C NMR (100 MHz, CDCl<sub>3</sub>) δ 17.7, 27.2, 27.32, 27.34, 27.35, 27.7, 30.3, 30.55, 30.59, 30.6, 30.70 (×2), 30.71 (×2), 30.8 (×2), 31.78 (×2), 31.8 (×2), 32.0, 35.9 (×2), 48.4, 48.6, 52.3, 52.4, 53.0, 67.2, 71.5, 72.0, 73.7, 124.6, 124.8, 125.1, 127.5, 128.7, 128.8, 129.0, 129.8, 130.0, 130.1, 130.3, 130.7, 130.9, 132.2, 133.1, 133.2, 133.79, 133.8, 145.7, 152.6, 153.2, 159.1, 168.4; HRMS (FAB, 3-NOBA matrix): *m/z* = 1131.8861 [(M-H-2PF<sub>6</sub>)<sup>+</sup>] (anal. calcd. for C<sub>77</sub>H<sub>115</sub>N<sub>2</sub>O<sub>4</sub>: 1131.8857).

**(4-Hydroxymethyl benzyl)-{4-[(*E*)-2-(4-hydroxymethyl phenyl)-1-methyl vinyl]-benzyl} ammonium hexafluoro phosphate (*E*-6)**



To a solution of *E*-9 (200 mg, 0.359 mmol) in CH<sub>2</sub>Cl<sub>2</sub> (10 mL) was added HCl (20 mL, 1.0 M in diethyl ether, 20 mmol). The reaction was stirred at room temperature for 16 h then concentrated under reduced pressure. The residue was dissolved in acetone (10 mL). NH<sub>4</sub>PF<sub>6</sub> (3.00 g, 18.4 mmol) in water (10 mL) was added and the mixture stirred for a further 1 h. Volatile components were removed under reduced pressure then the residue was diluted with water (10 mL) and extracted with CHCl<sub>3</sub> (3 × 20 mL). The organic extracts were concentrated to furnish *E*-6 as a colourless solid (148 mg, 0.285 mmol, 79%): mp. 168-170 °C; <sup>1</sup>H NMR (400 MHz, d<sub>6</sub>-DMSO) δ 2.25 (s, 3 H, H<sub>h</sub>), 4.18 (s, 4 H, H<sub>d, e</sub>), 4.52 (s, 4 H, H<sub>a, l</sub>), 6.95 (s, 1 H, H<sub>i</sub>), 7.10-7.60 (m, 8 H, H<sub>Ph</sub>), 7.66 (s, 2 H, H<sub>Ph</sub>), 9.15 (br s, 2 H, H<sub>Ph</sub>); <sup>13</sup>C NMR (100 MHz, d<sub>6</sub>-DMSO) δ 17.0, 49.3, 49.5, 62.4, 62.6, 125.8, 126.3, 126.4, 127.6, 128.1, 128.3, 128.8, 129.8, 130.1, 135.4, 135.8, 141.0, 143.3, 143.6; HRMS (FAB, 3-NOBA matrix): *m/z* = 374.2123 [(M-PF<sub>6</sub>)<sup>+</sup>] (anal. calcd. for C<sub>25</sub>H<sub>28</sub>NO<sub>2</sub>: 374.2120).

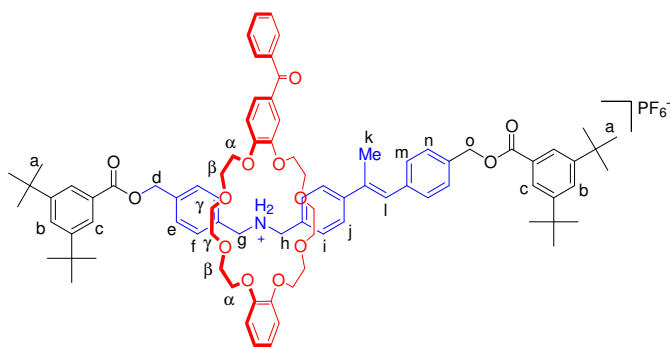
**[2]Rotaxane *E*-4**



To a solution of *E*-6 (80.0 mg, 0.156 mmol), dibenzo-24-crown-8 (111 mg, 0.248 mmol) and **S19** (152 mg, 0.336 mmol) in CH<sub>2</sub>Cl<sub>2</sub>/CH<sub>3</sub>CN (1:1, 4.0 mL) was added tributyl phosphine (10.0 μL, 0.0406 mmol) at room temperature. After 16 h, the reaction was concentrated under reduced pressure. Flash chromatography (SiO<sub>2</sub>,

CH<sub>2</sub>Cl<sub>2</sub>:methanol 9:1) afforded *E*-**4** as a colorless solid (120 mg, 0.0858 mmol, 55%): mp. 84-86 °C; <sup>1</sup>H NMR (400 MHz, CDCl<sub>3</sub>) δ 1.34 (s, 18 H, H<sub>a</sub>), 1.35 (s, 18 H, H<sub>a</sub>), 2.21 (s, 3 H, H<sub>k</sub>), 3.50 (s, 8 H, H<sub>γ</sub>), 3.70-3.85 (m, 8 H, H<sub>β</sub>), 4.00-4.16 (m, 8 H, H<sub>α</sub>), 4.55-4.70 (m, 4 H, H<sub>g, h</sub>), 5.28 (s, 2 H, H<sub>o</sub>), 5.39 (s, 2 H, H<sub>d</sub>), 6.73-6.80 (m, 5 H, H<sub>l</sub>, catechol), 6.82-6.6.88 (m, 4 H, H<sub>catechol</sub>), 7.24-7.33 (m, 4 H, H<sub>Ph</sub>), 7.33-7.40 (m, 4 H, H<sub>Ph</sub>), 7.47 (d, *J* = 8.4 Hz, 2 H, H<sub>Ph</sub>), 7.60-7.68 (m, 4 H, H<sub>Ph</sub>), 7.91 (d, *J* = 1.6 Hz, 2 H, H<sub>Ph</sub>), 7.94 (d, *J* = 2.0 Hz, 2 H, H<sub>Ph</sub>); <sup>13</sup>C NMR (100 MHz, CDCl<sub>3</sub>) δ 31.2, 31.4 (×2), 34.94, 34.95, 52.3, 65.7, 66.2, 68.1 (×2), 70.2, 70.6, 112.6, 121.7, 123.8, 123.9, 124.3, 126.1, 127.3, 127.4, 127.9, 128.0, 128.1, 129.1, 129.3, 129.40, 129.43, 130.3, 131.4, 134.8, 136.5, 137.70, 137.74, 144.5, 147.3, 151.1, 151.2, 166.9, 167.2.

## [2]Rotaxane (*E*-**5**)



To a solution of *E*-**6** (20 mg, 0.039 mmol), **3** (34 mg, 0.062 mmol) and **S19** (38 mg, 0.084 mmol) in CH<sub>2</sub>Cl<sub>2</sub>/CH<sub>3</sub>CN (1:1, 0.8 mL) was added tributyl phosphine (2.0 μL, 8.1 nmol) at room temperature. After 16 h, the reaction was concentrated under reduced pressure. Flash chromatography (SiO<sub>2</sub>, CH<sub>2</sub>Cl<sub>2</sub>:methanol 9:1) afforded *E*-**5** as a colorless solid (41 mg, 0.027 mmol, 69%): mp. 118-120 °C; <sup>1</sup>H NMR (400 MHz, CDCl<sub>3</sub>) δ 1.33 (s, 18 H, H<sub>a</sub>), 1.35 (s, 18 H, H<sub>a</sub>), 2.16 (s, 3 H, H<sub>k</sub>), 3.45-3.70 (m, 8 H, H<sub>γ</sub>), 3.70-4.00 (m, 8 H, H<sub>β</sub>), 4.00-4.30 (m, 8 H, H<sub>α</sub>), 4.60-4.75 (m, 4 H, H<sub>g, h</sub>), 5.29 (s, 2 H, H<sub>o</sub>), 5.39 (s, 2 H, H<sub>d</sub>), 6.65-6.75 (m, 3 H, H<sub>l</sub>, catechol), 6.75-6.85 (m, 3 H, H<sub>catechol</sub>), 7.22-7.48 (m, 14 H, H<sub>Ph</sub>), 7.48-7.56 (m, 2 H, H<sub>Ph</sub>), 7.62-7.70 (m, 5 H, H<sub>Ph</sub>), 7.93 (d, *J* = 2.0 Hz, 2 H, H<sub>Ph</sub>), 7.95 (d, *J* = 1.6 Hz, 2 H, H<sub>Ph</sub>); <sup>13</sup>C NMR (100 MHz, CDCl<sub>3</sub>) δ 31.32, 31.34 (×2), 34.9 (×2), 52.20, 52.25, 65.7, 66.2, 67.9 (×2), 68.1, 68.4, 70.0, 70.1, 70.2, 70.6 (×2), 70.7, 70.8 (×2), 111.1, 112.2, 112.3, 113.0, 121.5, 121.7, 123.8,

123.9, 126.0, 126.1, 127.3, 127.4, 127.9, 128.18, 128.20, 129.0, 129.2, 129.3 (×2), 129.4, 129.6 (×2), 130.1, 130.4, 131.4, 132.1, 134.7, 136.4, 137.7, 137.8, 144.4, 146.92, 146.94, 147.5, 151.1, 151.2, 151.5, 157.7, 166.9, 167.2, 195.2; HRMS (FAB, 3-NOBA matrix):  $m/z$  = 1358.7505 [(M-PF<sub>6</sub>)<sup>+</sup>] (anal. calcd. for calcd. for C<sub>86</sub>H<sub>104</sub>NO<sub>13</sub>: 1358.7508).

### 3.3. References and notes.

- (1) Kitazume, T.; Lin, J. T.; Takeda, M.; Yamazaki, T. *J. Am. Chem. Soc.* **1991**, *113*, 2123-2126.
- (2) A high *Z:E* ratio of olefin products was initially deemed desirable as a rotaxane-forming reaction using a fully deprotected diammonium *Z*-stilbene thread precursor had been envisaged. Inseparable product mixtures and low yields made this route impractical, however, and so it was decided to develop the *E*-olefin series to a monoammonium thread precursor (*E*-12).
- (3) Allard, E.; Delaunay, J.; Cousseau, J. *Org. Lett.* **2003**, *5*, 2239-2242.
- (4) Klopsch, R.; Franke, P.; Schlüter, A.-D. *Chem. Eur. J.* **1996**, *2*, 1330-1334.
- (5) Jakobsen, C. M.; Denmeade, S. R.; Isaacs, J. T.; Gady, A.; Olsen, C. E.; Christensen, S. B. *J. Med. Chem.* **2001**, *44*, 4696-4703.
- (6) Naito, H.; Kawahara, E.; Maruta, K.; Maeda, M.; Sasaki, S. *J. Org. Chem.* **1995**, *60*, 4419-4427.
- (7) Cantrill, S. J.; Youn, G. Y.; Stoddart, J. F.; Williams, D. J. *J. Org. Chem.* **2001**, *66*, 6857-6872.
- (8) (a) Kawasaki, H.; Kihara, N.; Takata, T. *Chem. Lett.* **1999**, 1015-1016. (b) Watanabe, N.; Yagi, T.; Kihara, N.; Takata, T. *Chem. Commun.* **2002**, 2720-2721. (c) Tachibana, Y.; Kawasaki, H.; Kihara, N.; Takata, T. *J. Org. Chem.* **2006**, *71*, 5093-5104.